

NASA
CR
3170
c.1

NASA Contractor Report 3170

LOAN/COPY IN
AEWIC/TECHNIC
KIRTLAND AFB
0061925



Rotary Balance Data for a Single-
Engine General Aviation Design Having
a High Aspect-Ratio Canard for an
Angle-of-Attack Range of 30° to 90°

William J. Mulcay and Robert Rose

CONTRACT NAS1-14849
DECEMBER 1980

NASA



0061925

NASA Contractor Report 3170

**Rotary Balance Data for a Single-
Engine General Aviation Design Having
a High Aspect-Ratio Canard for an
Angle-of-Attack Range of 30° to 90°**

William J. Mulcay and Robert Rose
Birbile Applied Research, Inc.
Jericho, New York

Prepared for
Langley Research Center
under Contract NAS1-14849



National Aeronautics
and Space Administration

**Scientific and Technical
Information Branch**

1980

SUMMARY

Aerodynamic characteristics obtained in a helical flow environment utilizing a rotary balance located in the Langley spin tunnel are presented in plotted form for a 1/4.5-scale single-engine general aviation model having a high aspect-ratio canard. The configurations tested included the basic airplane, two canard locations, and wing leading-edge modifications, as well as airplane components. Data are presented without analysis for an angle-of-attack range of 30° to 90° and clockwise and counter-clockwise rotations covering an $\frac{\Omega b}{2V}$ range between 0 and 0.90.

INTRODUCTION

The NASA Langley Research Center has a broad general aviation stall/spin research program underway which includes spin-tunnel and free-flight radio control model tests, as well as full-scale flight tests for a number of configurations typical of light, general aviation airplanes. To support this effort, rotary balance wind tunnel force tests covering these same configurations will be conducted to establish a data base for analysis of model and full-scale flight results, and to develop design charts for desirable stall/spin characteristics.

As part of this program, it was desired to obtain fundamental information on a 1/4.5-scale general aviation model having a high aspect-ratio canard. This report presents the data obtained for the basic configuration, two canard positions, and wing leading-edge modifications, as well as airplane components.

SYMBOLS

The units for physical quantities used herein are presented in the International System of Units (SI) and U.S. Customary Units. The measurements were made in the U.S. Customary Units; equivalent dimensions were determined by using the conversion factors given in reference 1.

b	wing span, m (ft)
\bar{c}	mean aerodynamic chord, cm (in.)
C_L	lift-force coefficient, $\frac{\text{Lift force}}{qS}$
C_N	normal-force coefficient, $\frac{\text{Normal force}}{qS}$
C_A	axial-force coefficient, $\frac{\text{Axial force}}{qS}$
C_λ	rolling moment coefficient, $\frac{\text{Rolling moment}}{qSb}$
C_m	pitching-moment coefficient, $\frac{\text{Pitching moment}}{qSc}$
C_n	yawing-moment coefficient, $\frac{\text{Yawing moment}}{qSb}$
q	free-stream dynamic pressure, N/m ² (lb/ft ²)
S	wing area, m ² (ft ²)
V	free-stream velocity, m/sec (ft/sec)
α	angle of attack, deg
β	angle of sideslip, deg
Ω	angular velocity about spin axis, rad/sec
$\frac{\Omega b}{2V}$	spin coefficient, positive for clockwise spin
δ_{C_f}	canard flap deflection, positive when trailing edge is down, deg

Abbreviations:

cg	center of gravity
SR	spin radius
LE	leading edge

TEST EQUIPMENT

A rotary balance measures the forces and moments acting on an airplane while subjected to rotational flow conditions; the background for this apparatus is discussed in reference 2. A photograph and sketch of the rotary balance apparatus installed in the Langley spin tunnel are shown in figures 1 and 2, respectively. The rotating portion of the balance system, mounted on a horizontal supporting boom which is hinged at the wall, is moved from the wall to the center of the tunnel by cables. The rotary arm of the balance system, which rotates about a vertical axis, is attached to the outer end of the horizontal supporting boom and is driven by a drive shaft through couplings and gears.

A test model is mounted on a strain gauge balance which is affixed to the bottom of the rotary balance apparatus. Controls located outside the tunnel are used to activate motors on the rig which position the model to the desired attitude. The angle-of-attack range of the rig is 8 to 90 degrees and the sideslip angle range is ± 15 degrees. The spin radius and the lateral displacement motors allow the operator to position the moment center of the balance on the spin axis or at a specific distance from the spin axis. This is done for each combination of angle of attack and sideslip angle. The general practice is to mount the moment center of the balance at the cg location about which the aerodynamic moments are desired. Electrical current from the balance, and to the motors on the rig, is conducted through slip-rings located at the rig head. Examples of how the rig is positioned for different angles of attack and sideslip angles are shown in figures 2a and 2b, respectively.

The model can be rotated up to 90 rpm in either direction. By using different rotational speeds and a specific airflow in the tunnel, the motions of a steady spinning airplane can be simulated. The aerodynamic forces and moments can then be

measured for values of $\frac{\Omega b}{2V}$, including the case of $\frac{\Omega b}{2V} = 0$, where static aerodynamic forces and moments can be obtained.

A NASA six-component strain gauge balance is mounted inside the model and measures the normal, lateral, and longitudinal forces and the yawing, rolling, and pitching moments acting about the body axis. The interactions that exist between the six components are available from balance calibration tests and are accounted for after the balance voltages are converted to forces and moments.

The data acquisition, reduction and presentation system for the rotary balance set-up is composed of a 12-channel scanner/voltmeter, a mini-computer and a plotter. With this equipment, on-line digital print out and/or graphical plots of data are possible.

TEST PROCEDURES

Rotary aerodynamic data are obtained in two steps. The first step is to record the inertial forces and moments (tares) acting on the model at different attitudes and rotational speeds. To accomplish this, a covered bird cage-like structure, which encloses the model without touching it, is mounted on the upper portion of the rig and rotates with the model. In this manner, the air immediately surrounding the model is trapped by the structure and constrained to rotate with it. As the rig is rotated at the desired attitude and rate, the inertial forces and moments generated by the model are measured and stored on magnetic tape for later use.

The second step in the data-gathering process is to measure aerodynamic and inertial forces at different attitudes and rotational speeds for a selected tunnel velocity with, of course, the cage structure removed. The tares are subtracted from these values, and the remaining aerodynamic forces and moments are

then converted to coefficient form and stored on magnetic tape.

MODEL

A 1/4.5-scale model of a single-engine general aviation design having a high aspect-ratio canard was constructed of fiberglass-epoxy, wood and styrofoam. A three-view drawing of this model is shown in figure 3, dimensional characteristics of the model are presented in Table I, and a photograph of the model installed on the rotary balance located in the Langley spin tunnel is presented in figure 1.

Wing LE cuffs were removable such that two sets could be tested differing only in nose radius (see figure 4). Also, allowance was made to remove the wing, test the canard 8.26 cm (3.3 in.) below the basic canard location (see figure 5) and to replace the upper and lower vertical surfaces (see figure 6) mounted on the wing tips with conventional wing tip fairings. The body alone configuration tested is shown in figure 7.

The model control surfaces could be set to any position prior to the test. The maximum deflections for the control surfaces were:

Canard flap, deg	20 up, 23 down
Rudder, deg	35 right outboard, 35 left outboard
Aileron, deg	20 up, 20 down

TEST CONDITIONS

The tests were conducted in the spin tunnel at an airstream velocity of 7.62 m/sec (25 ft/sec) which corresponds to a Reynolds number of approximately 93,000 based on the model mean aerodynamic chord and 37,400 based on model canard chord. Unless

noted otherwise in Table II, all the configurations were tested through an angle-of-attack range of 30 to 90° at a zero side-slip angle with the spin axis passing through the full-scale airplane cg location.

For each angle of attack, data were obtained for nominal $\frac{\Omega b}{2V}$ values of .1, .2, .3, .4, .5, .6, .7, .8, and .9 in both clockwise and counter-clockwise directions, as well as for $\frac{\Omega b}{2V} = 0$ (static value).

DATA PRESENTATION

Table II identifies the configurations tested and the corresponding appendix figure numbers which present the aerodynamic data. The aerodynamic coefficients vs. $\frac{\Omega b}{2V}$ are presented for each configuration in six sequentially numbered figures in the following order: C_n , C_ℓ , C_m , C_N , C_Y , and C_A . Each figure, in turn, consists of two pages which present the subject aerodynamic coefficient vs. $\frac{\Omega b}{2V}$ for the following angles of attack.

- a) $\alpha = 30, 35, 40, 45, 50$ deg
- b) $\alpha = 55, 60, 70, 80, 90$ deg

All the moment data are presented for a cg position .748 \bar{c} forward of the LE of \bar{c} , which corresponds to 5.6 cm (2.22 in.) forward of the wing LE-strake intersection.

REFERENCES

1. Mechtly, E.A.: The International System of Units - Physical Constants and Conversion Factors. NASA SP-7012, 1973.
2. Bihrle, William, Jr.; Hultberg, Randy S.; Mulcay, William: Rotary Balance Data for a Typical Single-Engine Low-Wing General Aviation Design for an Angle-of-Attack Range of 30° to 90° . NASA CR-2972, 1978.

TABLE I.- DIMENSIONAL CHARACTERISTICS OF THE BASIC MODEL

Overall length, m (ft)894 (2.933)
Wing:	
Span, m (ft)	1.504 (4.933)
Area, m^2 (ft^2)246 (.647)
Root chord, cm (in.)	23.7 (9.33)
Tip chord, cm (in.)	8.94 (3.52)
Mean aerodynamic chord, cm (in.)	17.5 (6.88)
Leading edge of \bar{C} , distance rearward of leading edge of wing-strake intersection, cm (in.)	7.34 (2.89)
Aspect ratio	9.19
Anhedral along wing leading-edge, deg	4
Incidence:	
At strake intersection, deg	+1.13
Tip, deg	-1.75
Sweepback of leading edge, deg	28
Canard:	
Span, m (ft)847 (2.78)
Area, m^2 (ft^2)0596 (.642)
Chord, cm (in.)	7.06 (2.78)
Aspect ratio	12.02
Incidence, deg	0
Airfoil section . . . Glasgow Univ. designation GU 25-5(11)8	
Upper vertical surface:	
Span, cm (in.)	20.8 (8.17)
Area, m^2 (ft^2)01596 (.1718)
Root chord, cm (in.)	11.2 (4.40)
Tip chord, cm (in.)	3.91 (1.54)
Dihedral	Perpendicular to wing upper surface
Incidence:	
Root, deg	0
Tip, deg	-1
Sweepback of leading edge, deg	30
Lower vertical surface:	
Span, cm (in.)	4.06 (1.60)
Root chord, cm (in.)	3.35 (1.32)
Tip chord, cm (in.)	1.96 (.77)
Incidence, deg	0
Sweepback along trailing edge, deg	0

TABLE II.- CONFIGURATIONS TESTED AND FIGURE INDEX

(All configurations tested through $\alpha = 30^\circ$ to 90° at $\beta = 0^\circ$.)

FIGURE NO.	CONFIGURATION	δc_f deg	δa deg	δr deg
A1-A6	Basic	0	0	0
A7-A12	Canard lowered	0	0	0
A13-A18	Canard off			↓
A19-A24	LE cuff having increased nose radius			↓
A25-A30	Vertical surfaces off	↓	↓	Off
A31-A36	Wing off	+23	off	
A37-A42	Wing and canard off (body alone)	off	↓	↓

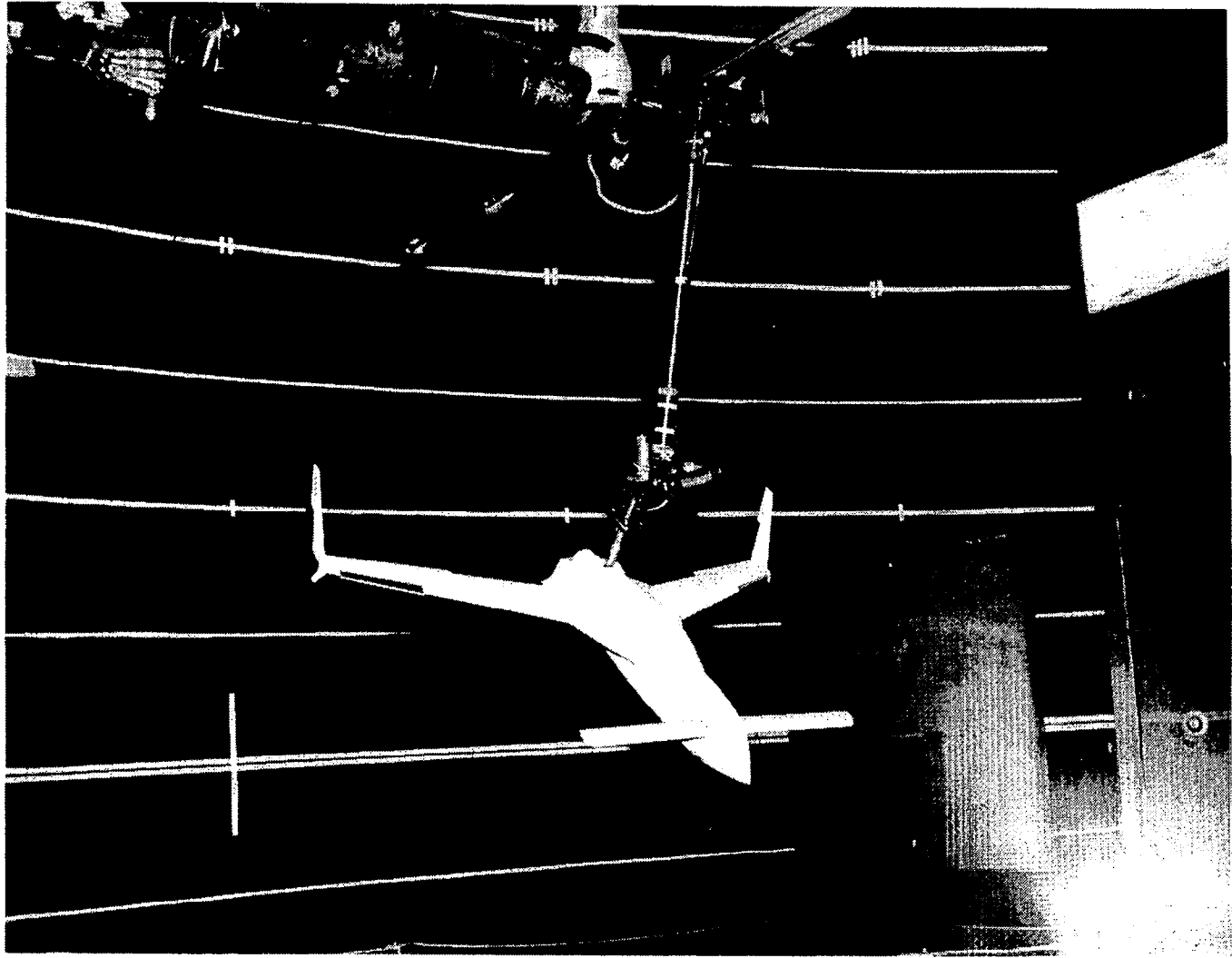
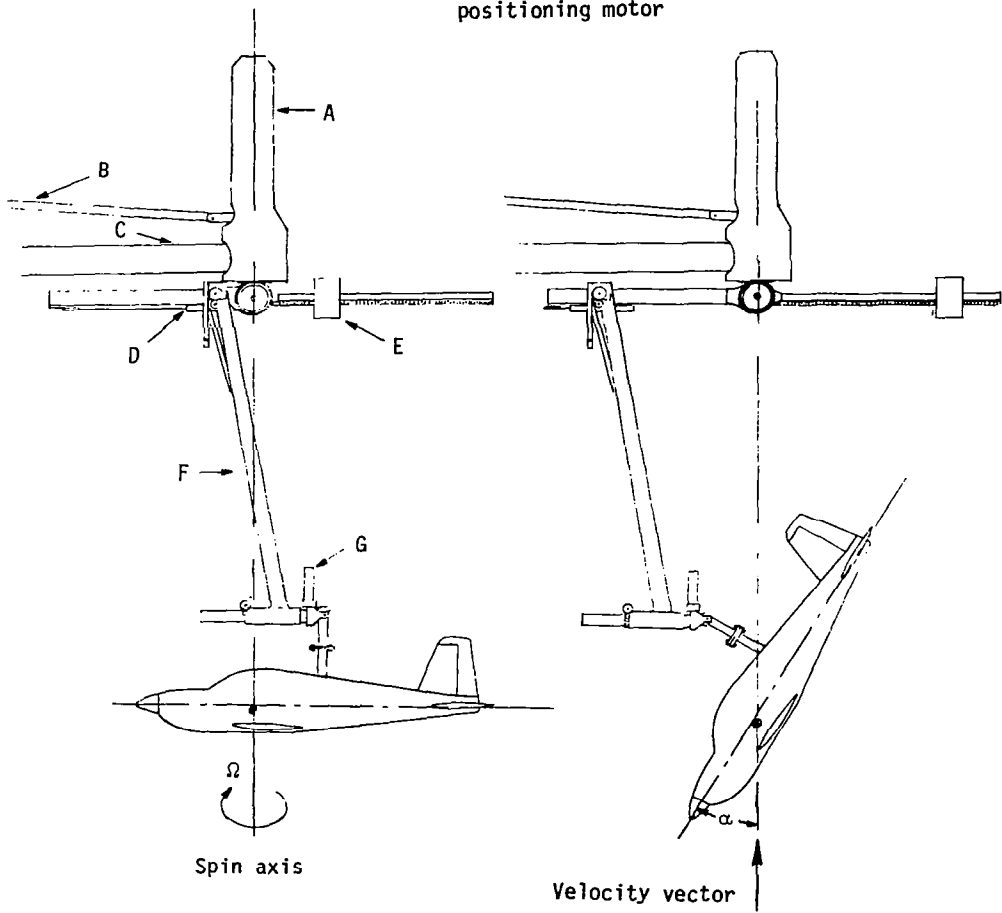


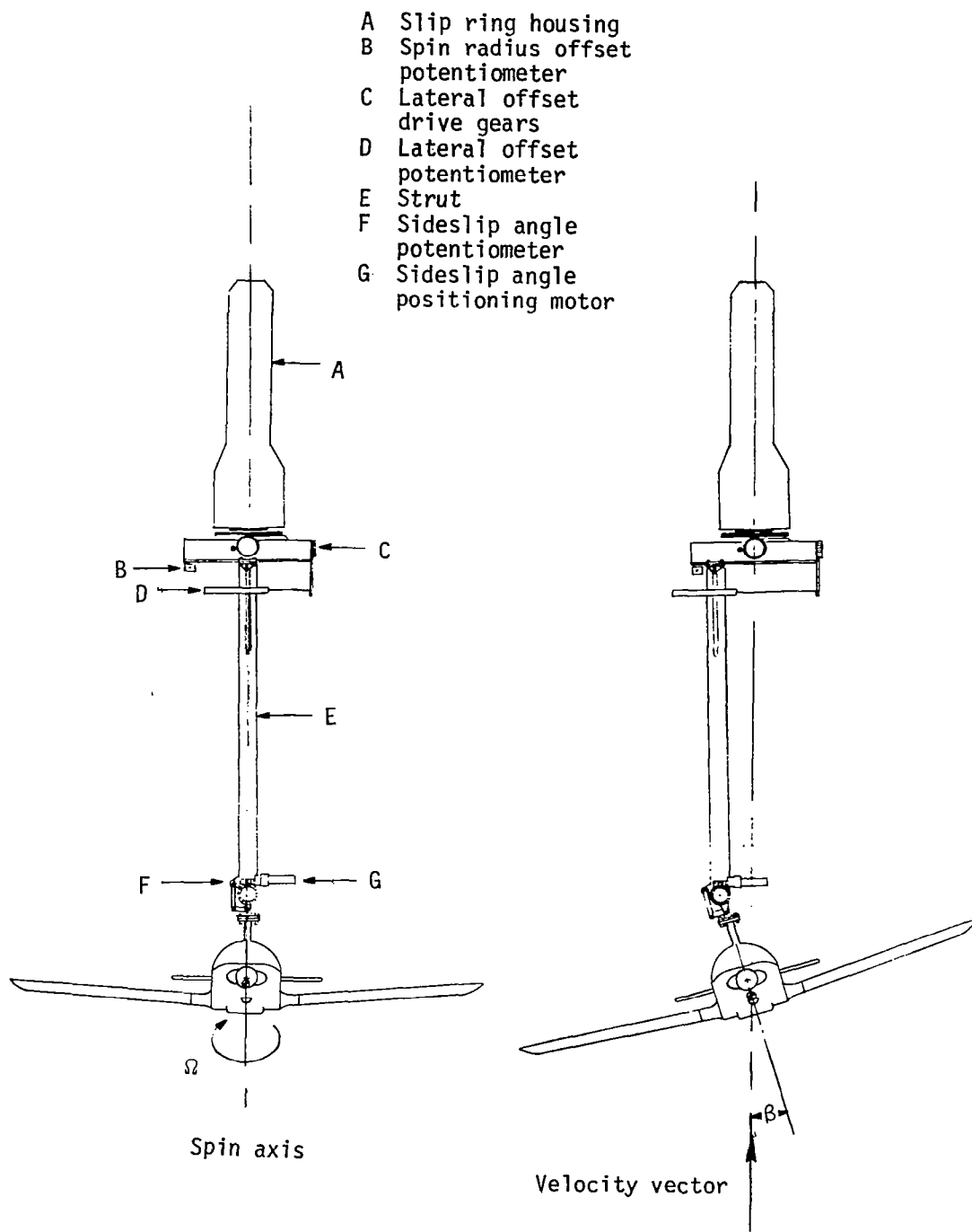
Figure 1. - Photograph of 1/4.5-scale model installed on rotary balance apparatus.

- A Slip ring housing
- B Drive shaft
- C Support boom
- D Spin radius offset potentiometer
- E Counterweight
- F Strut
- G Angle of attack positioning motor



(a) Side view of model.

Figure 2.- Sketch of rotary balance apparatus.



(b) Front view of model.

Figure 2.- Concluded.

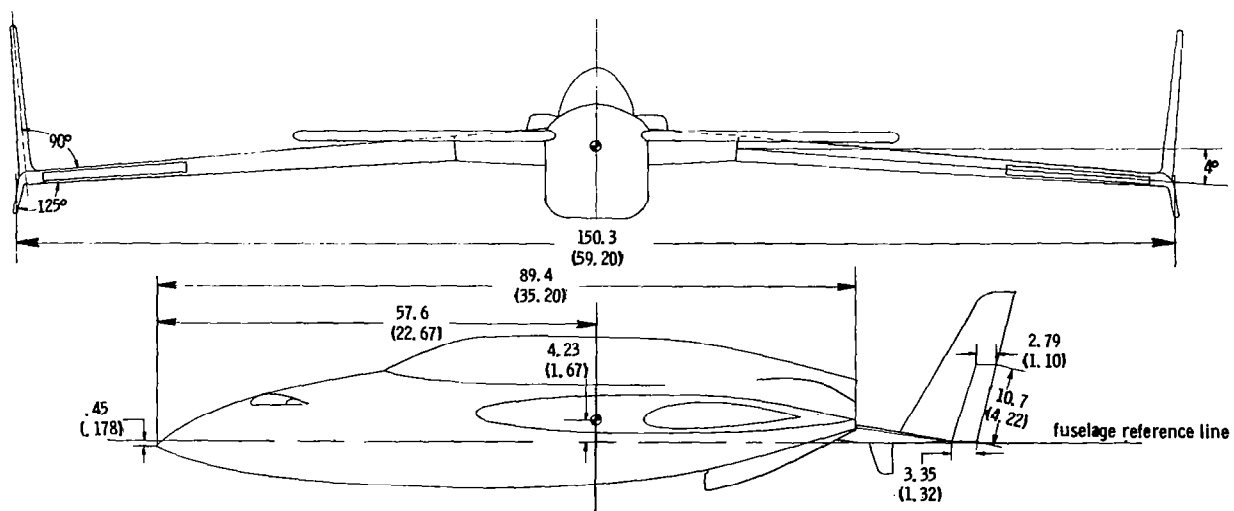
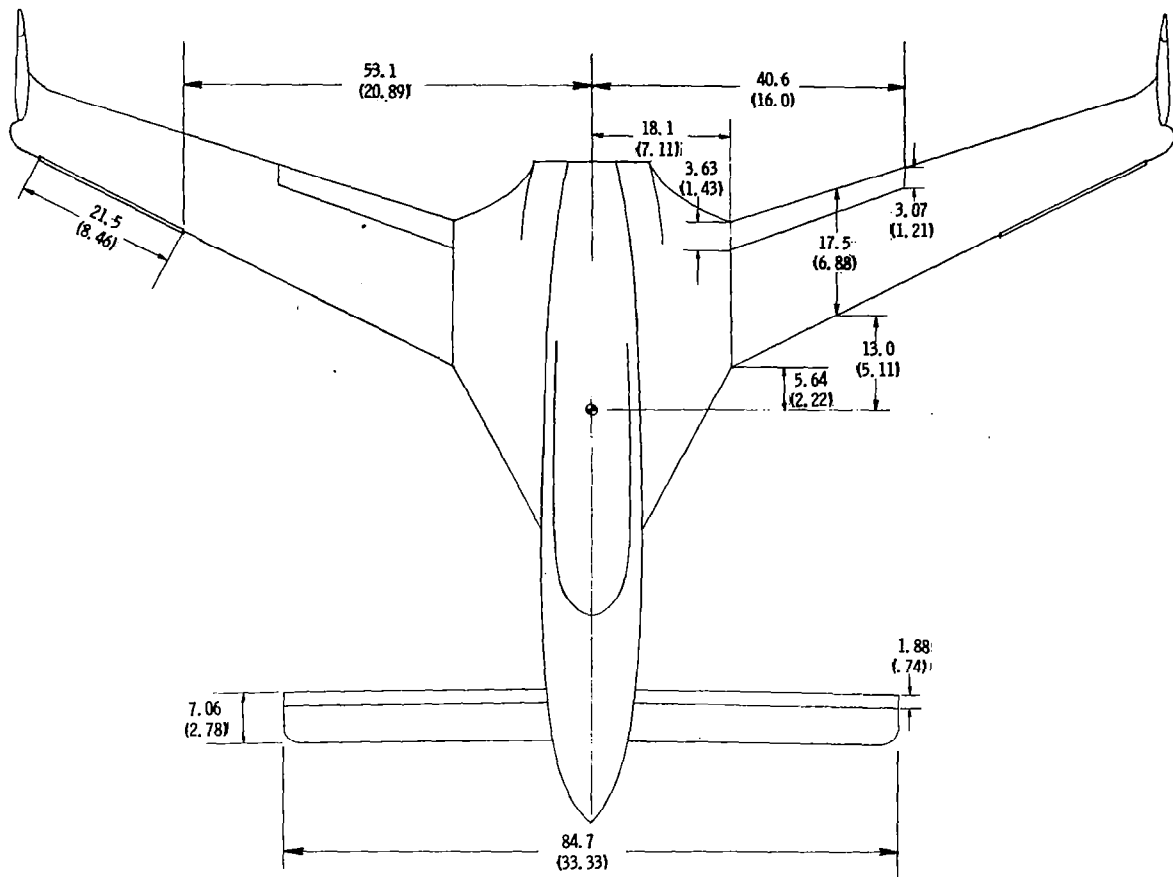


Figure 3. - Three-view drawing of basic 1/4.5-scale general aviation model having high aspect-ratio canard. Dimensions are given in centimeters (inches), model scale.

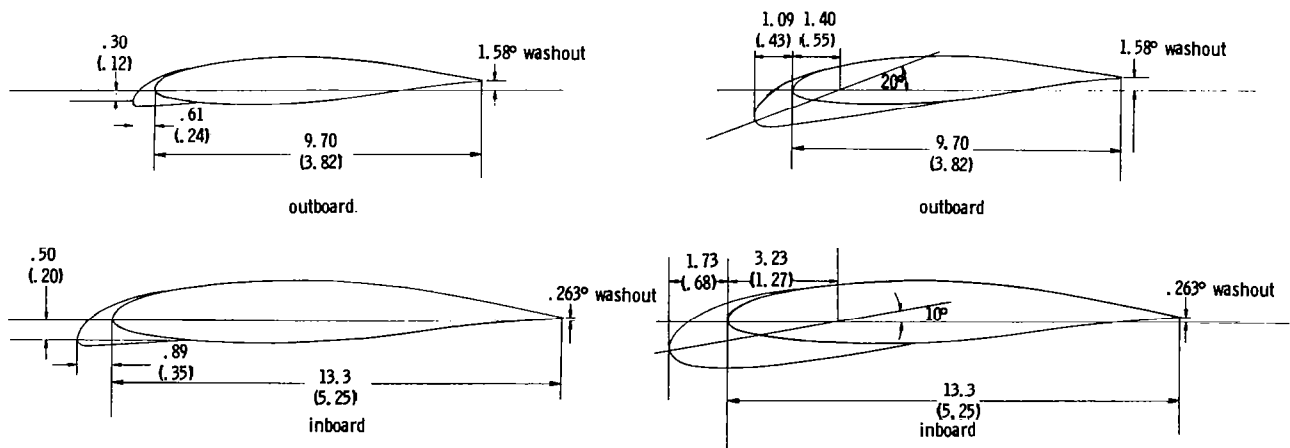
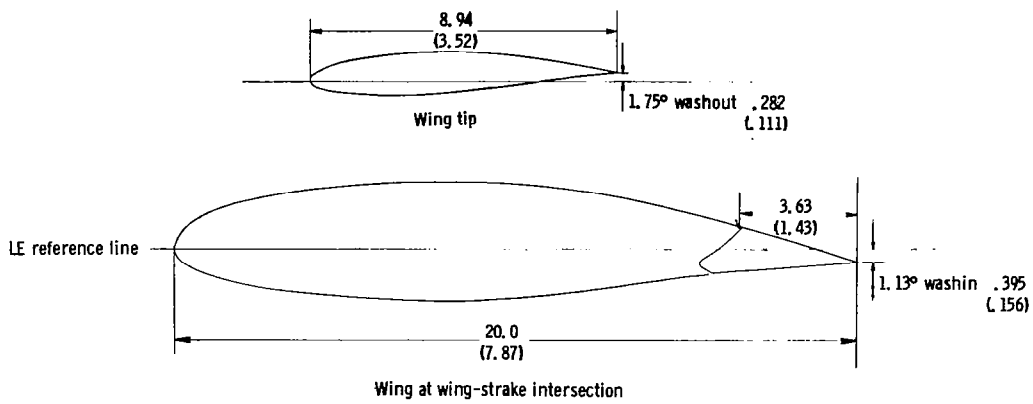


Figure 4. - Wing, canard and cuff airfoils tested on model. Dimensions are given in centimeters (inches), model scale.

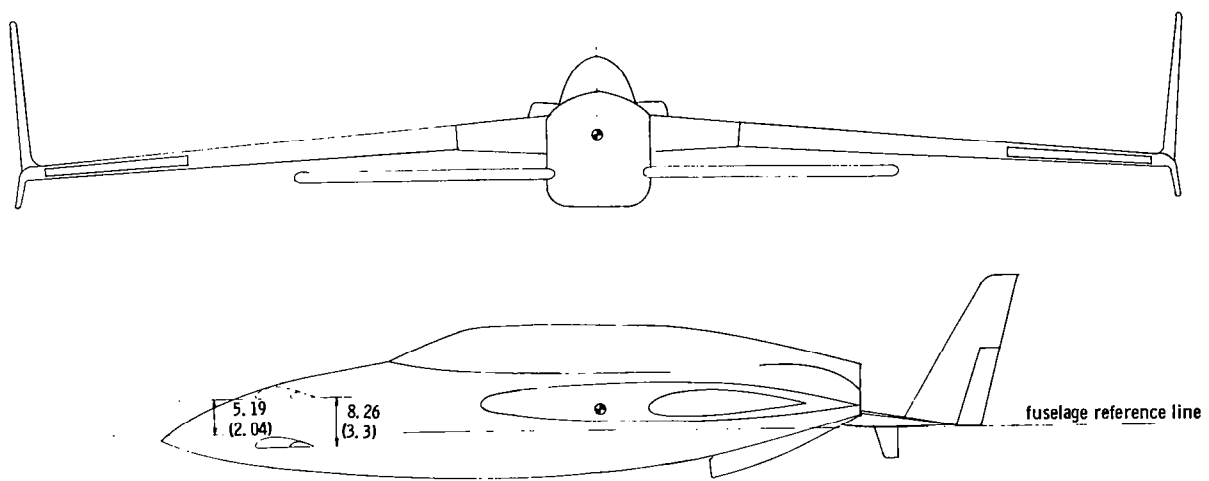


Figure 5.- Location of lowered canard tested on model. Dimensions are given in centimeters (inches), model scale.

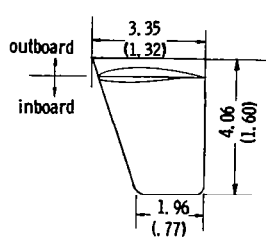
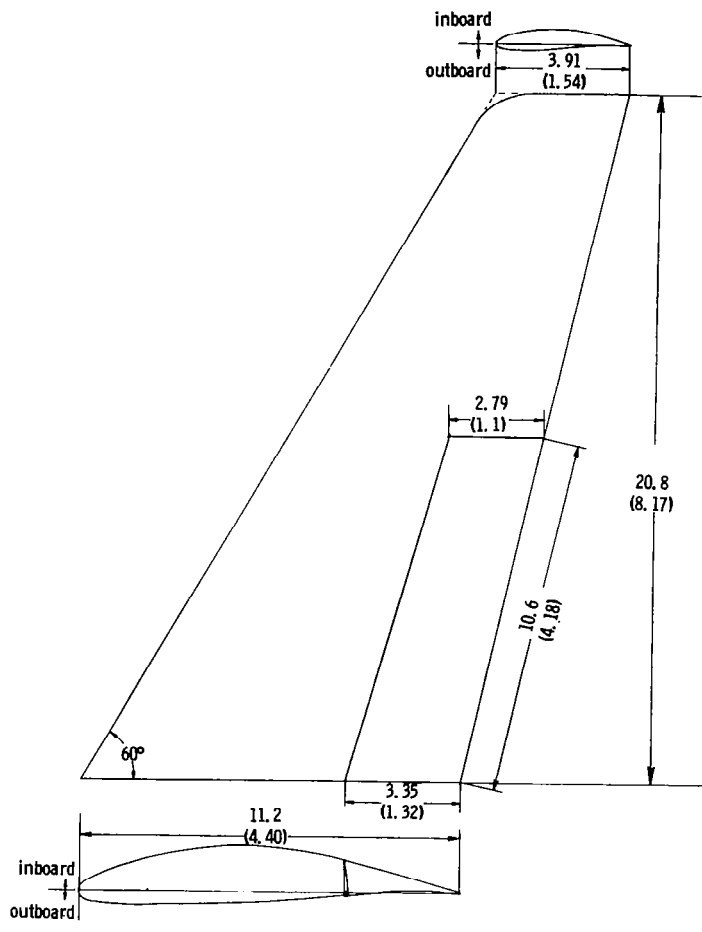


Figure 6. - Wing tip vertical surfaces tested on model. Dimensions are given in centimeters (inches), model scale.

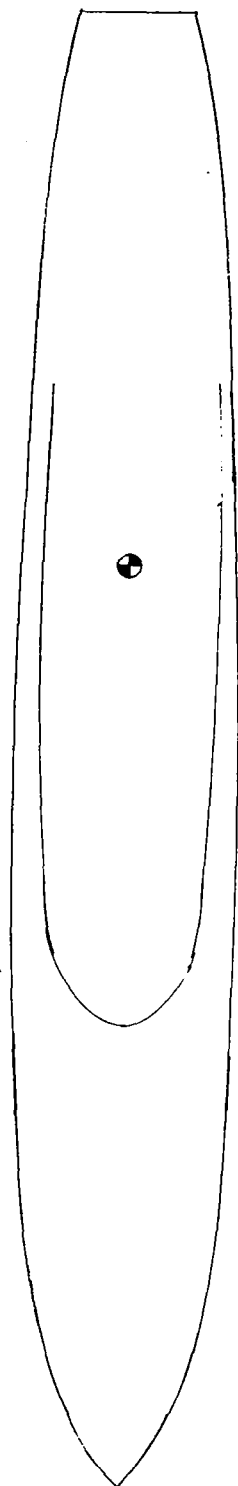
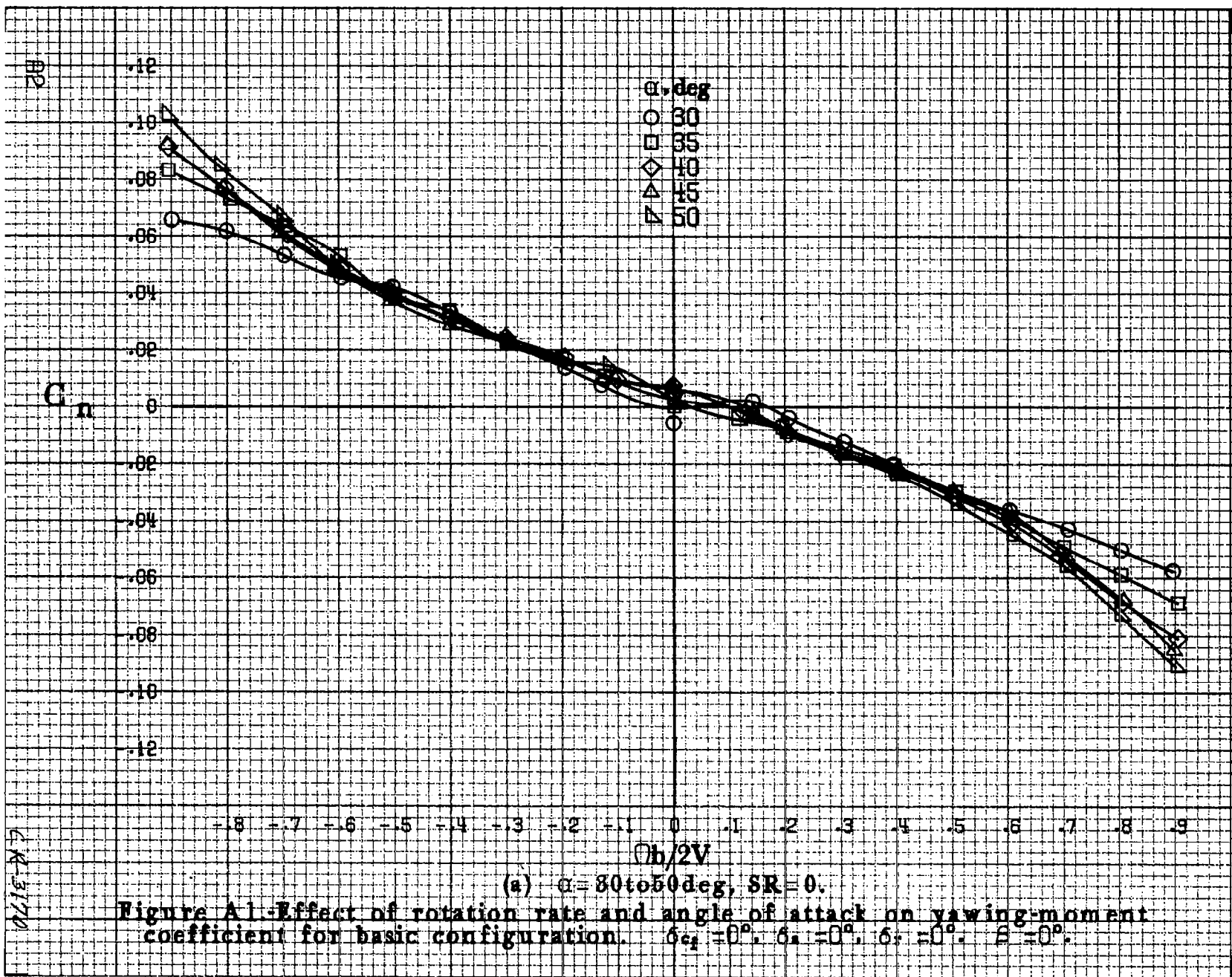
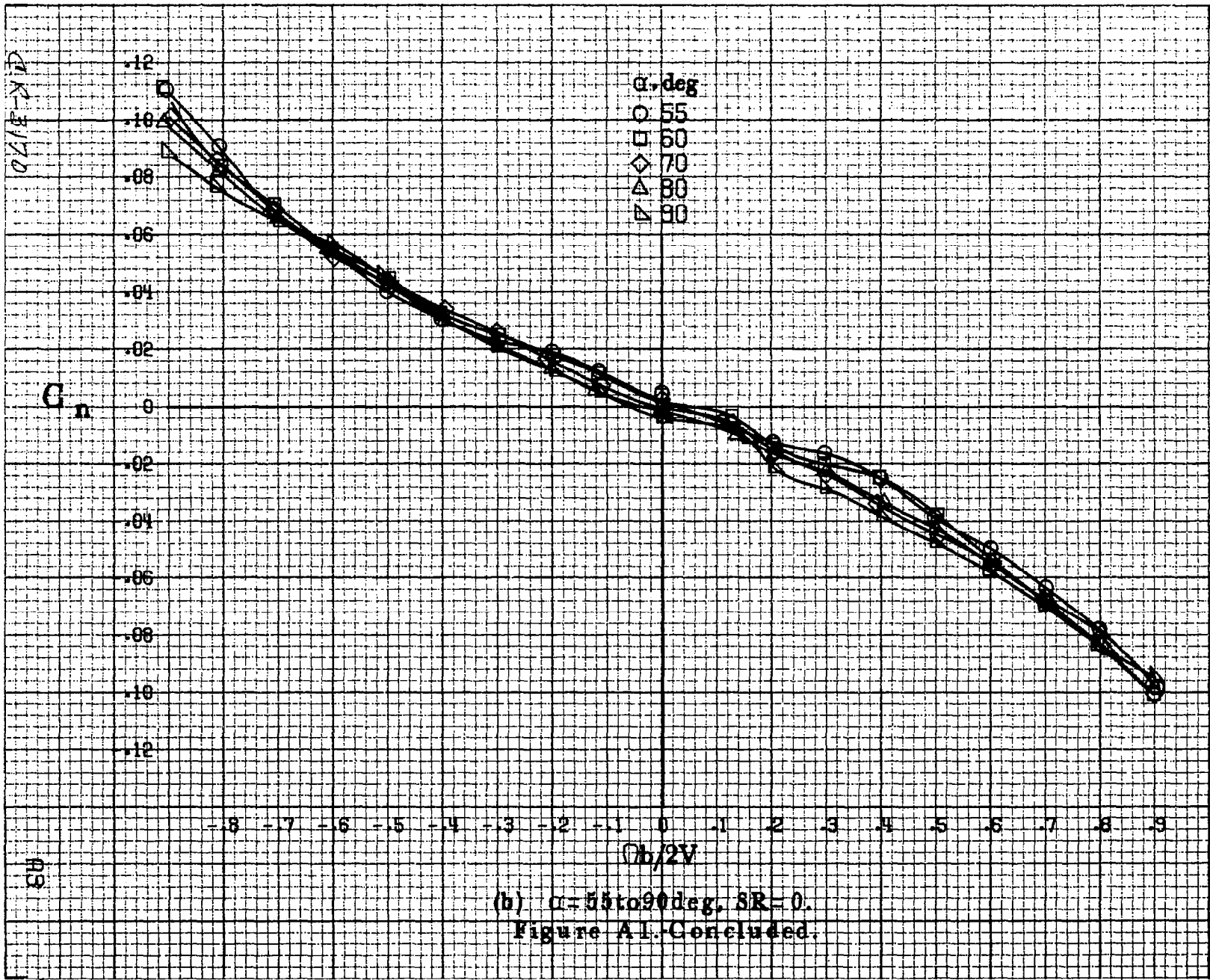


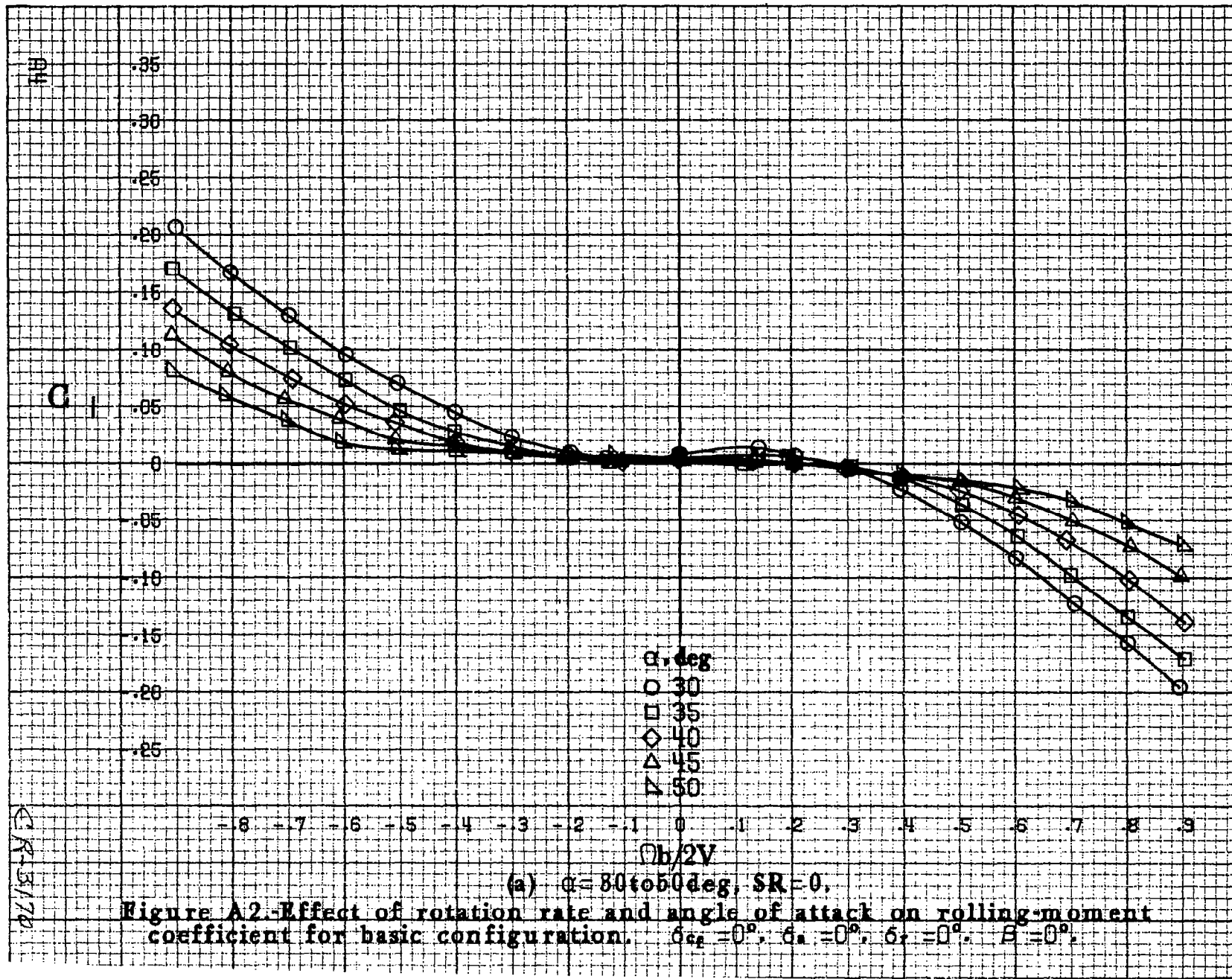
Figure 7. Body alone configuration as tested

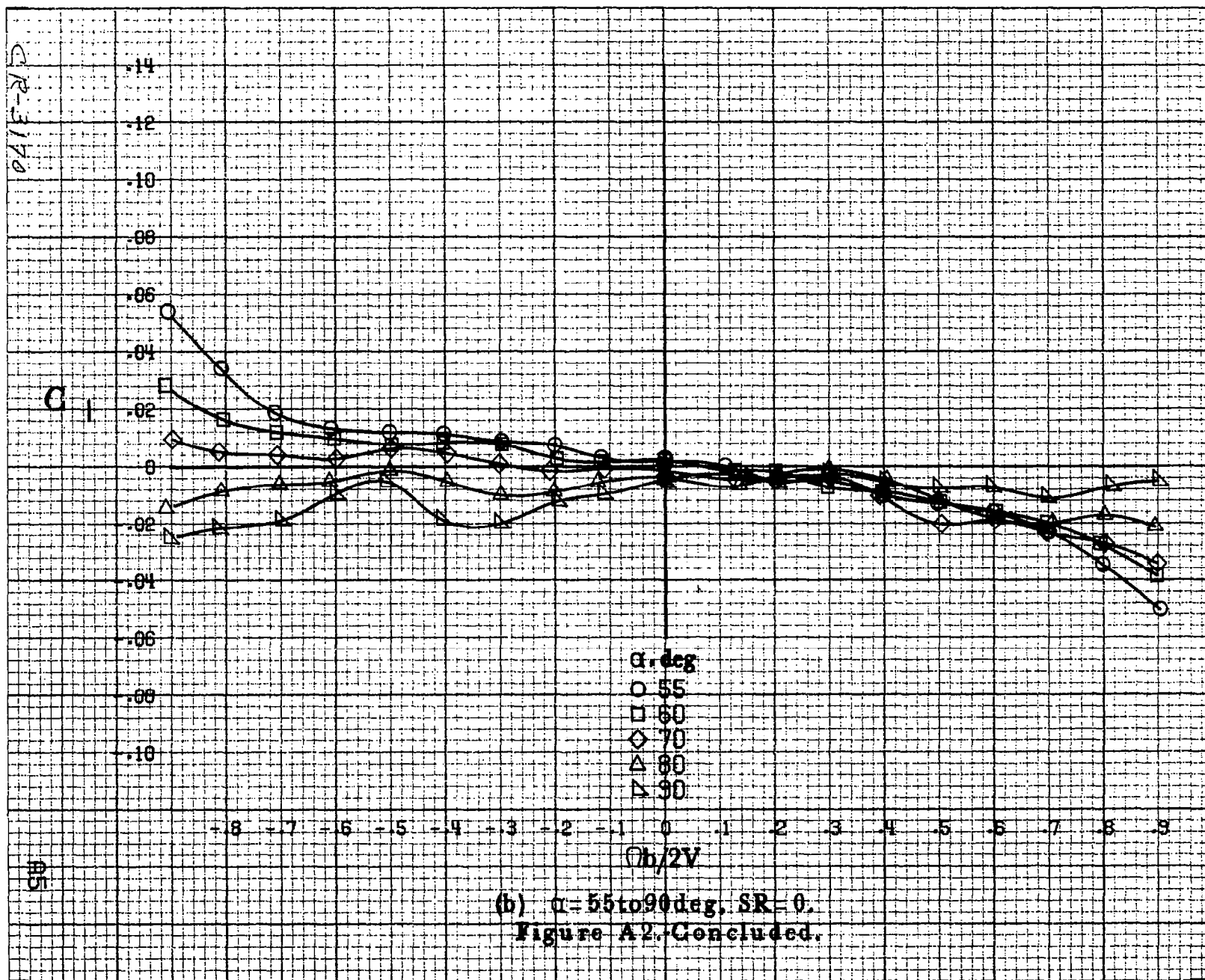


APPENDIX

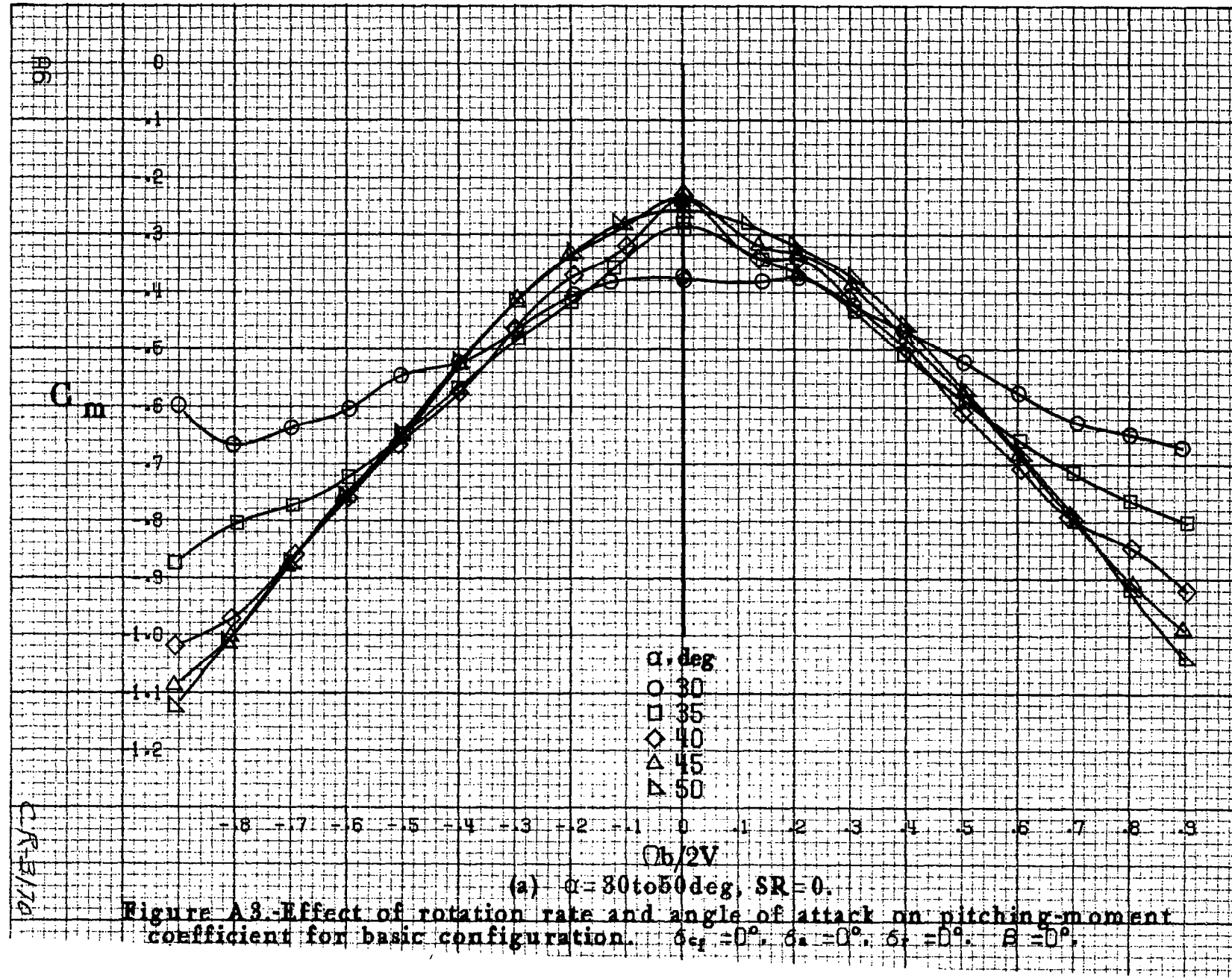


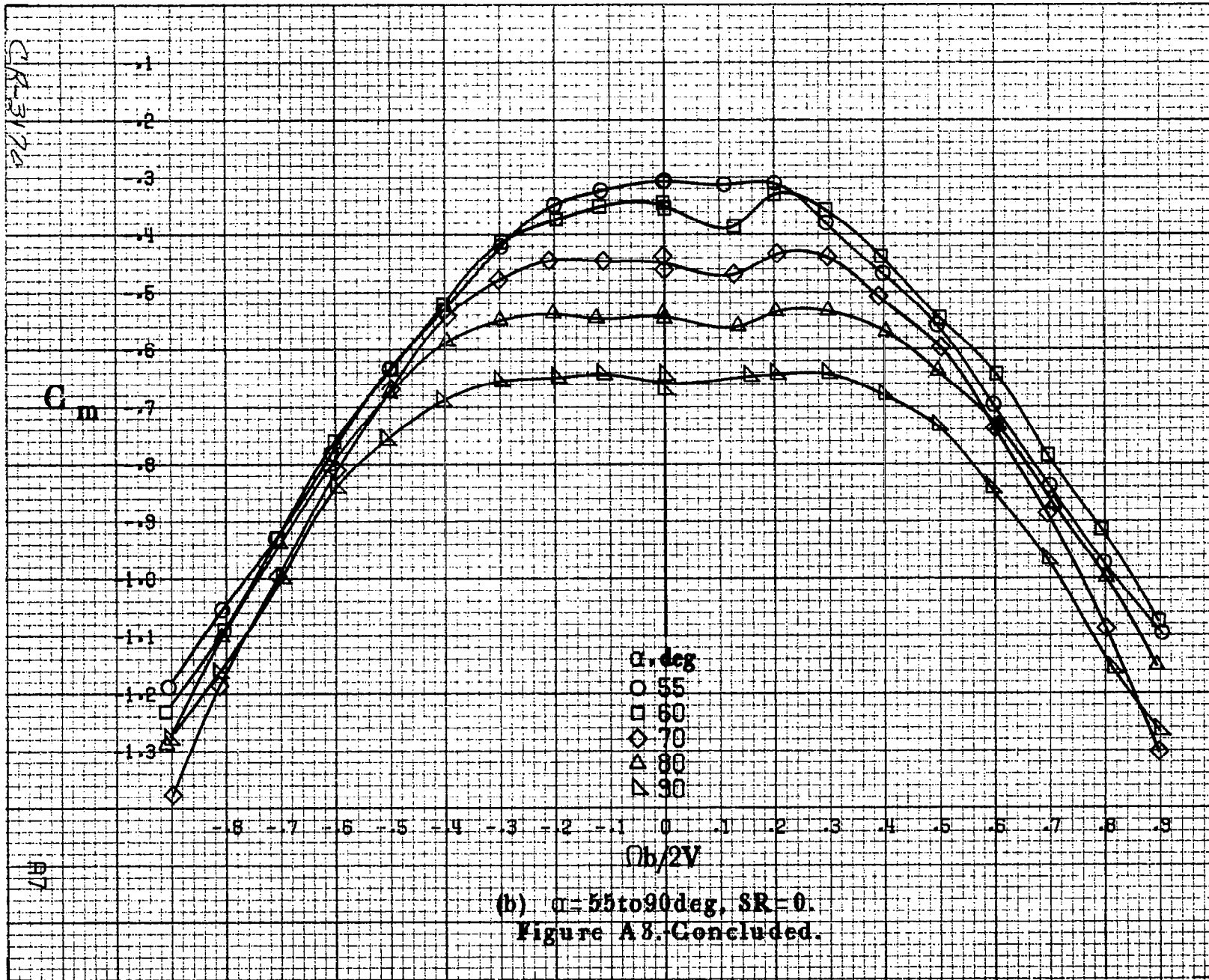


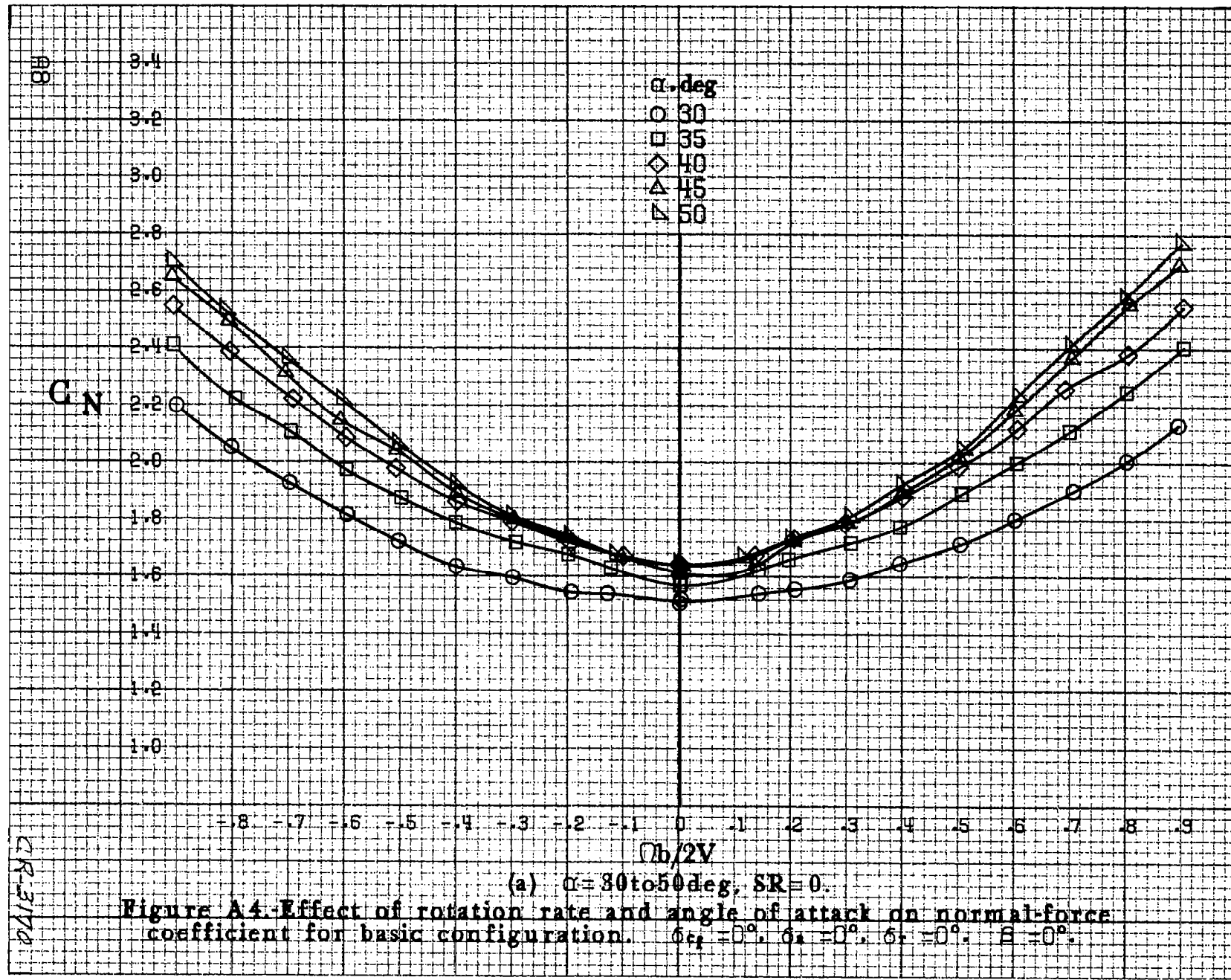


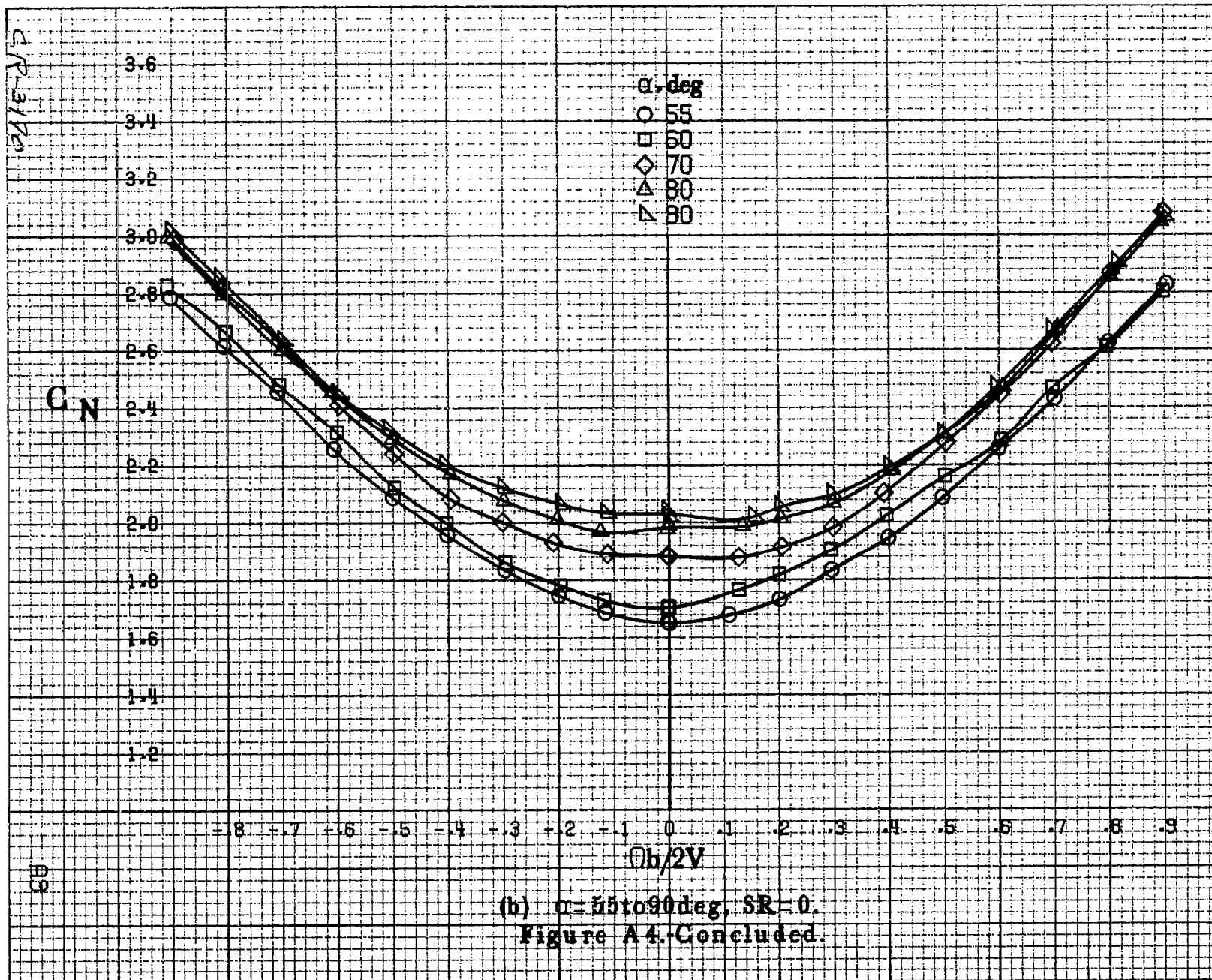


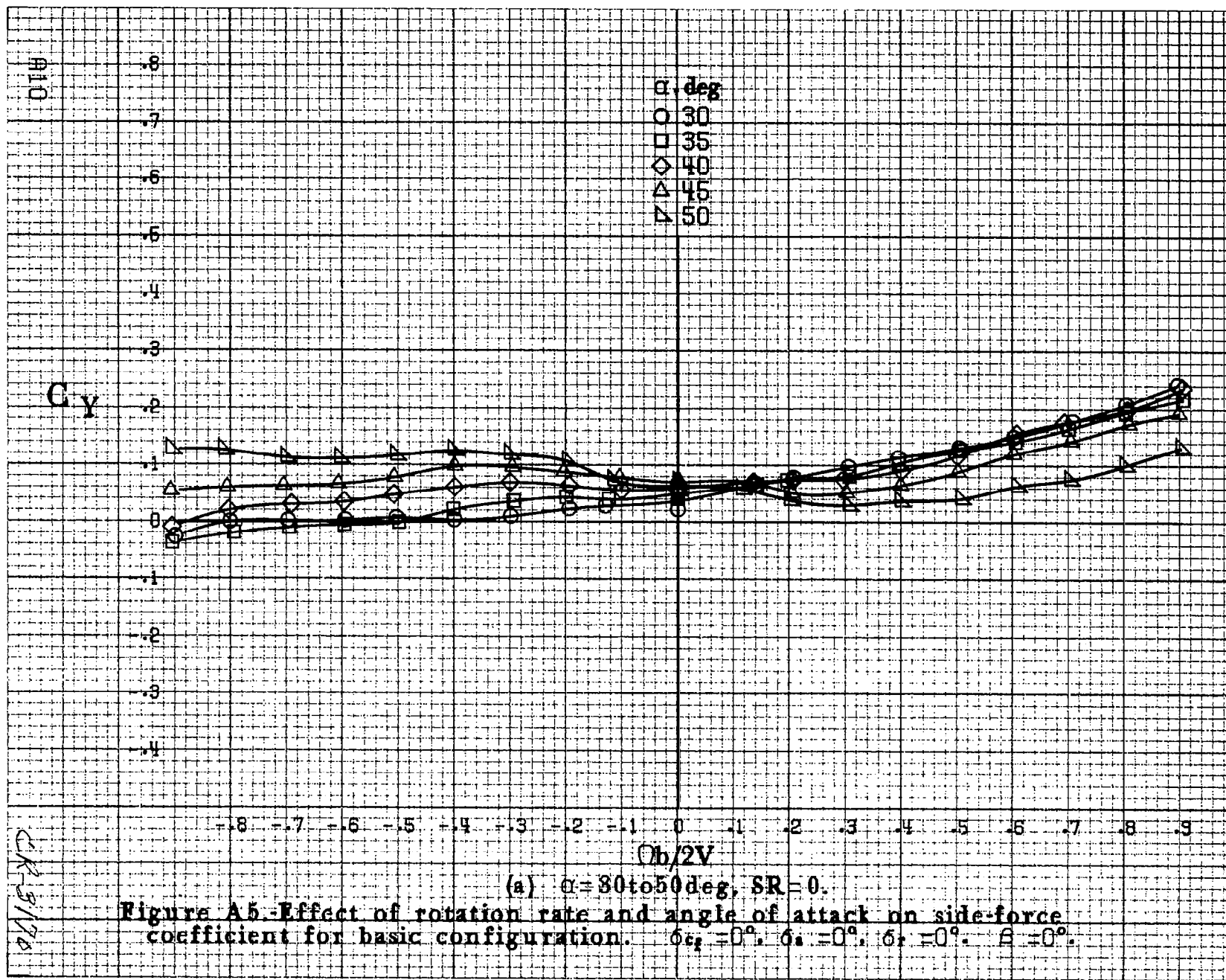
(b) $\Omega = 55$ to 90 deg., $SR = 0$.
Figure A2. Concluded.

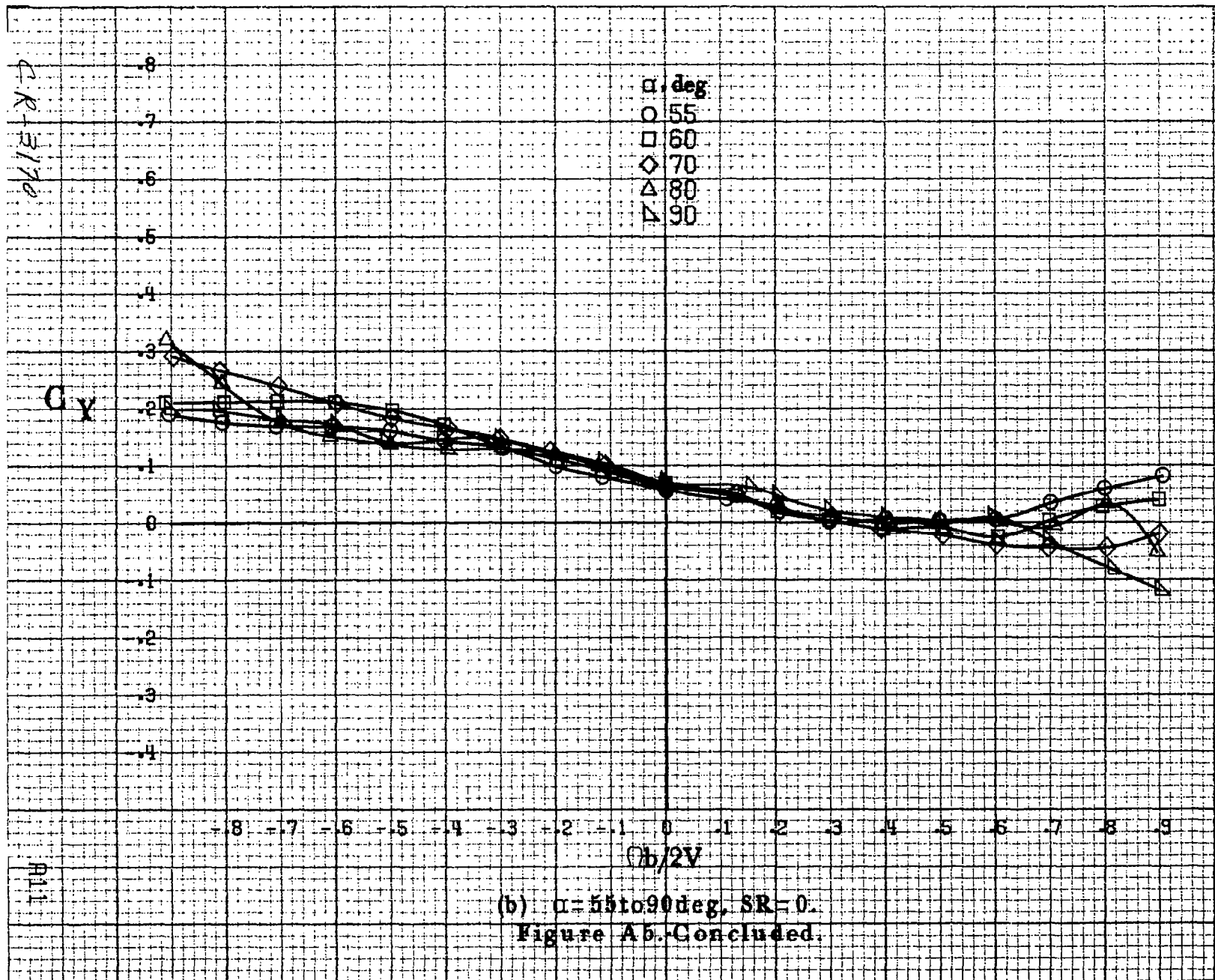


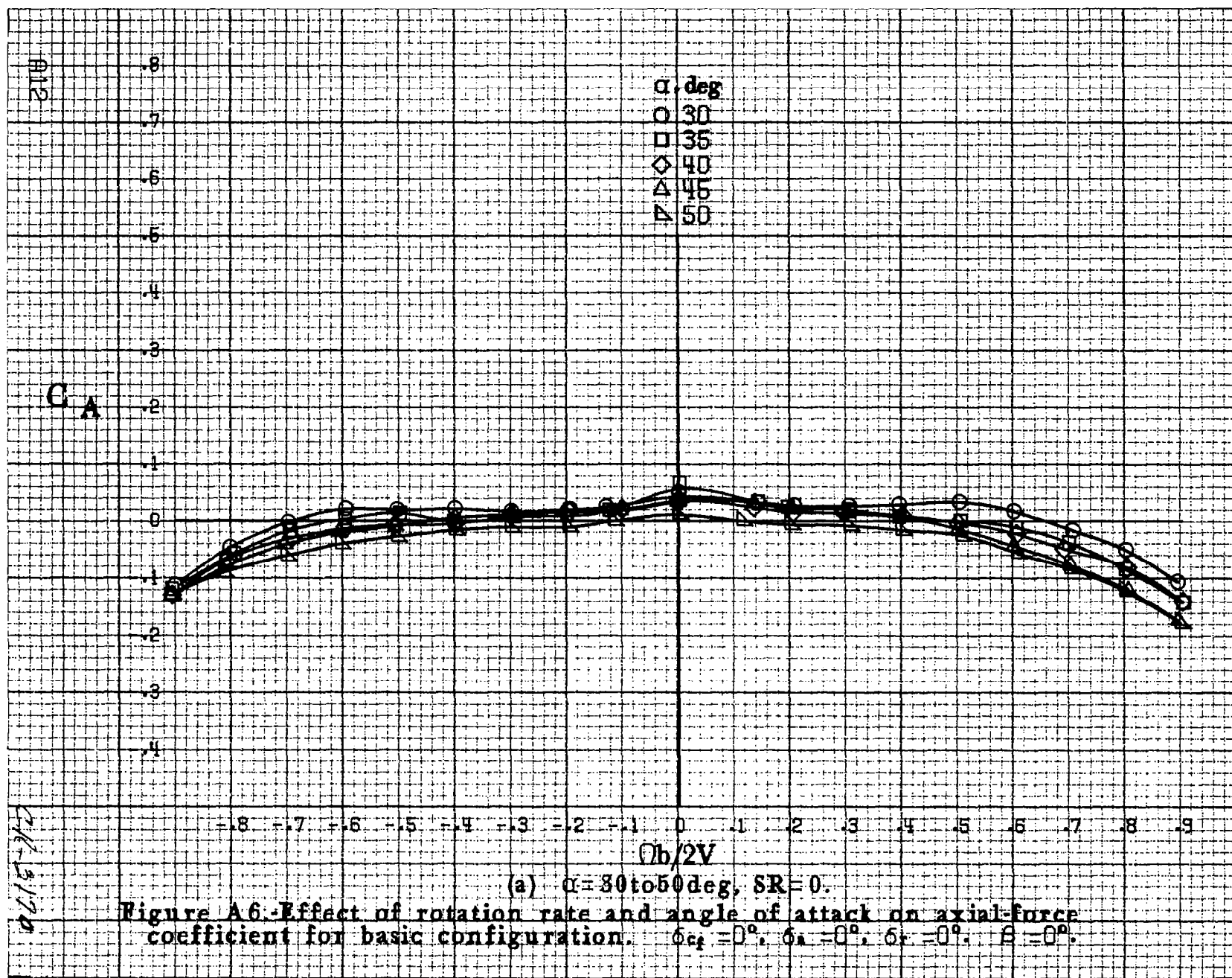


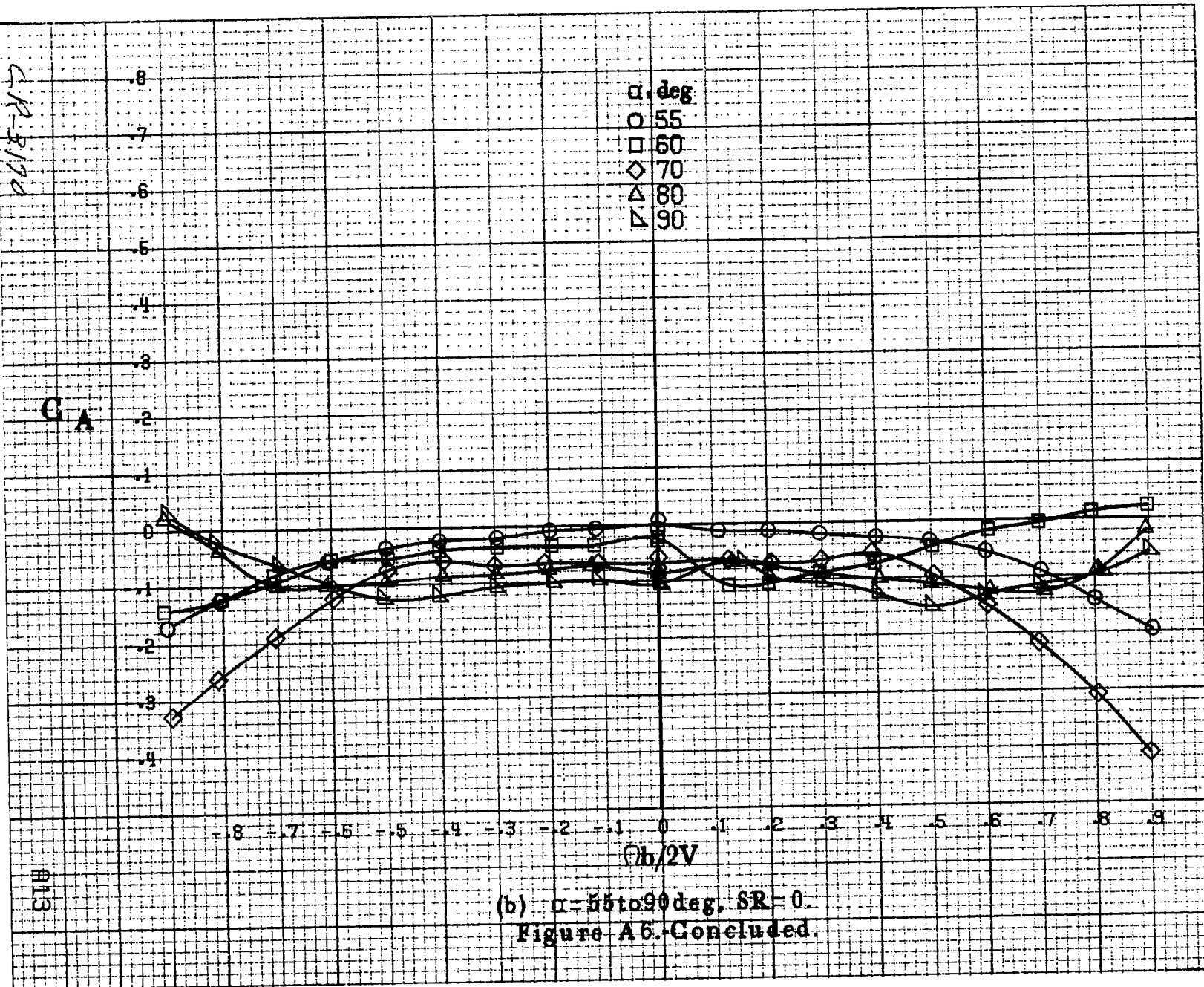


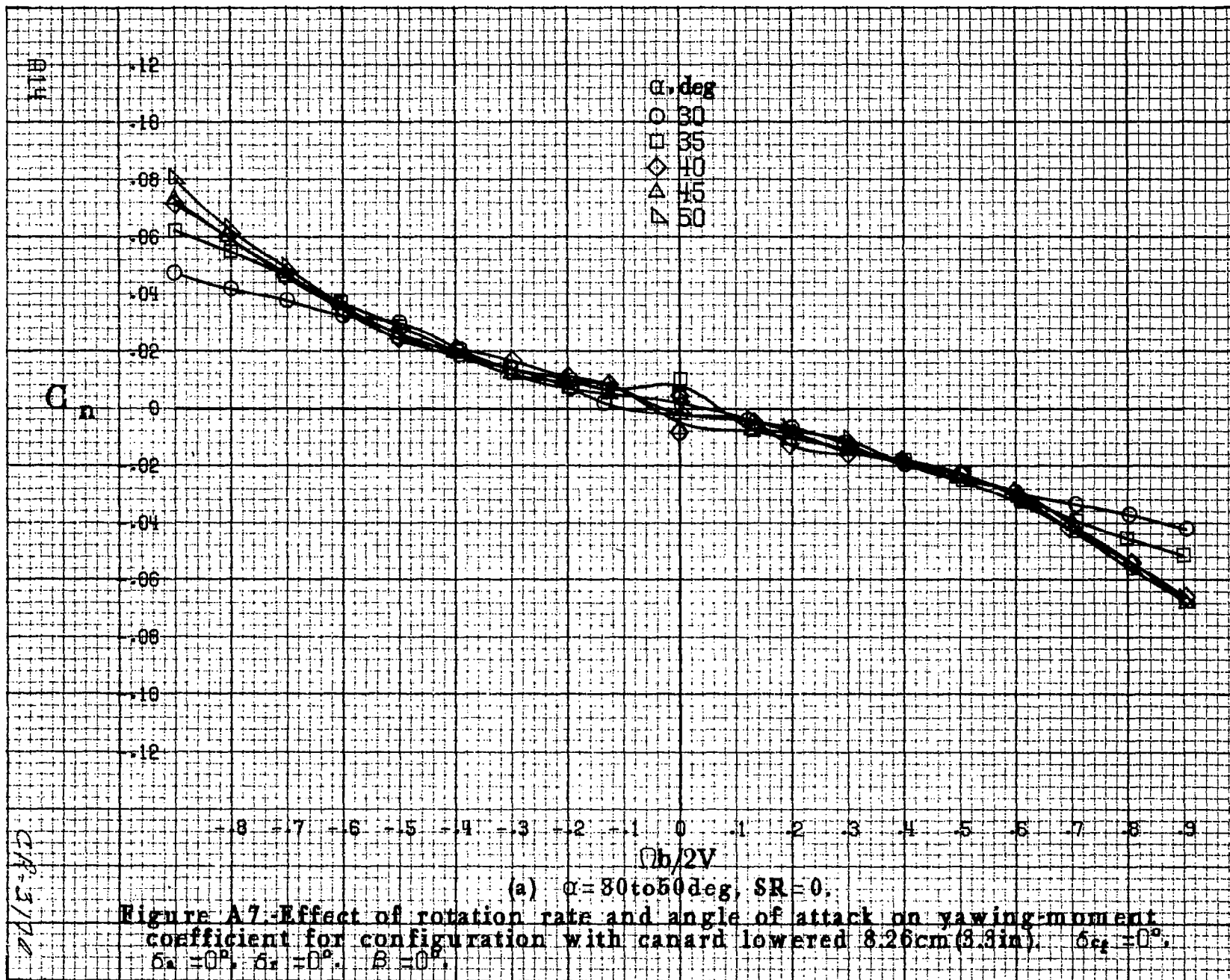






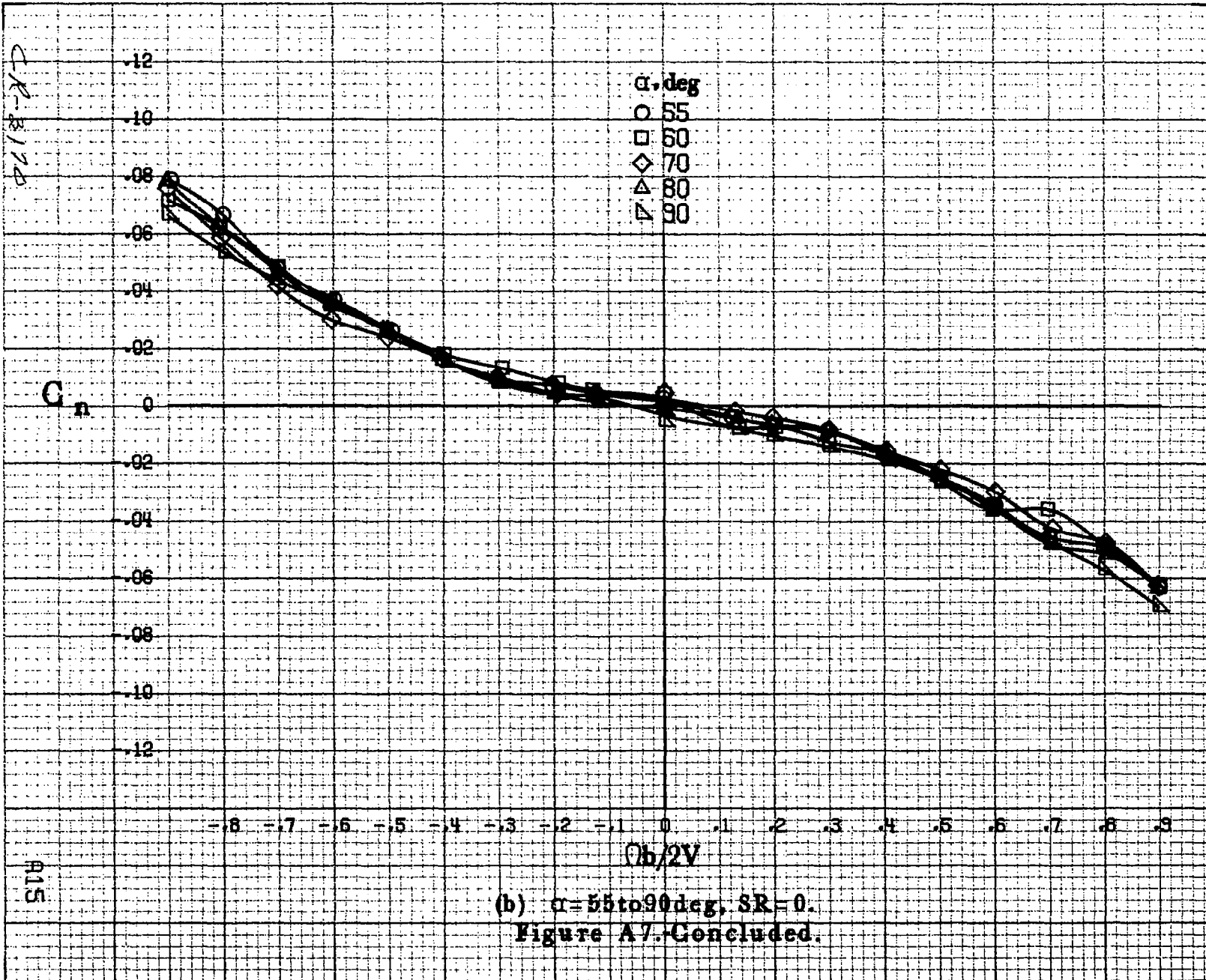


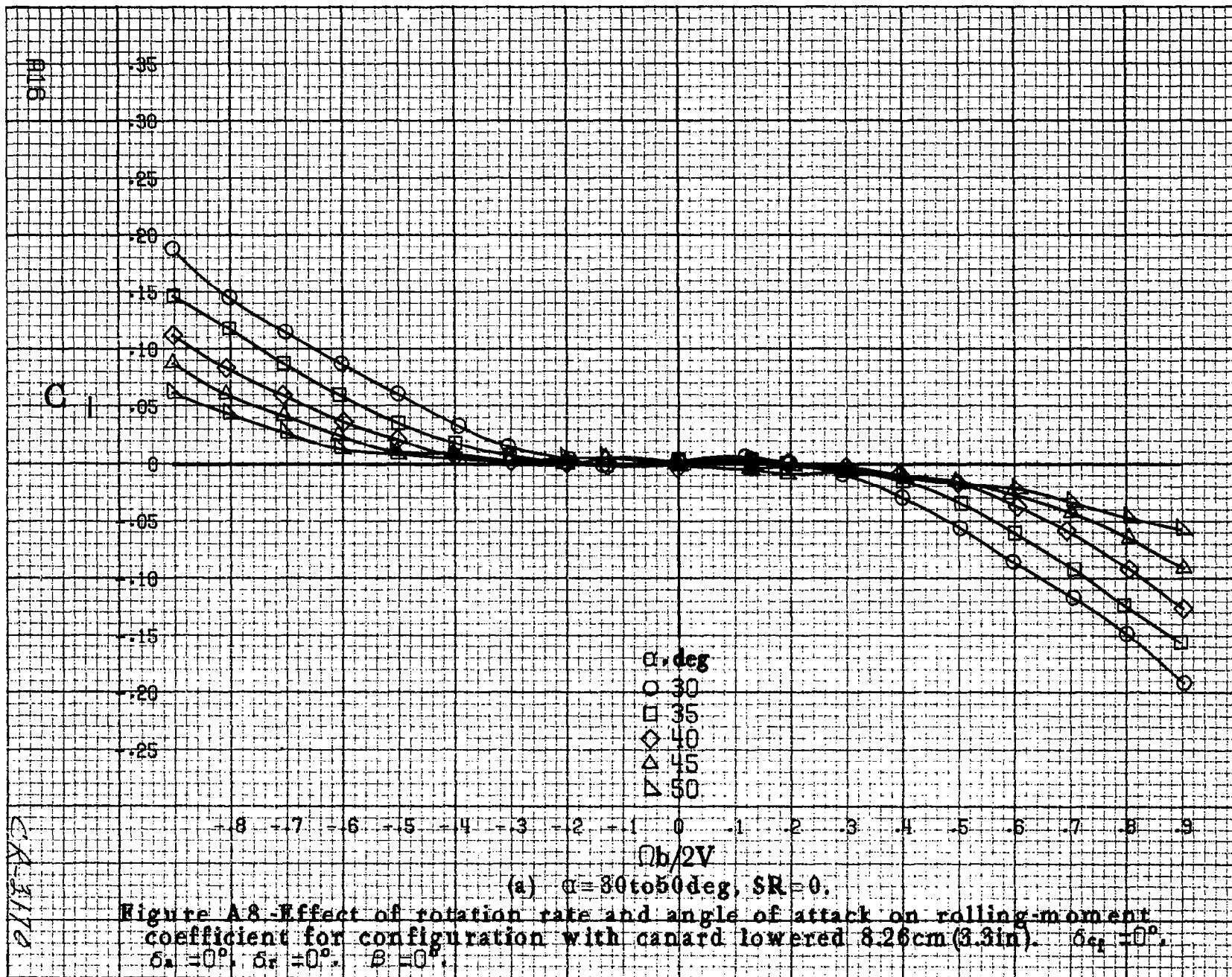


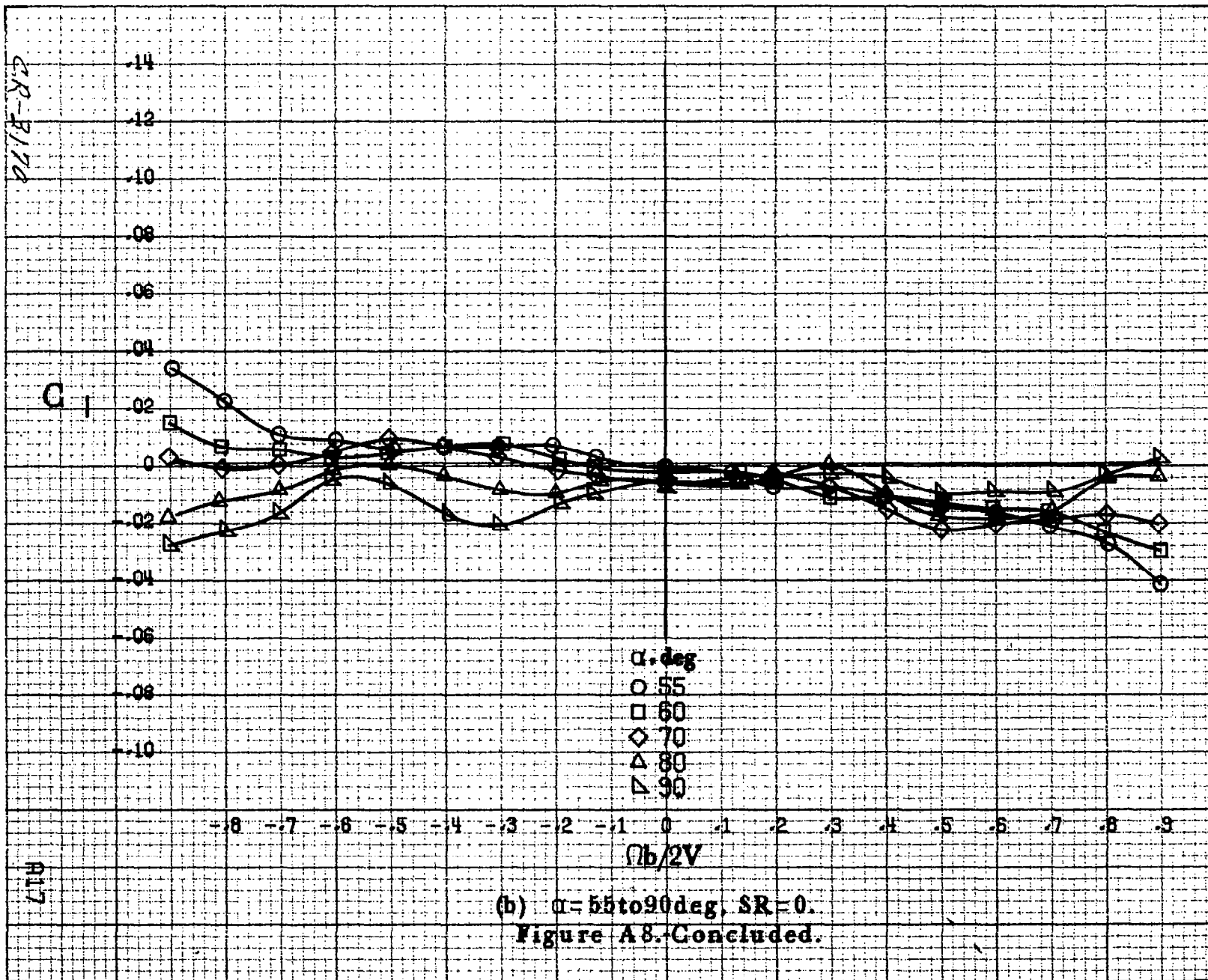


(a) $\alpha = 30$ to 50 deg, SR = 0.

Figure A7. Effect of rotation rate and angle of attack on yawing-moment coefficient for configuration with canard lowered 8.26cm(3.2in). $\delta_{ca} = 0^\circ$, $\delta_a = 0^\circ$, $\delta_r = 0^\circ$, $B = 10\%$.







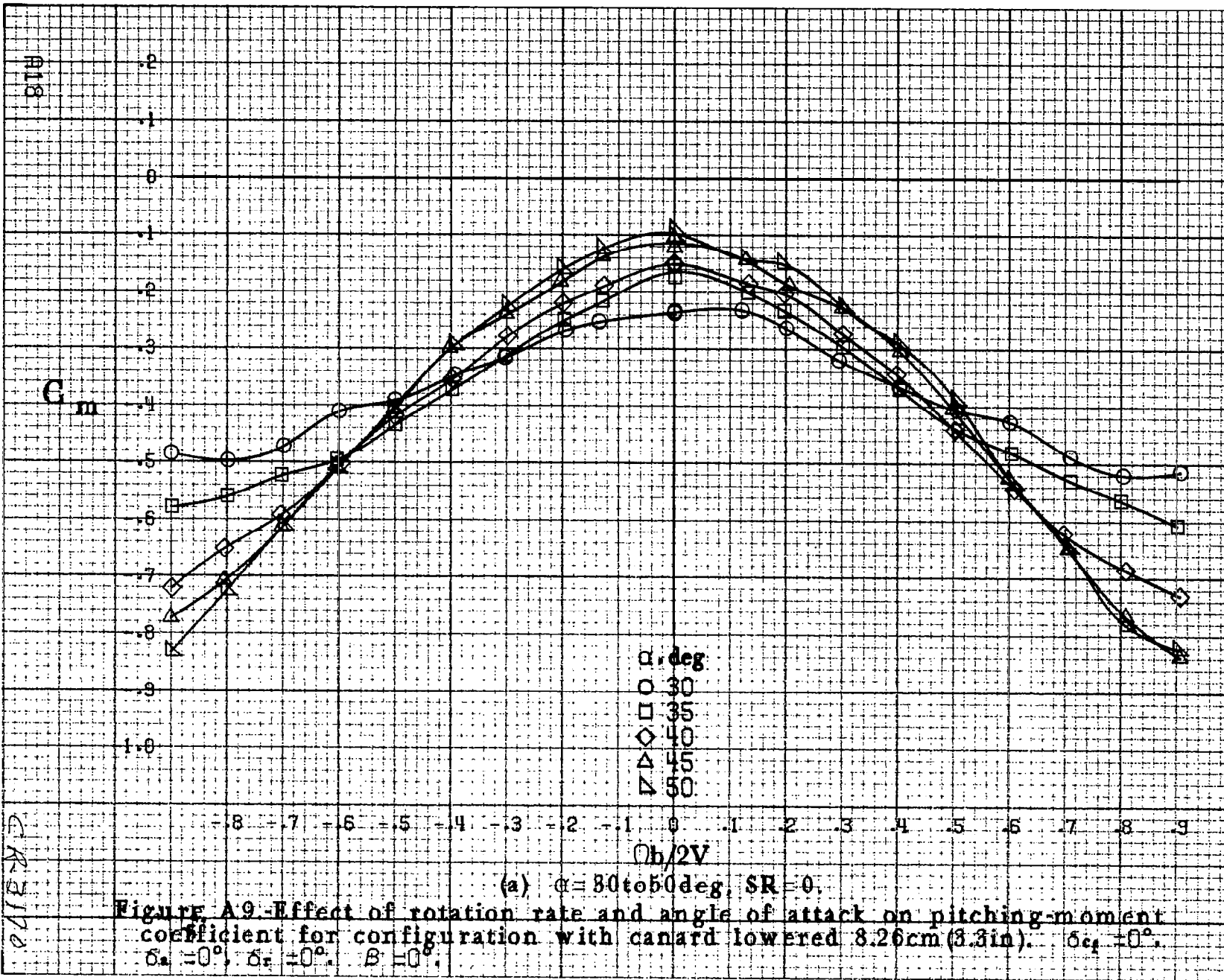


Figure A.9 -Effect of rotation rate and angle of attack on pitching-moment coefficient for configuration with canard lowered 8.26cm (3.3in). $\delta_{ca} = 0^\circ$, $\delta_r = 0^\circ$, $B = 0^\circ$.

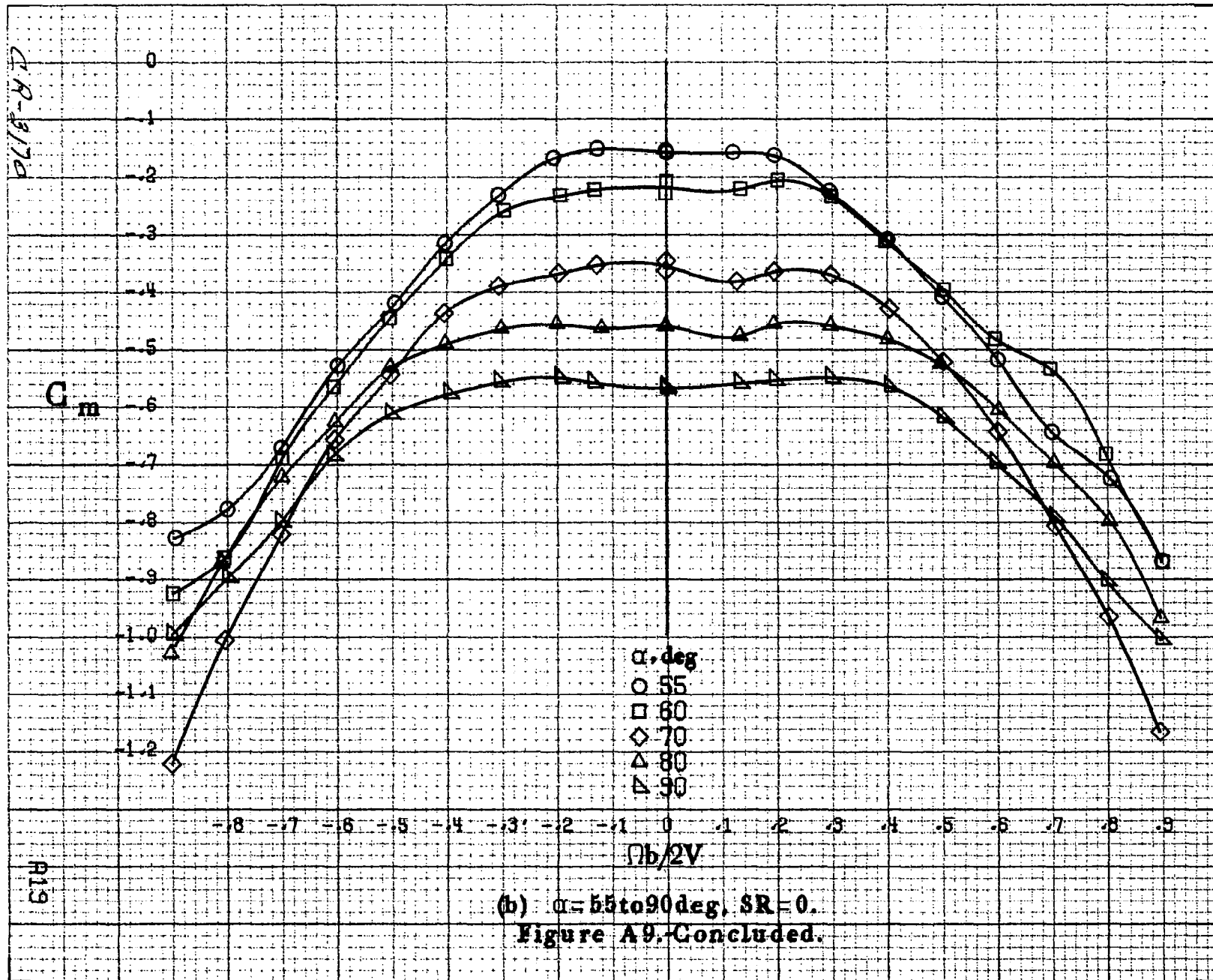
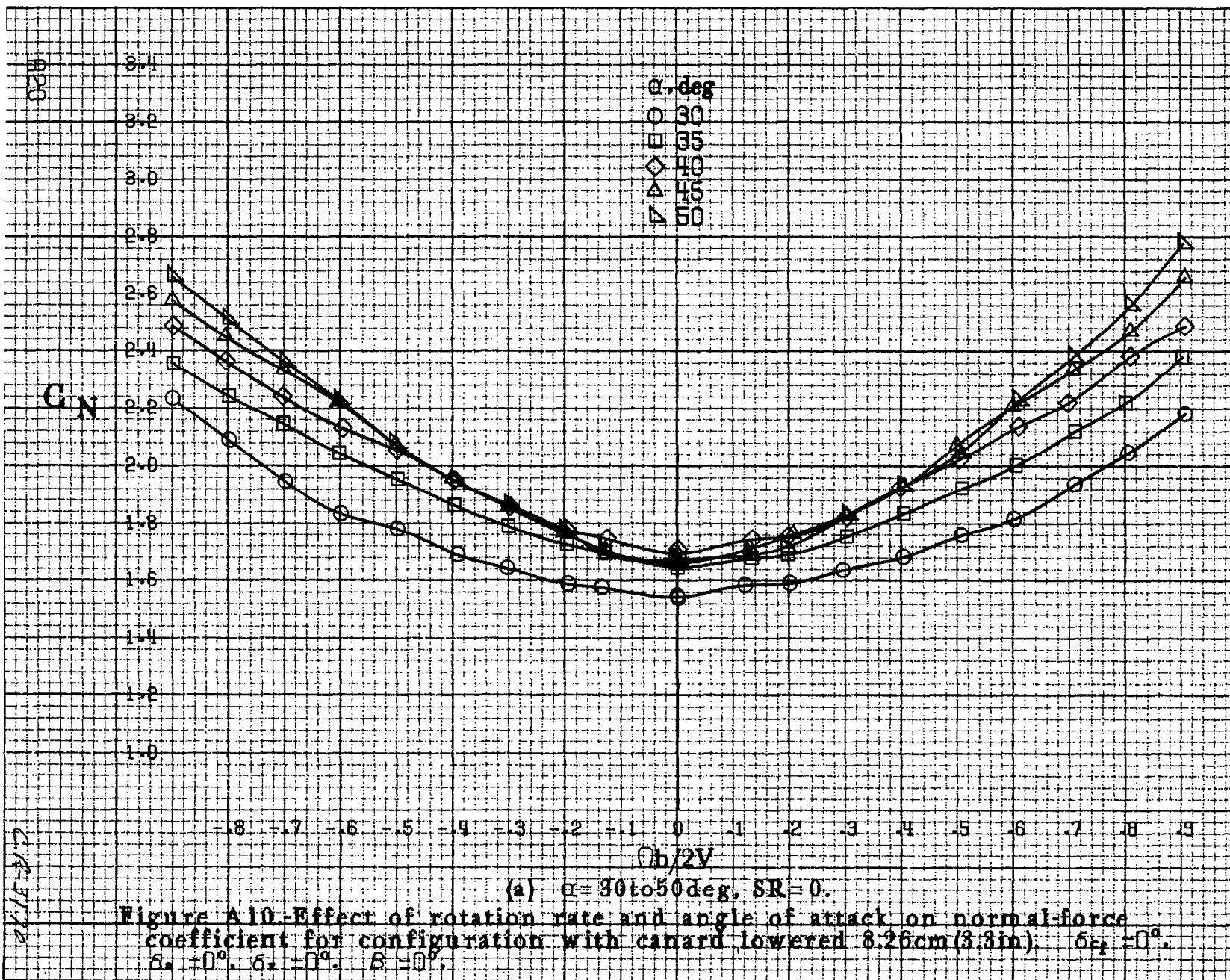
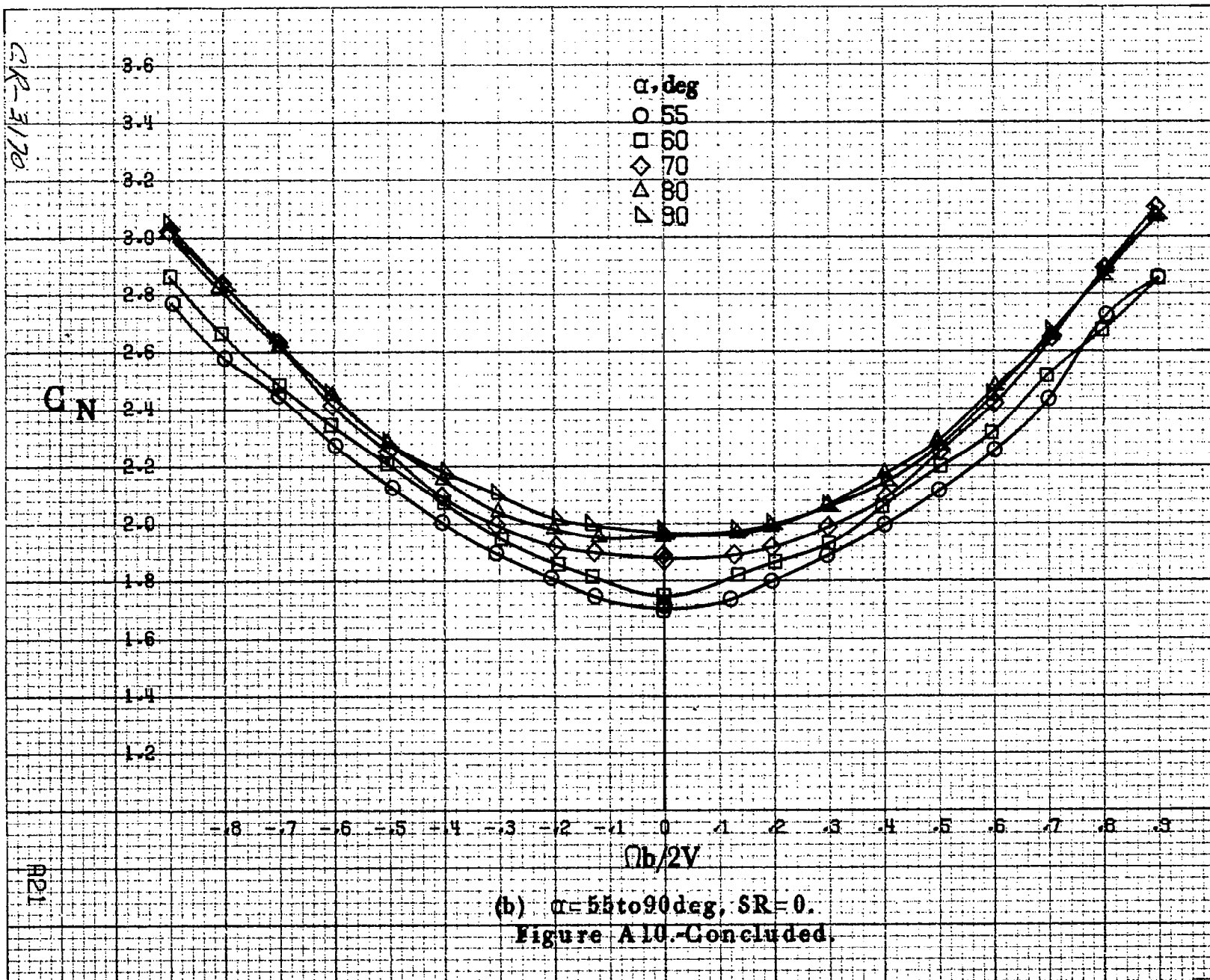
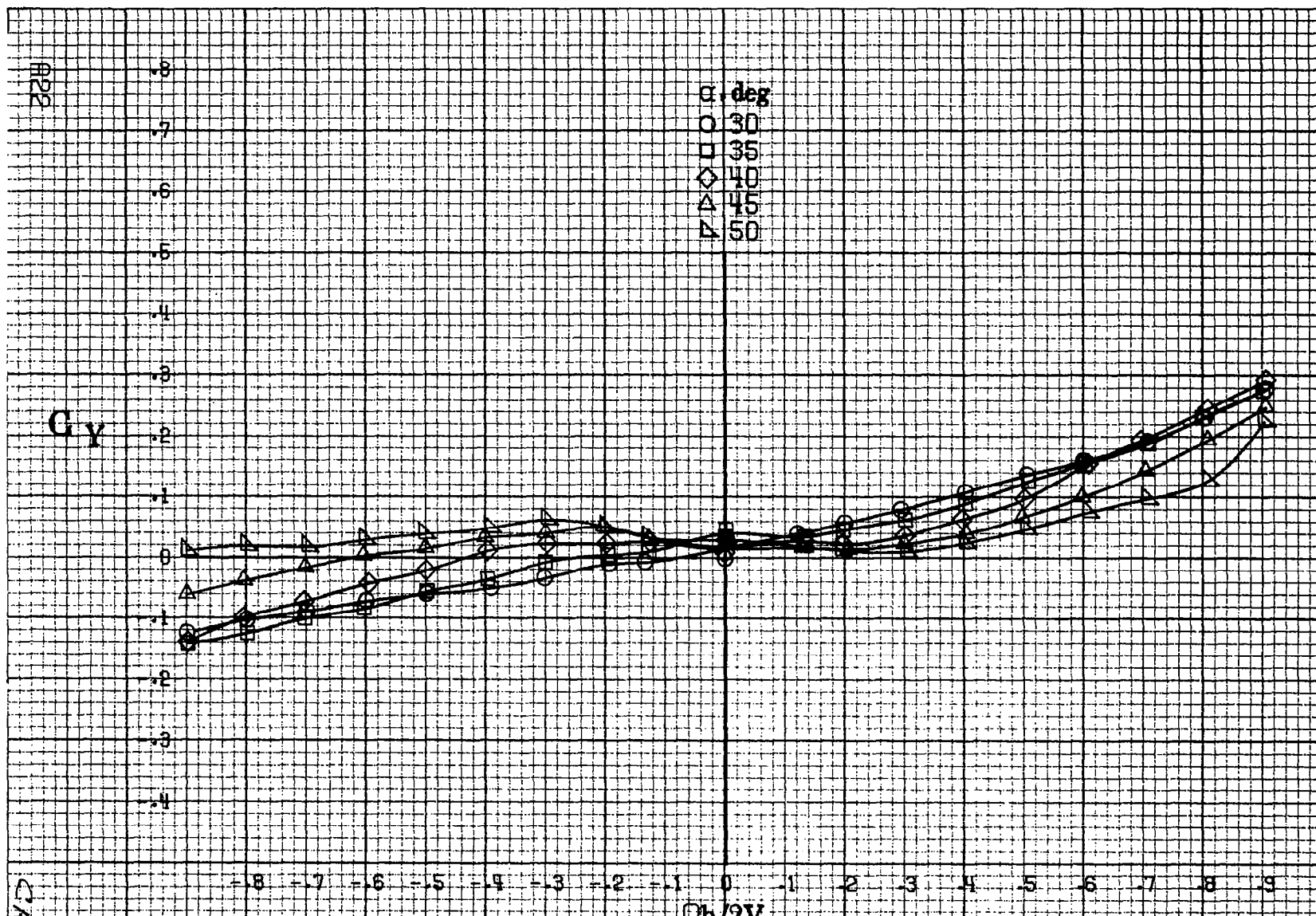


Figure A9. Concluded.

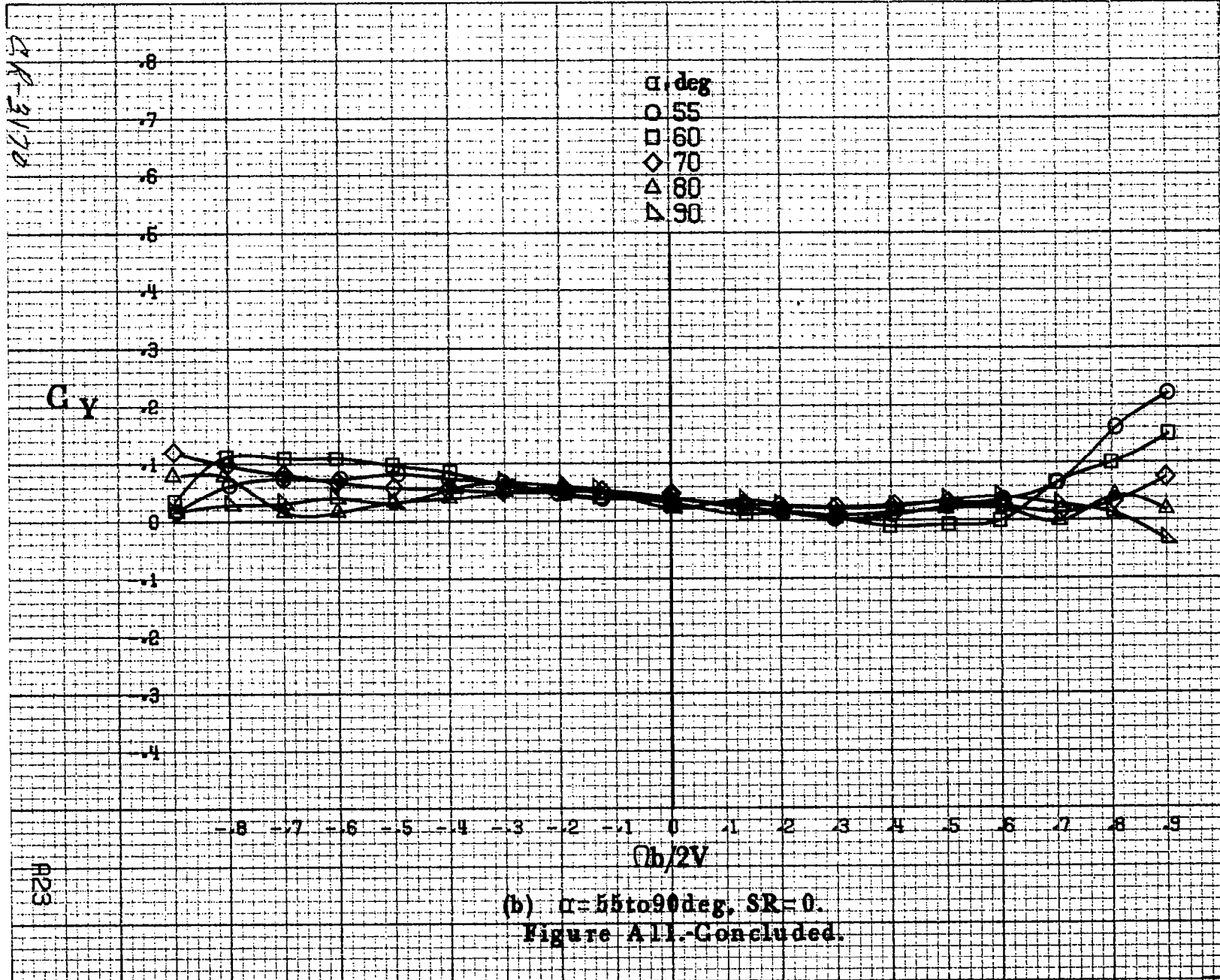


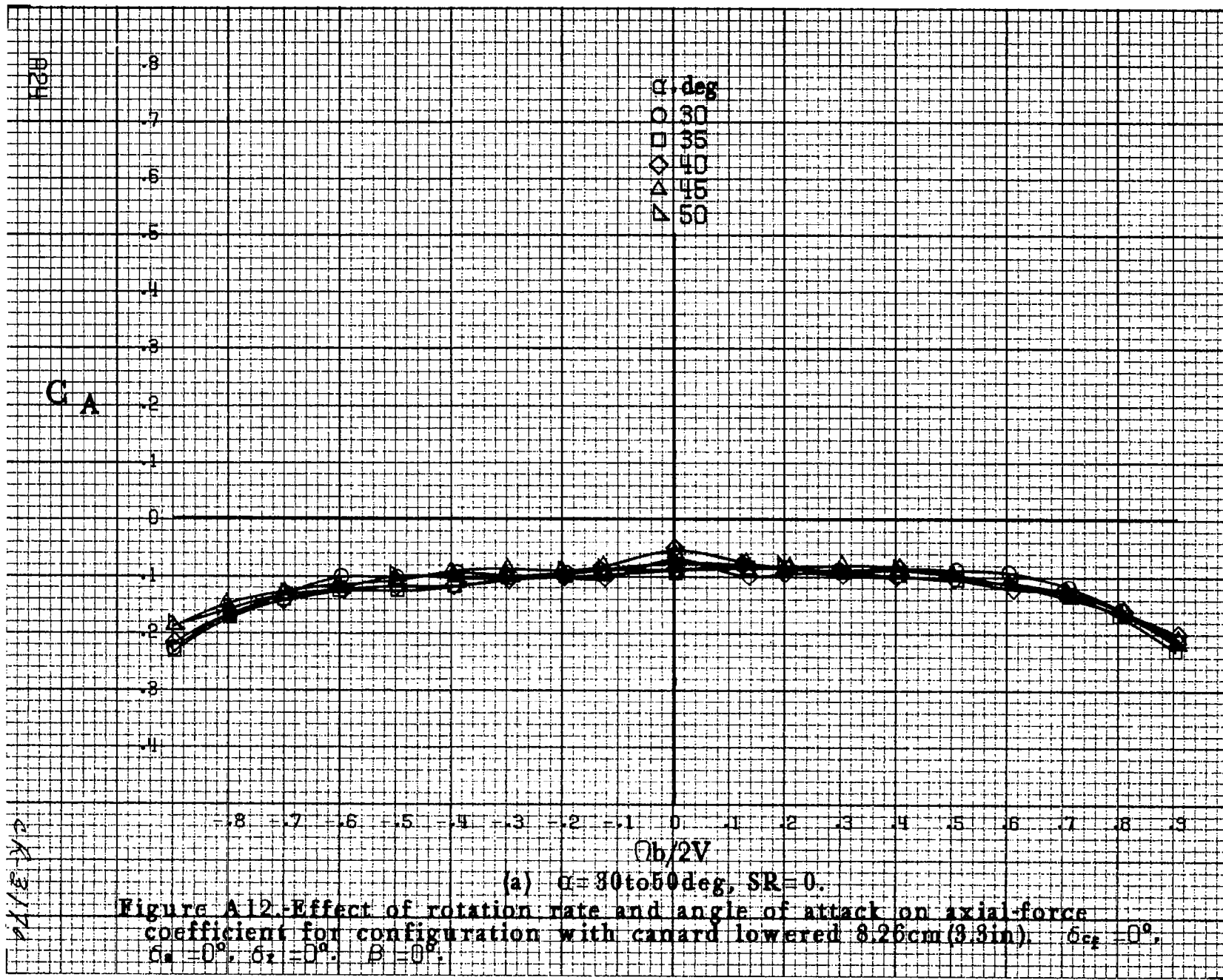




(a) $\alpha = 30$ to 50 deg, SR = 0.

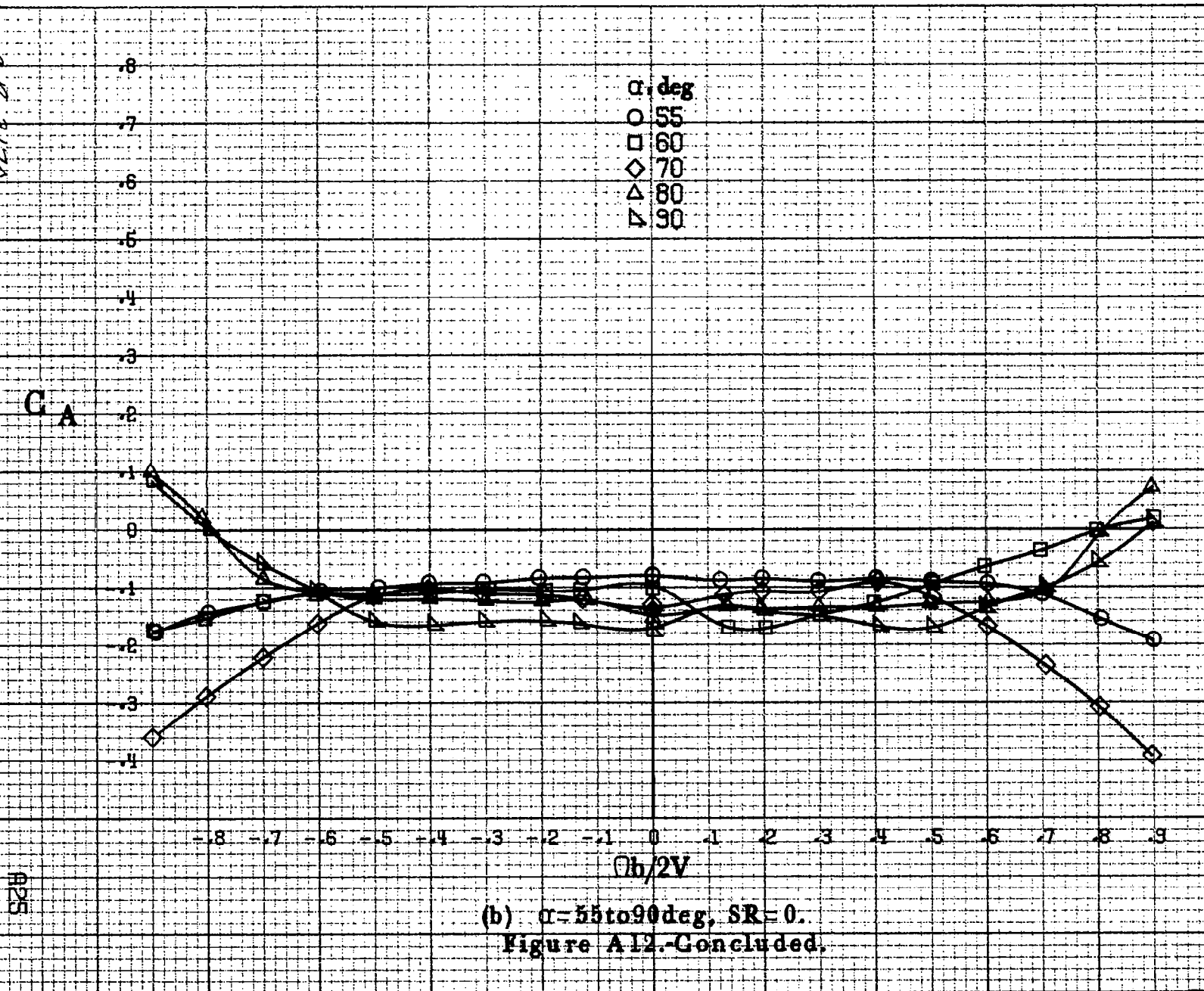
Figure A11 -Effect of rotation rate and angle of attack on side-force coefficient for configuration with canard lowered 8.26cm (3.3in). $\delta_{rf} = 0^\circ$, $\delta_a = 0^\circ$, $\delta_r = 0^\circ$, $B = 0^\circ$.





24-3/12

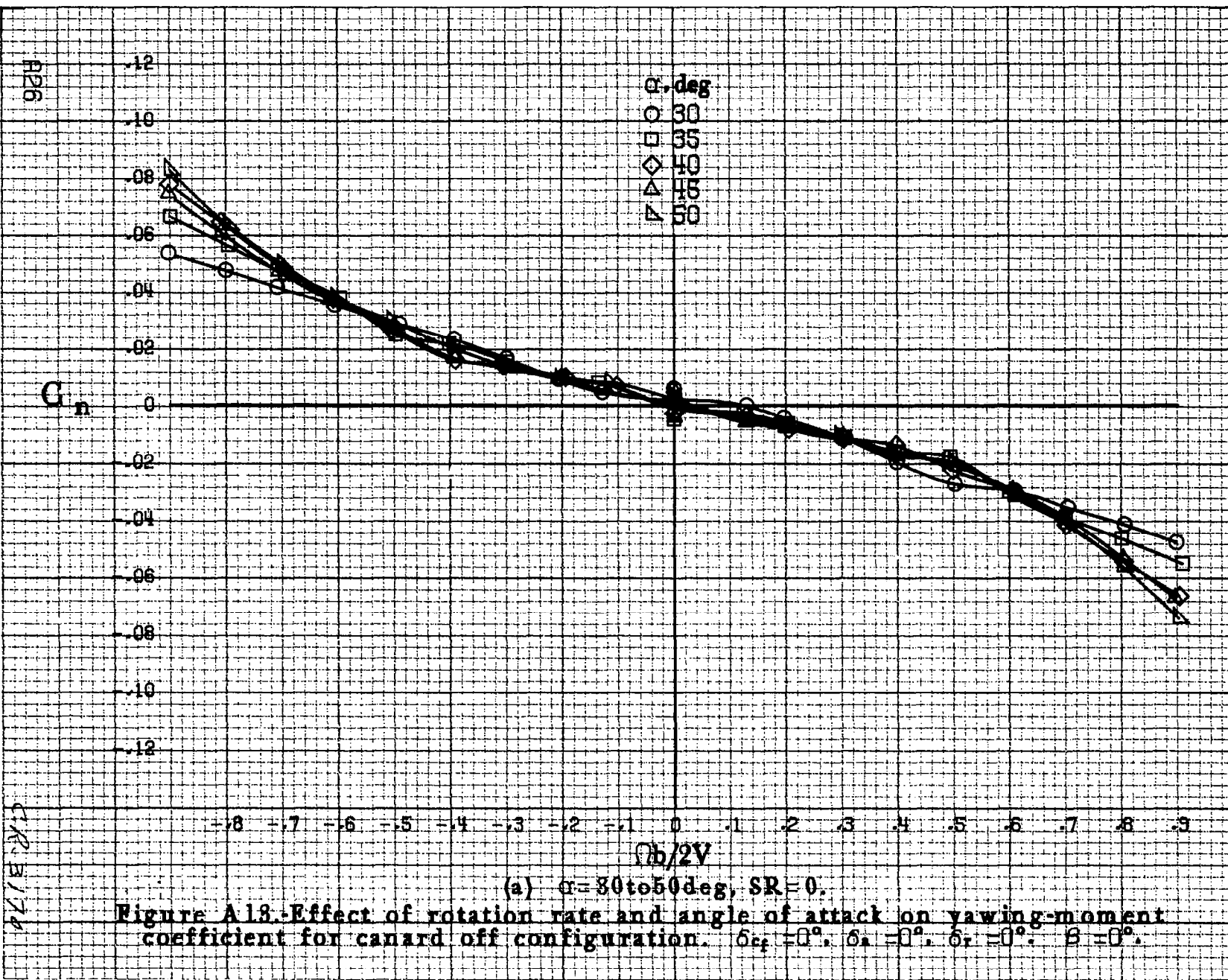
C A

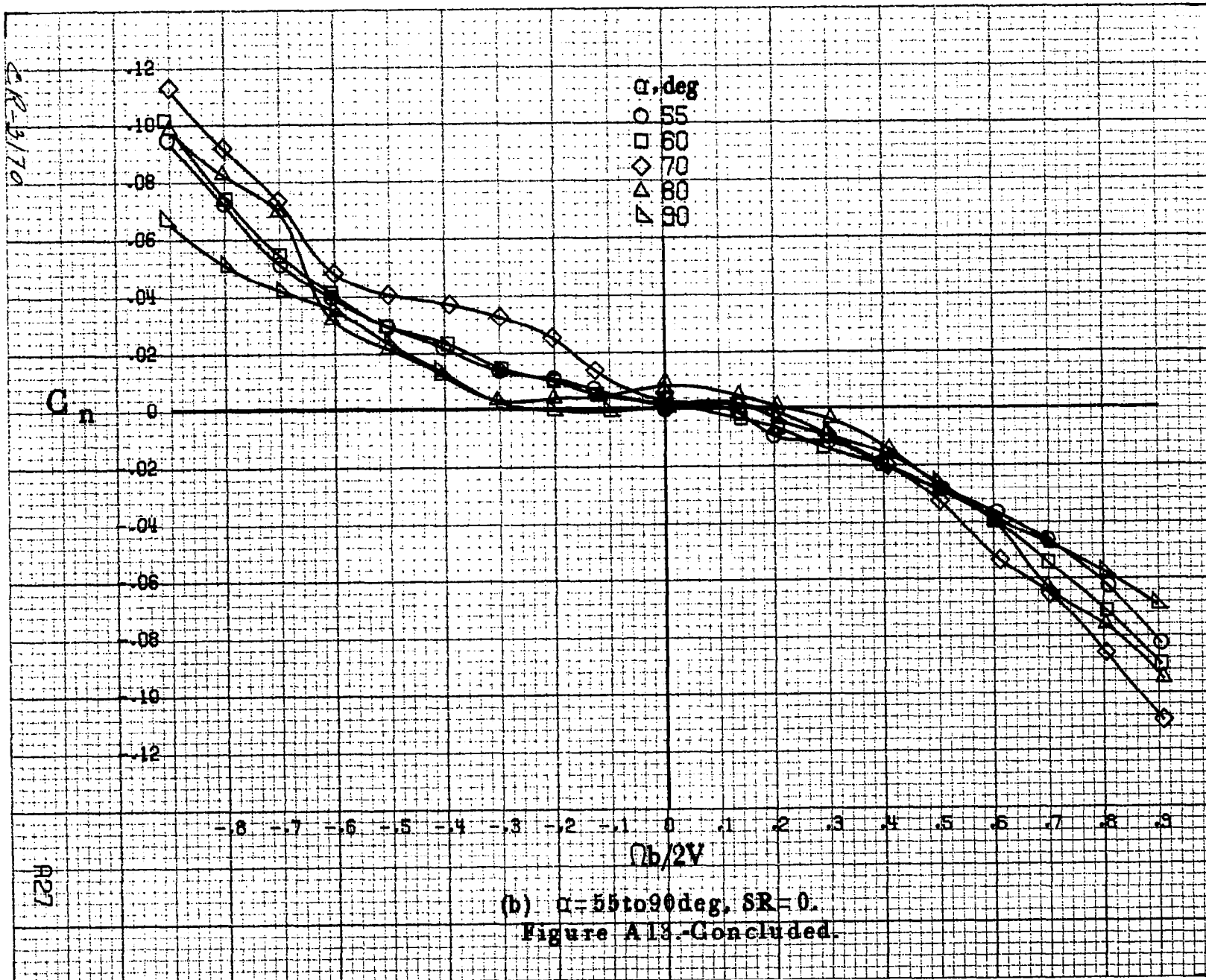


(b) $\alpha=55$ to 90 deg, SR = 0.

Figure A12-Concluded.

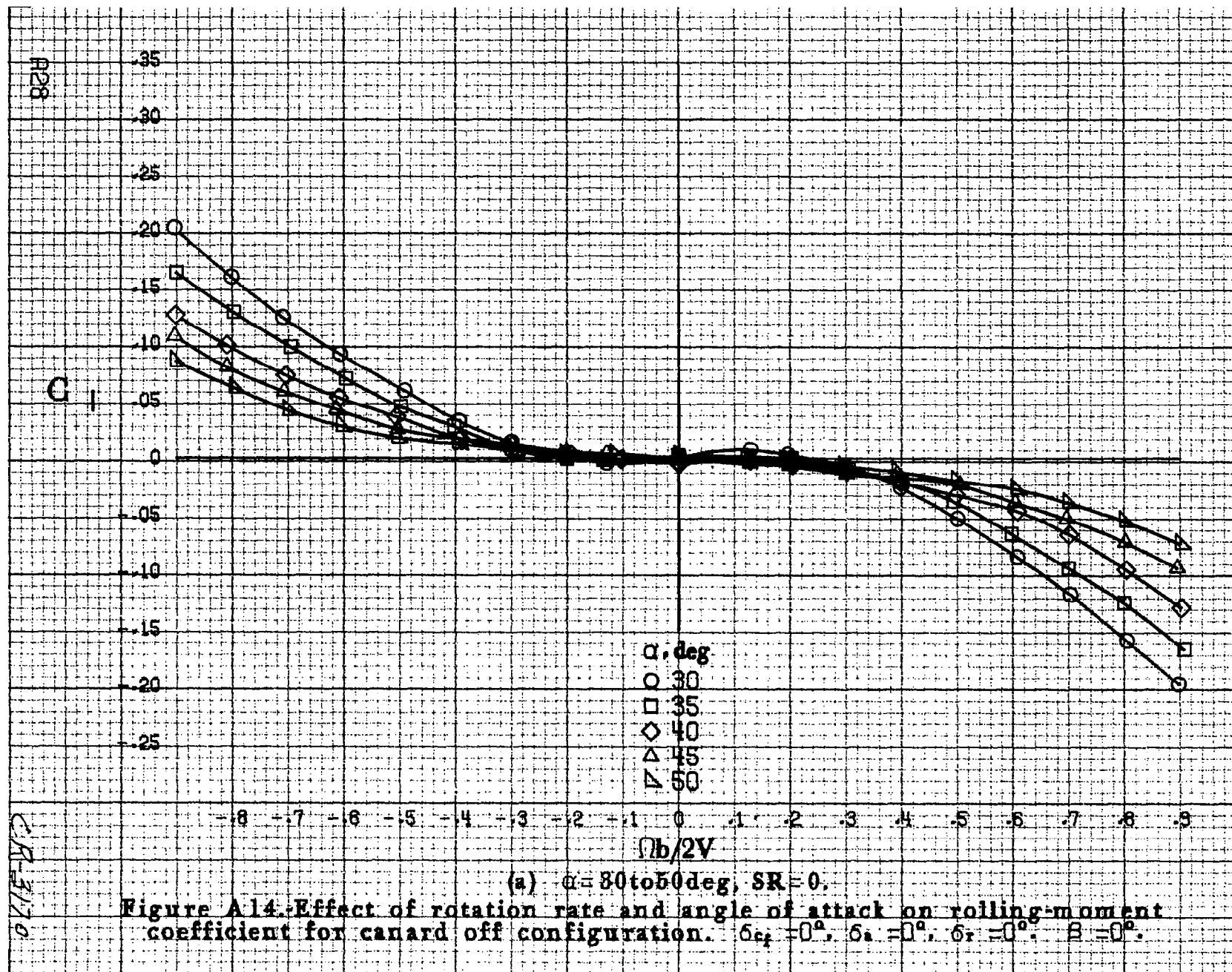
B25

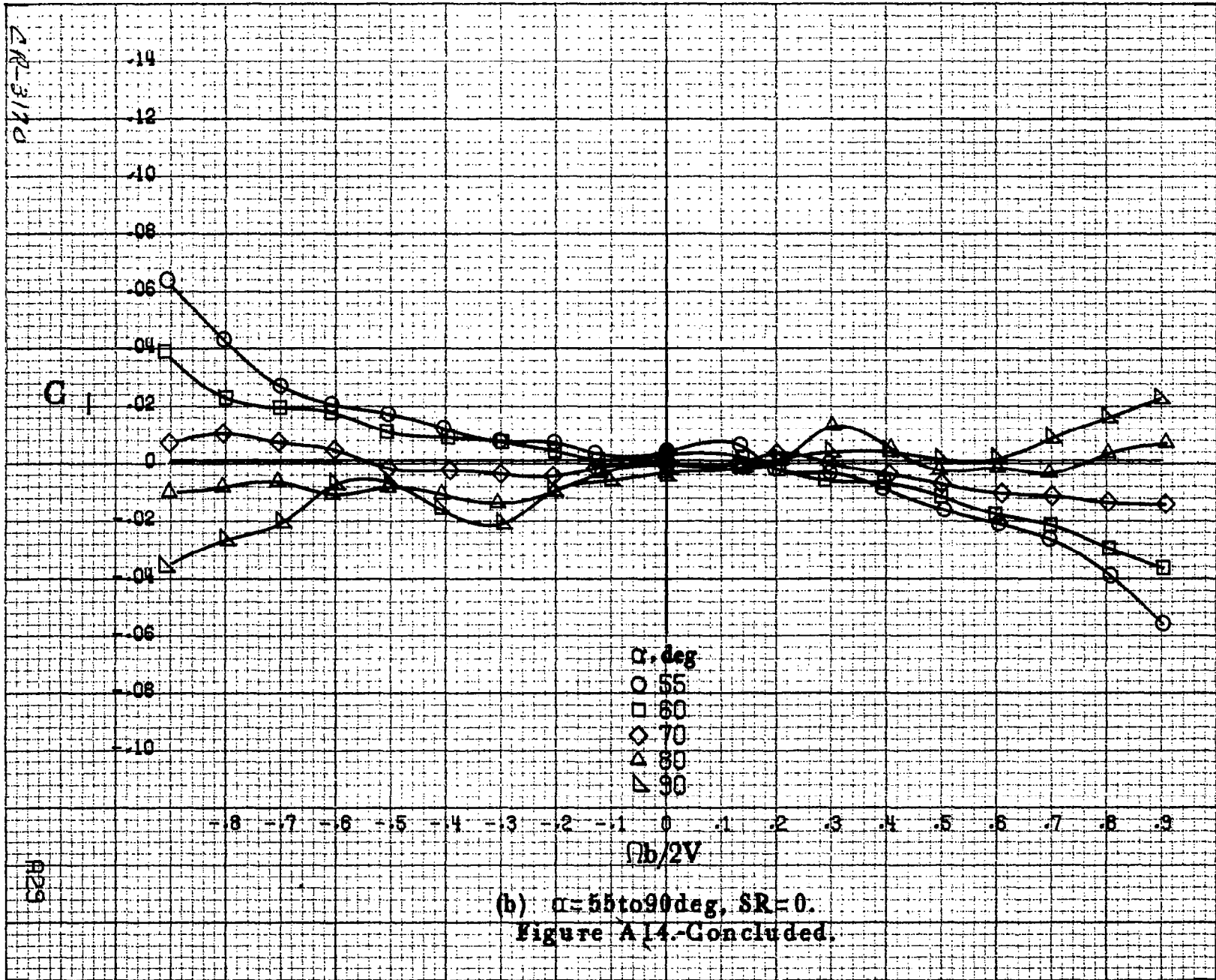


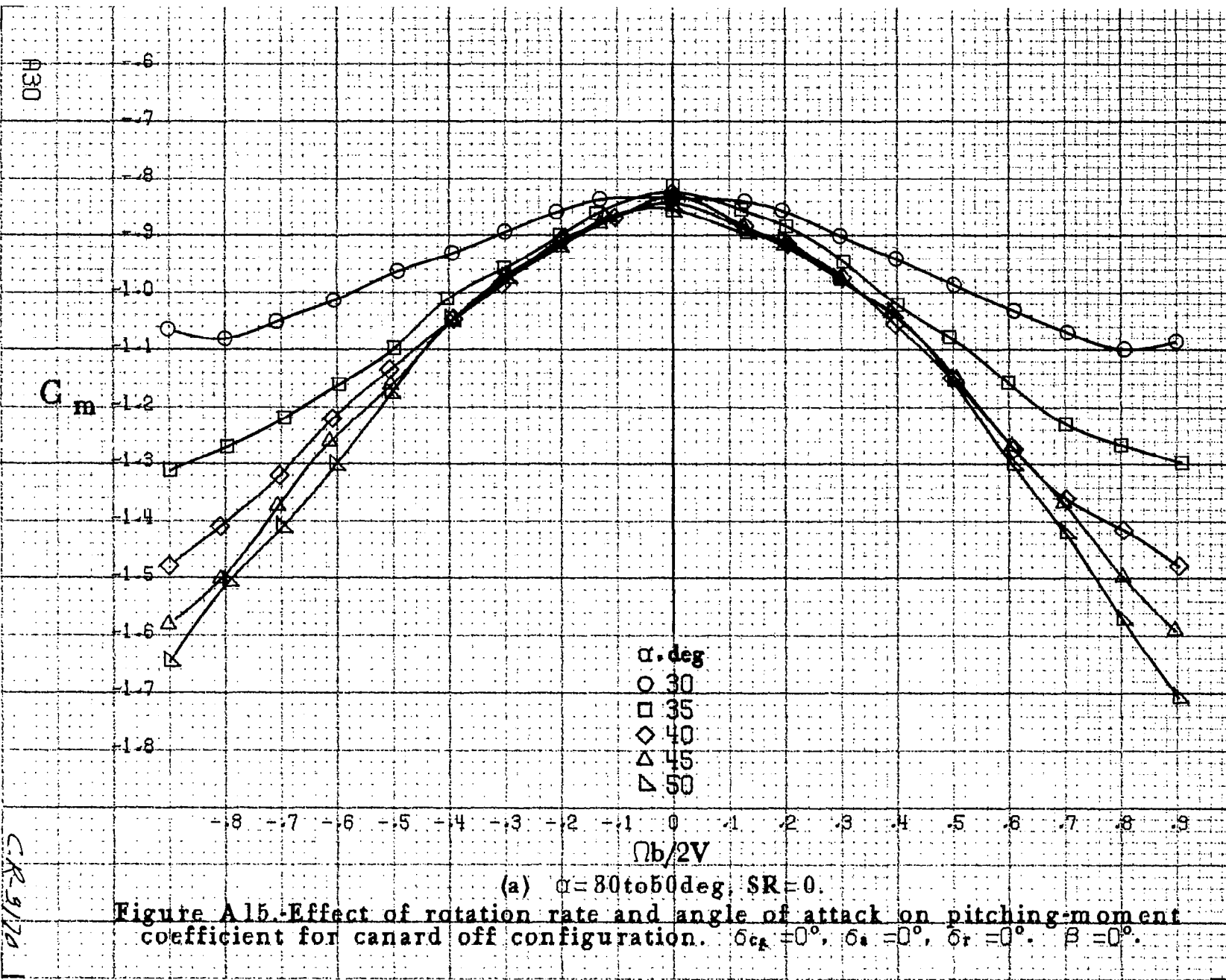


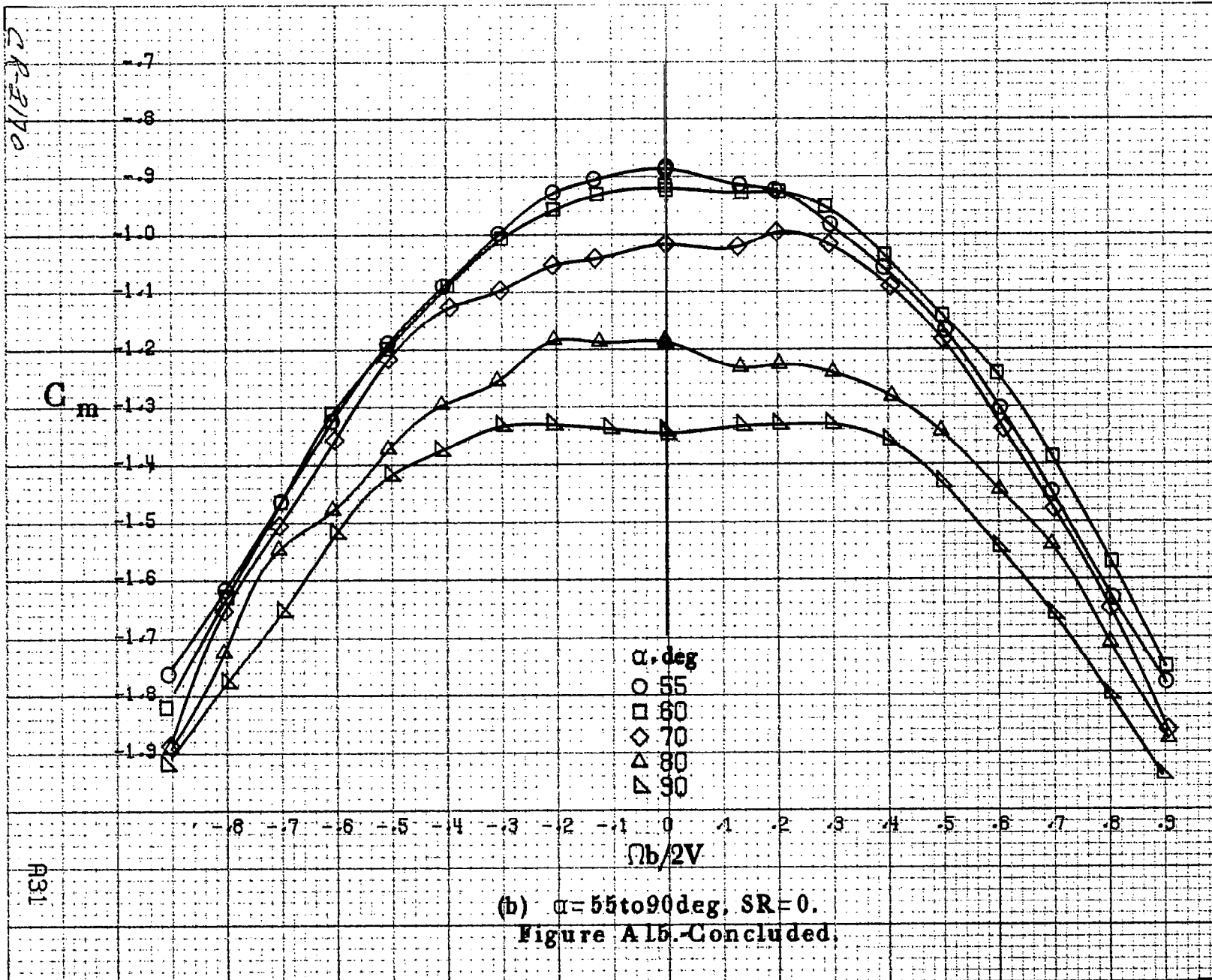
(b) $\alpha=55\text{to}90\deg$, SR=0.

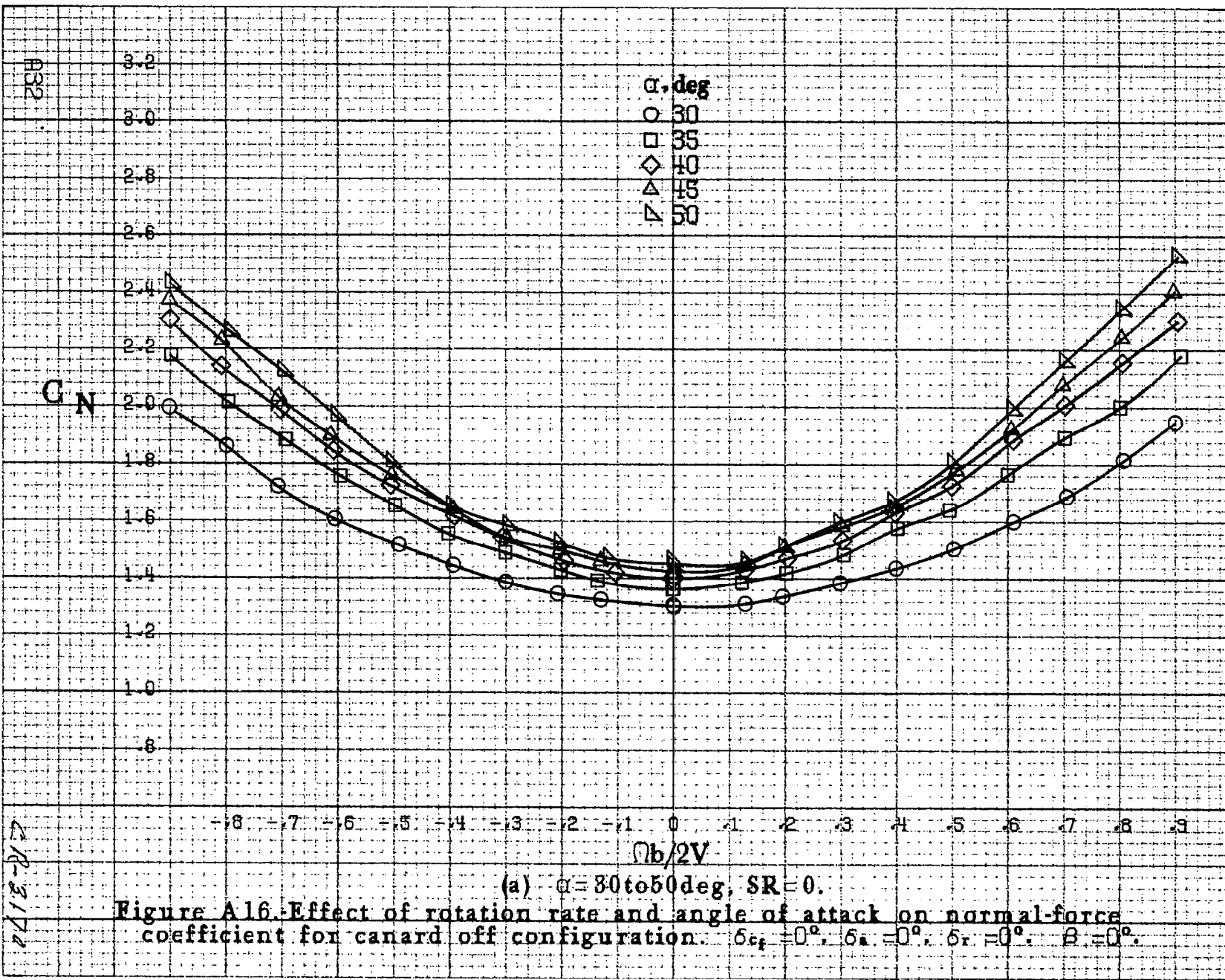
Figure A13.-Concluded.

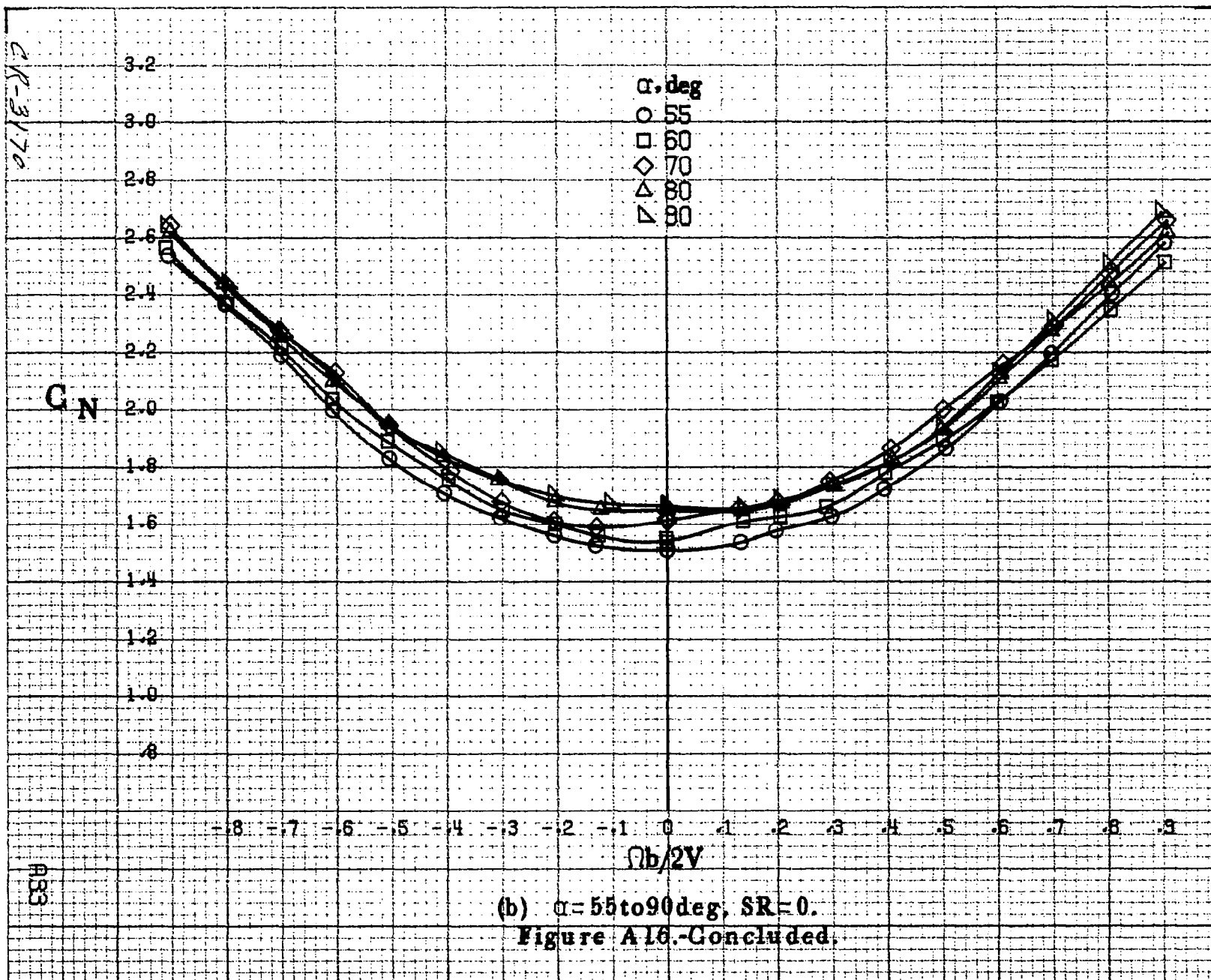


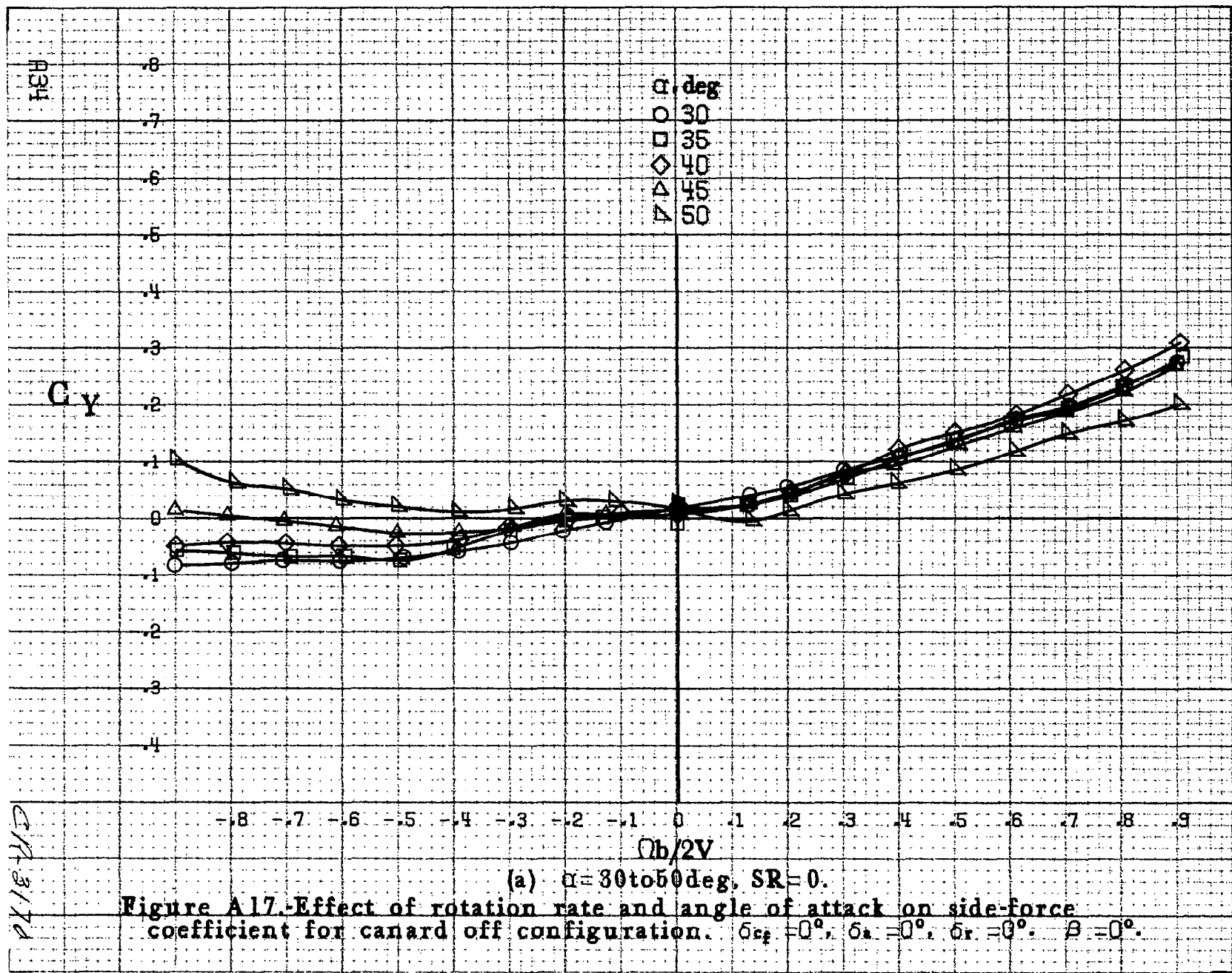


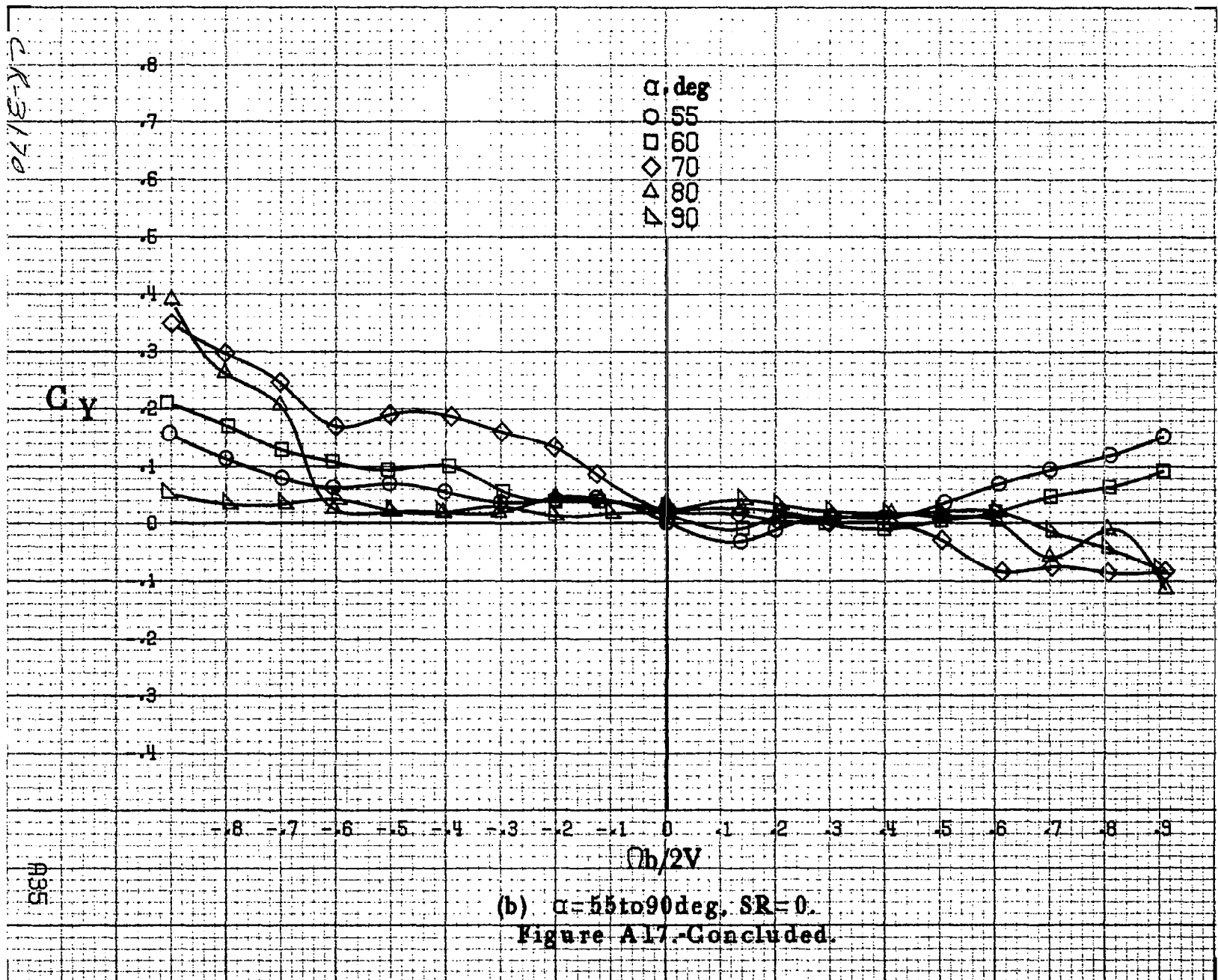












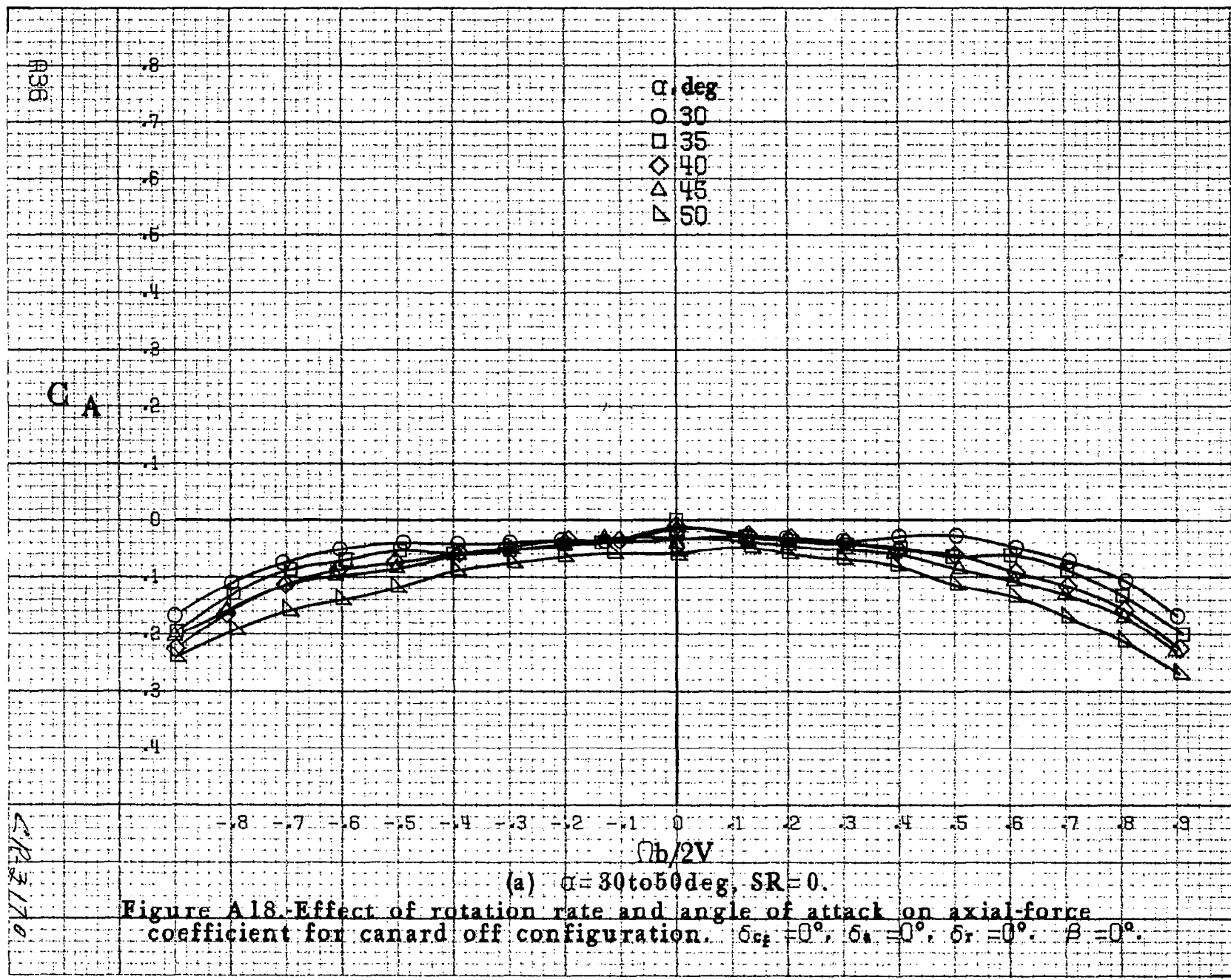
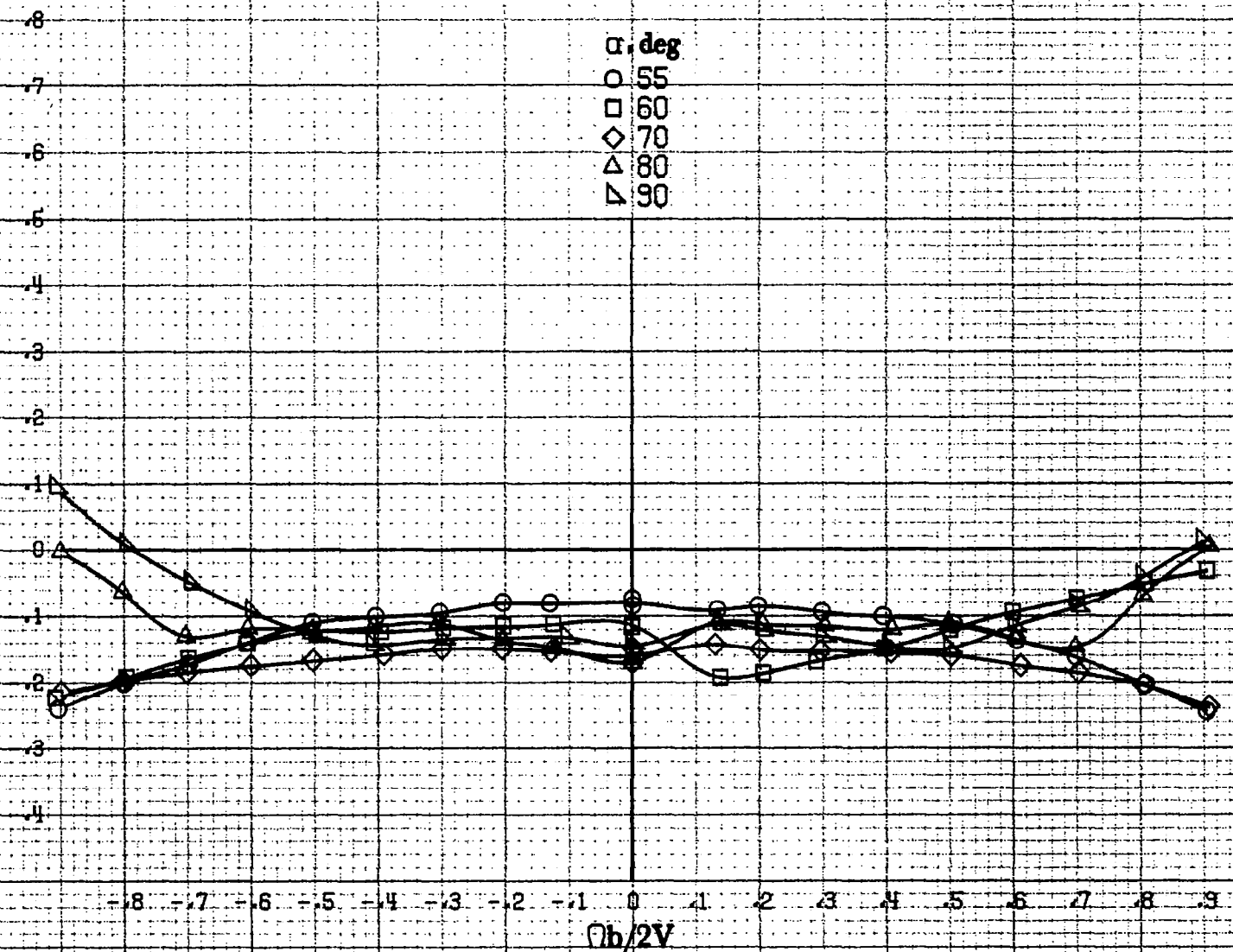


Figure A18. Effect of rotation rate and angle of attack on axial-force coefficient for canard off configuration. $\delta_{c1} = 0^\circ$, $\delta_c = 0^\circ$, $\delta_r = 0^\circ$, $B = 0^\circ$.

CR-3170

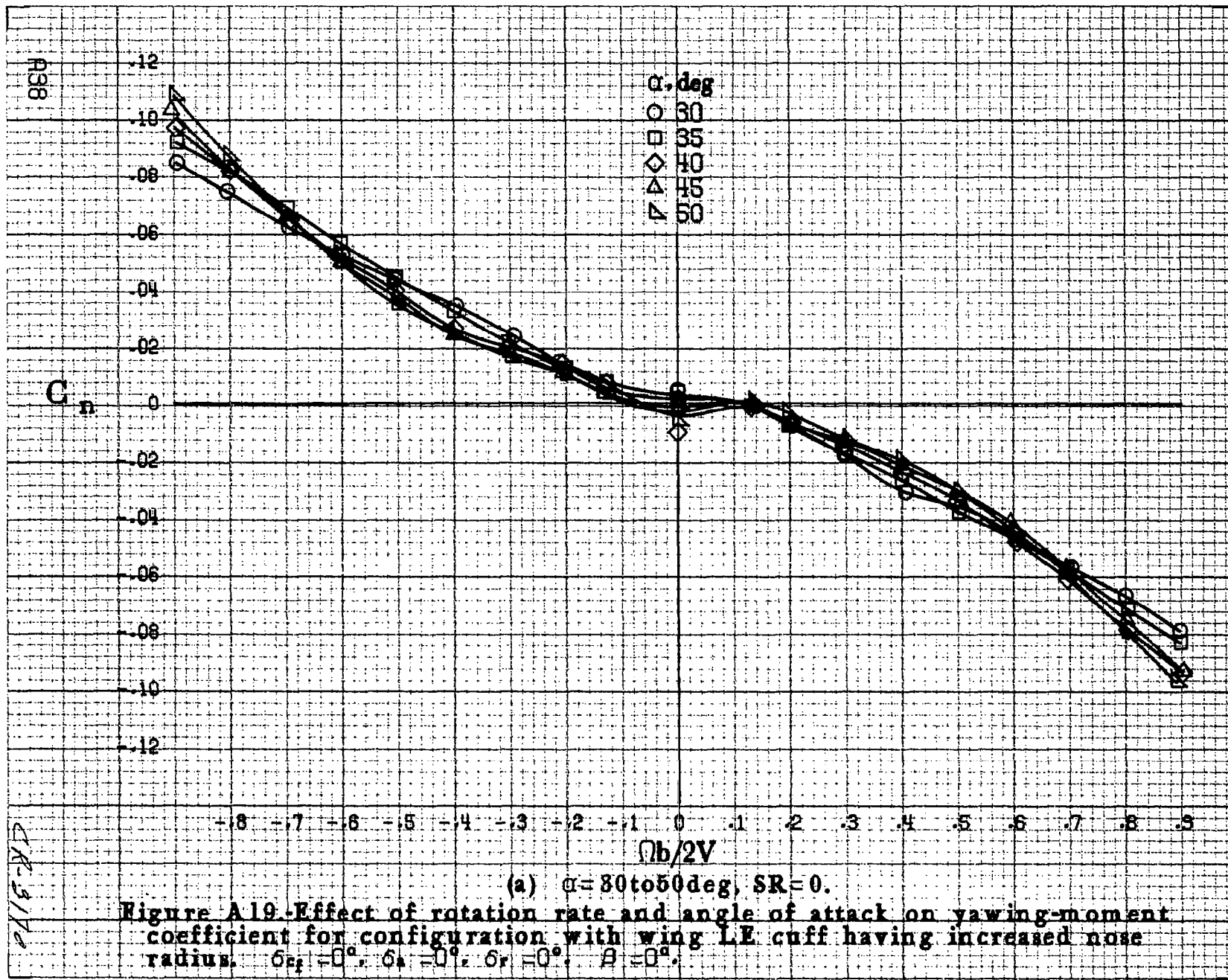
C A

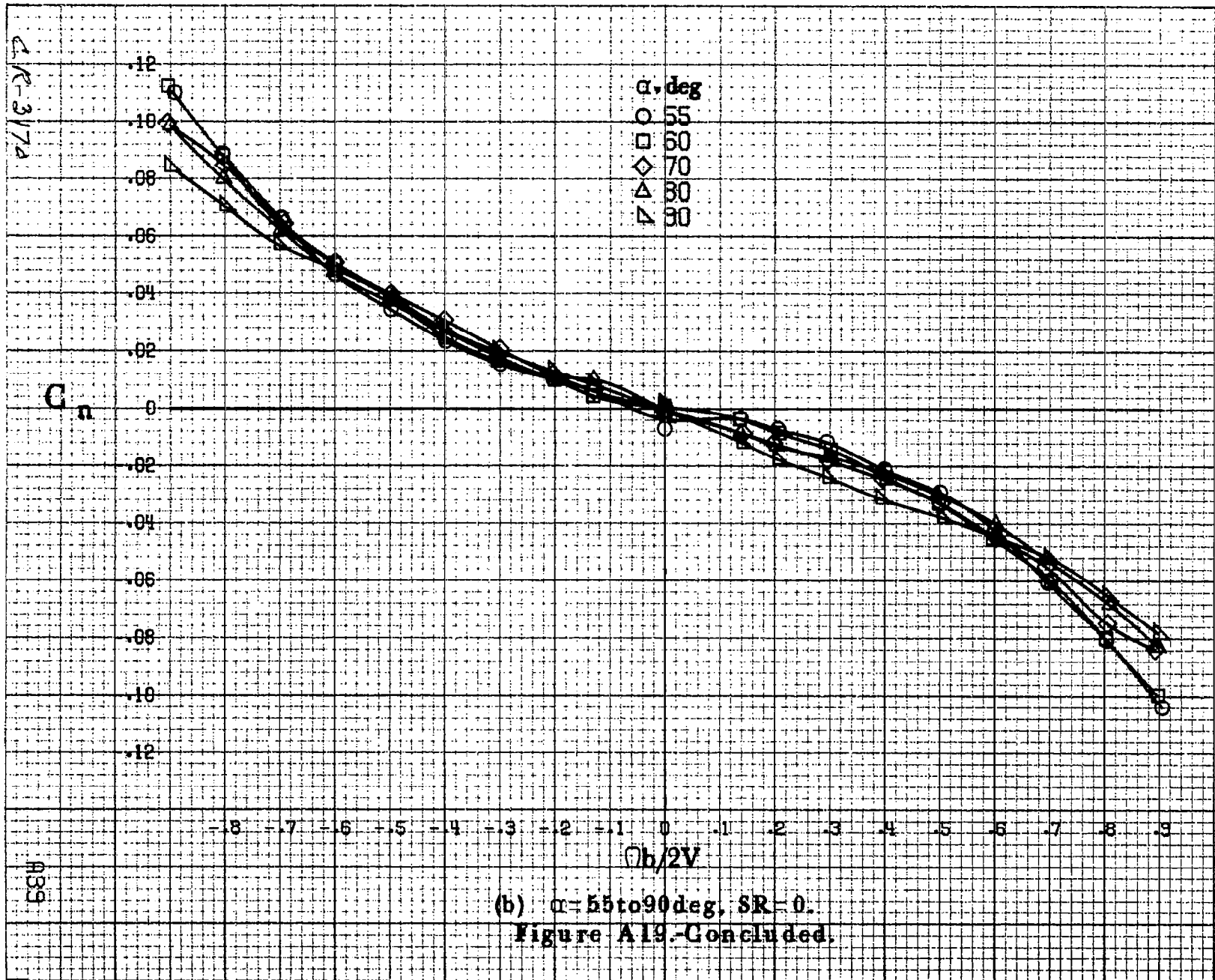
P37



(b) $\alpha = 55$ to 90 deg, SR = 0.

Figure A1d-Concluded.





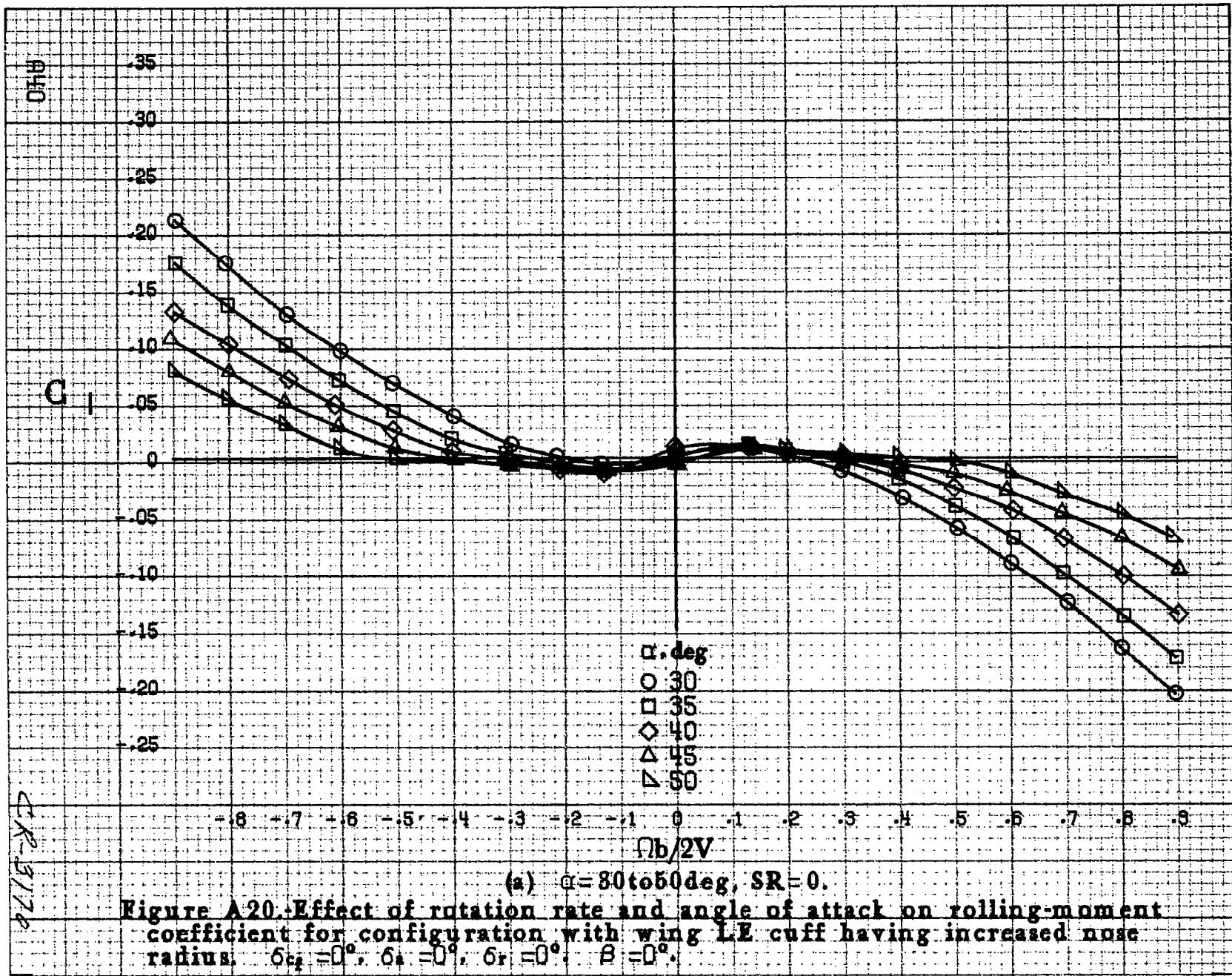
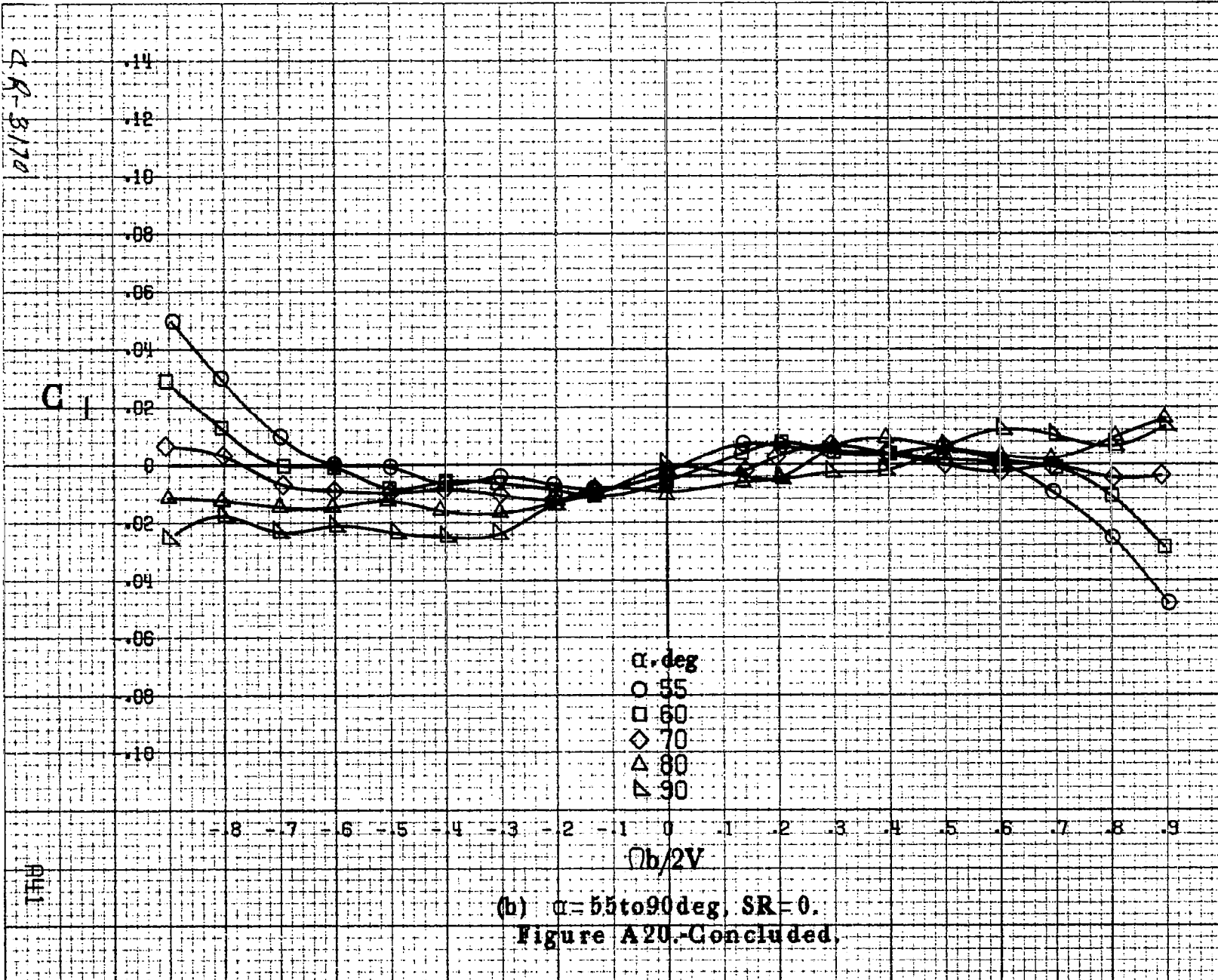
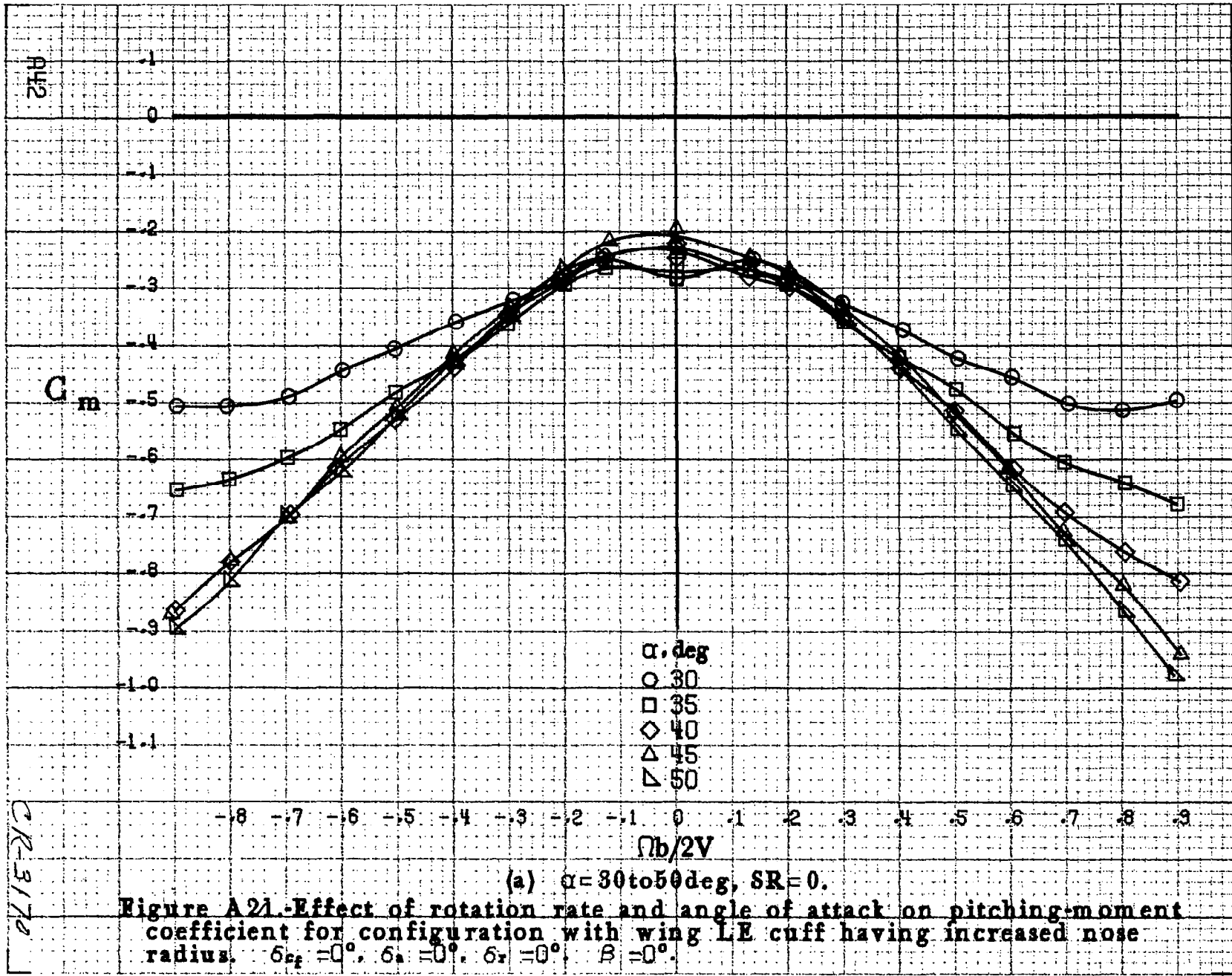
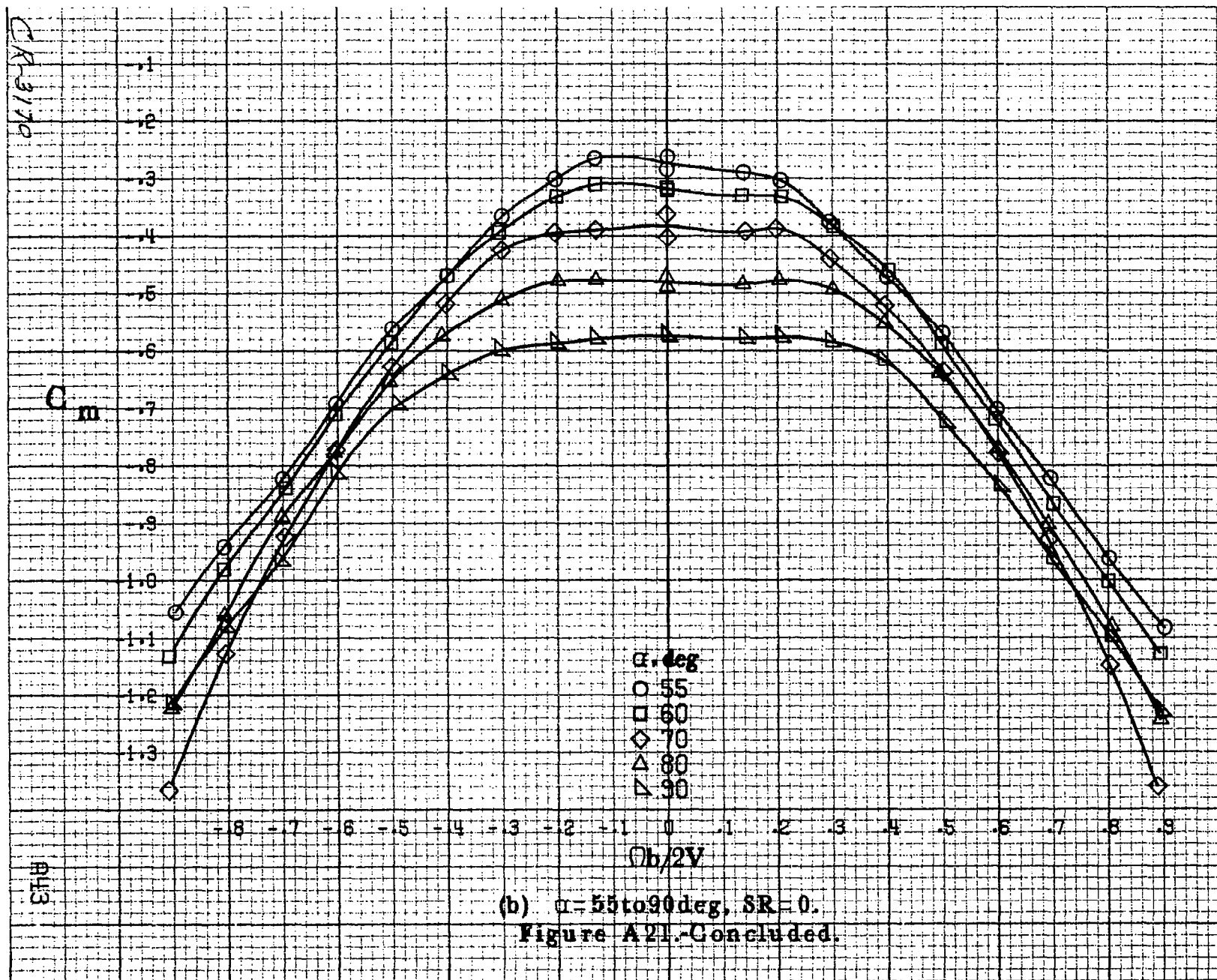
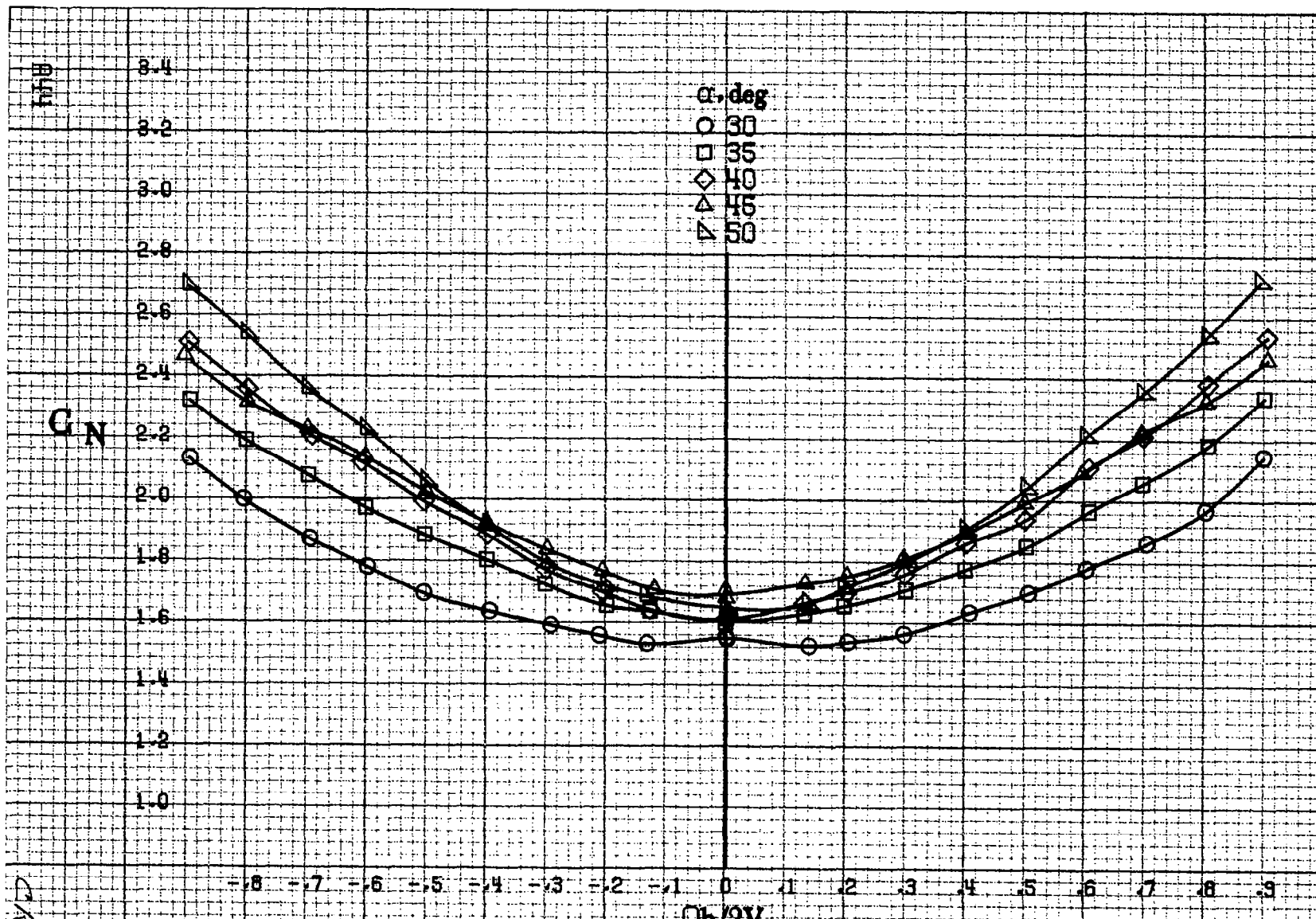


Figure A20. Effect of rotation rate and angle of attack on rolling-moment coefficient for configuration with wing LE cuff having increased nose radius: $\delta_{c_2} = 0^\circ$, $\delta_t = 0^\circ$, $\delta_r = 0^\circ$, $\beta = 0^\circ$.



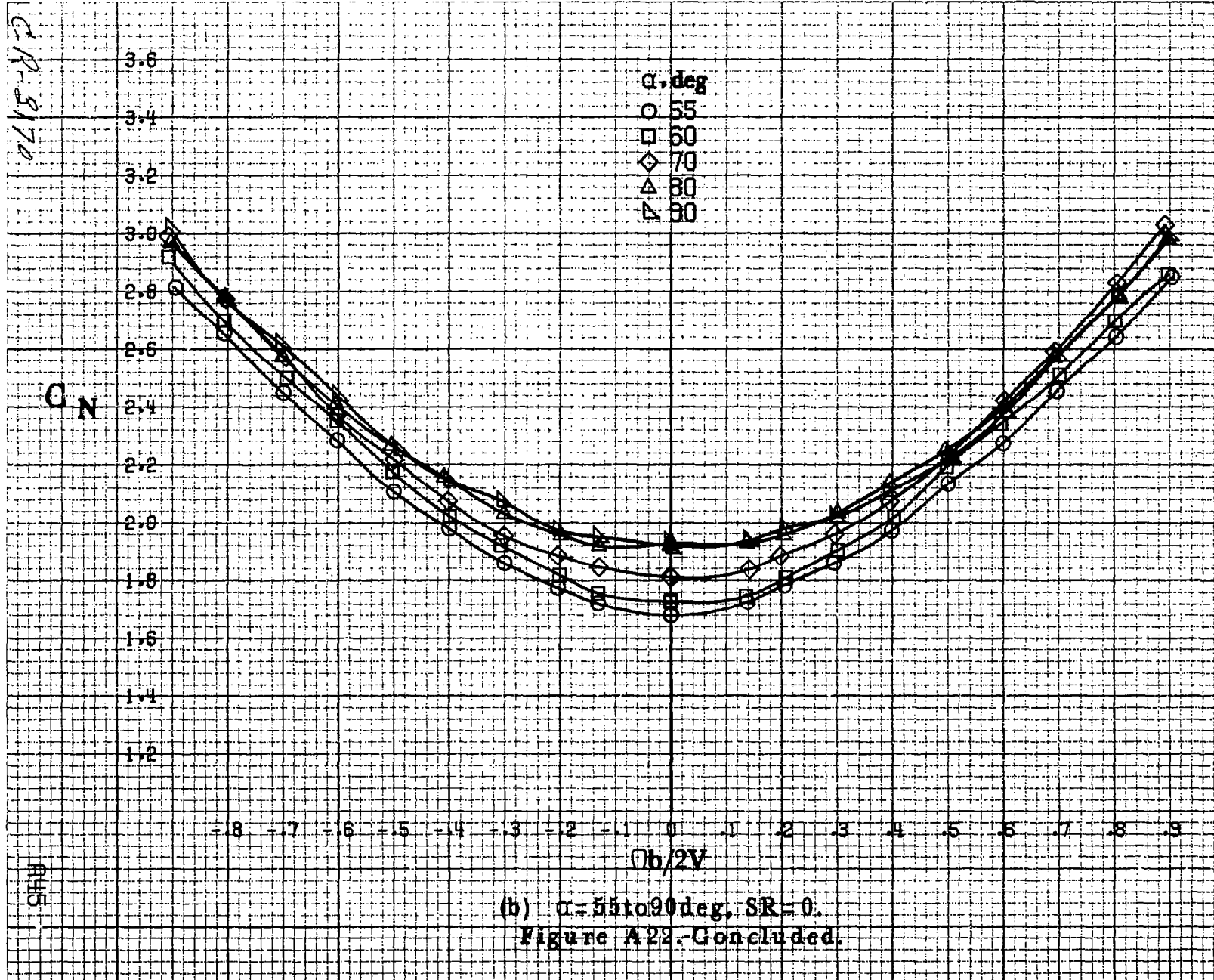


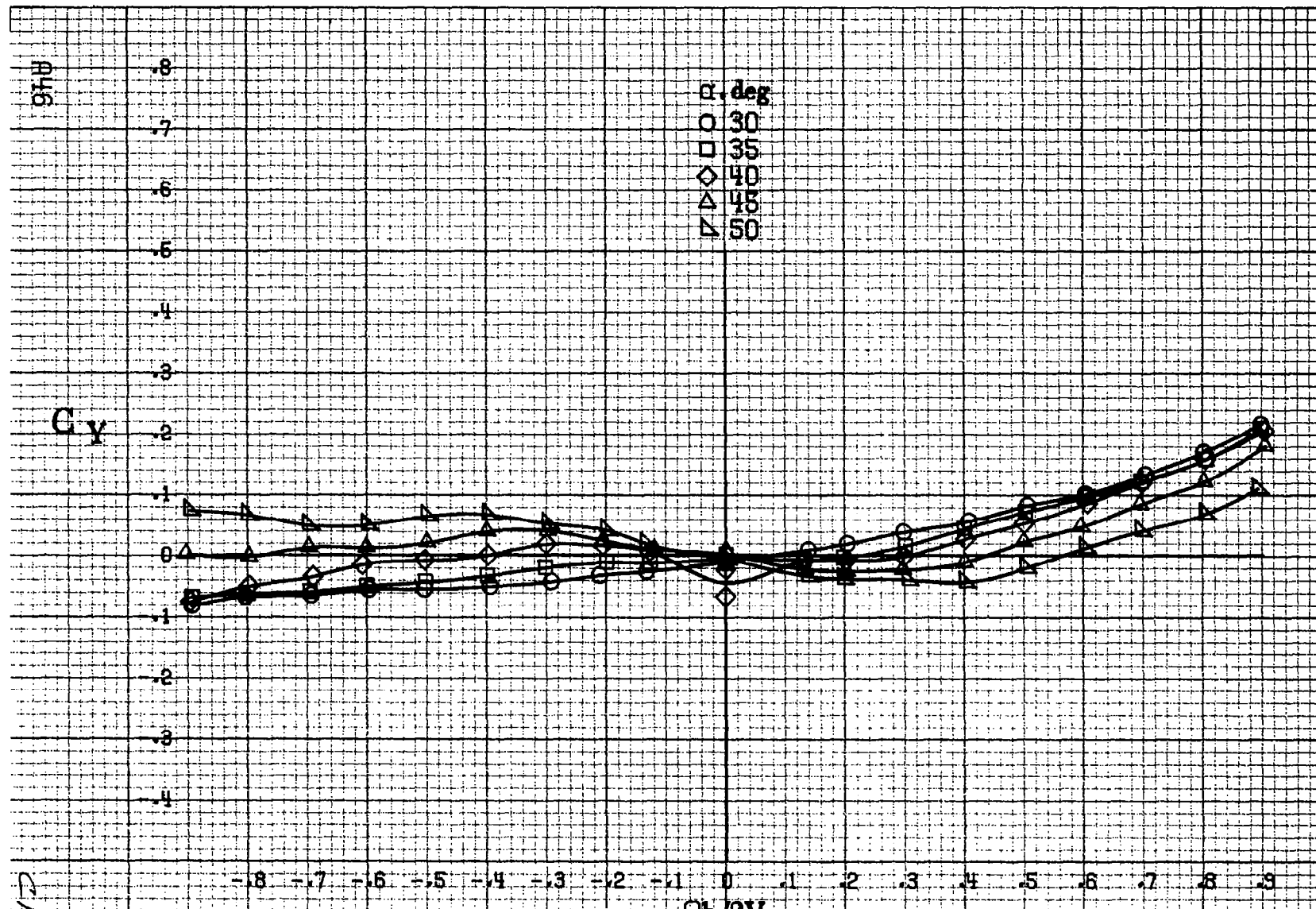




(a) $\alpha = 30$ to 50 deg, SR = 0.

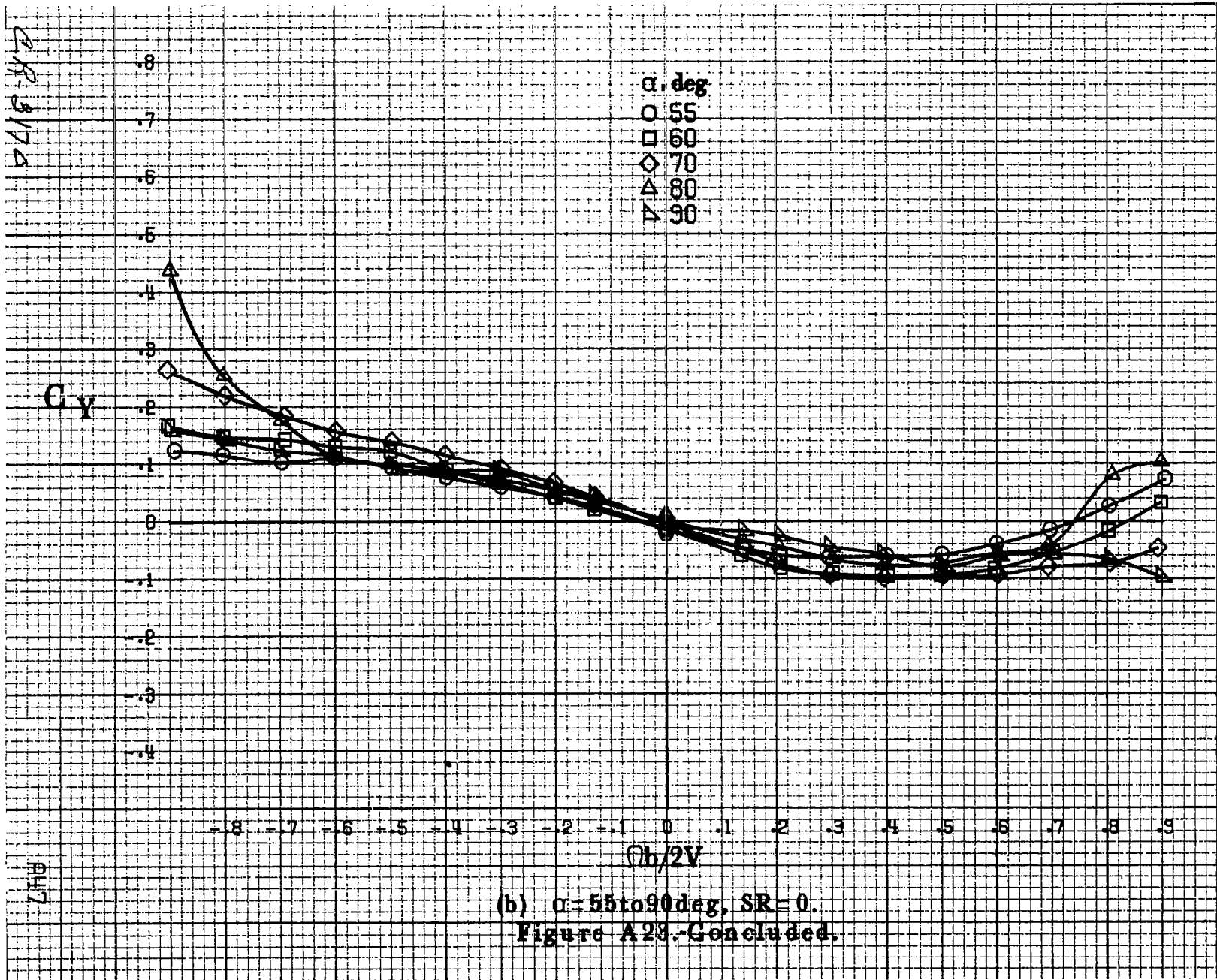
Figure A22. Effect of rotation rate and angle of attack on normal-force coefficient for configuration with wing LE cuff having increased nose radius. $\delta_{c_1} = 0^\circ$, $\delta_a = 0^\circ$, $\delta_r = 0^\circ$, $\beta = 0^\circ$.

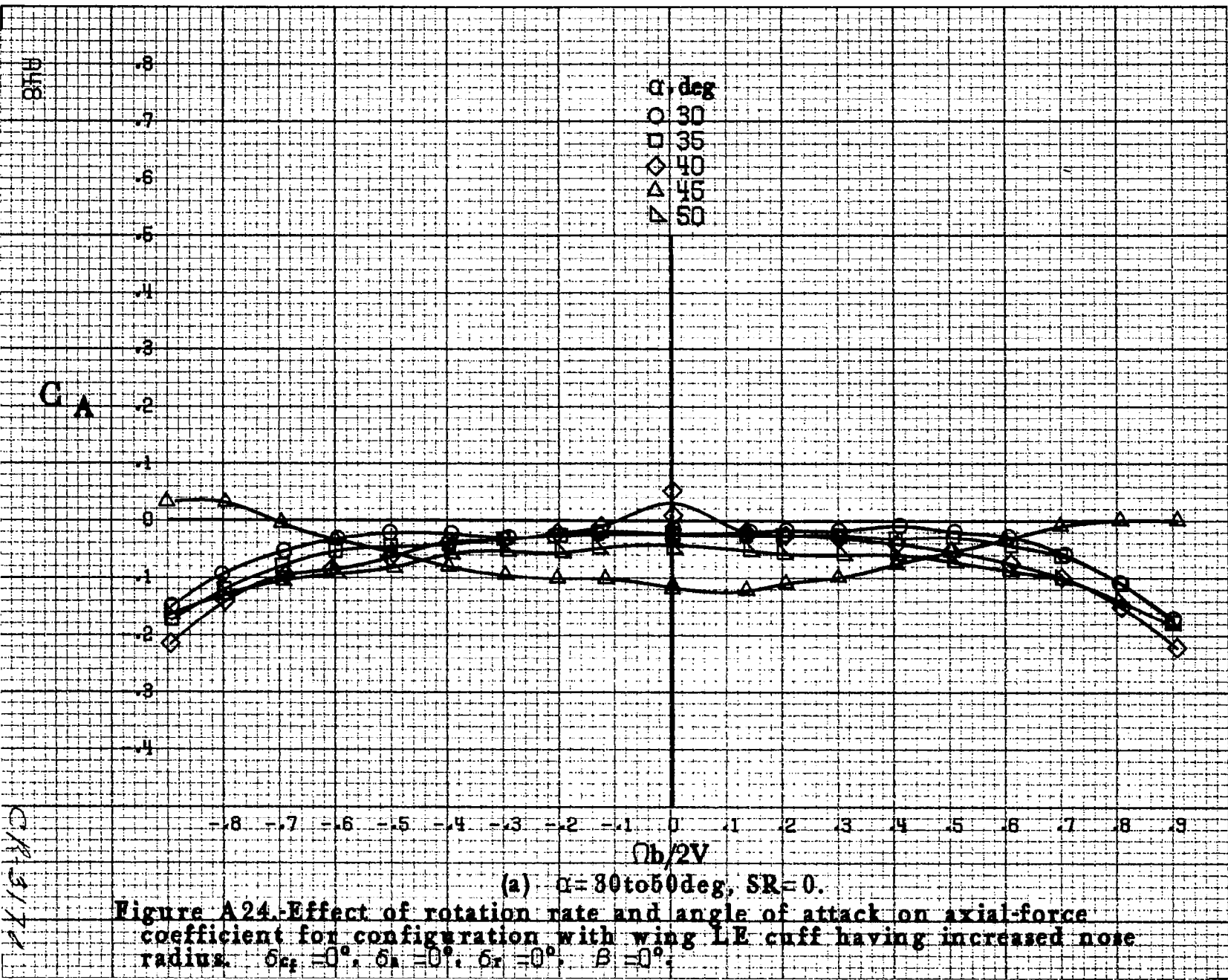


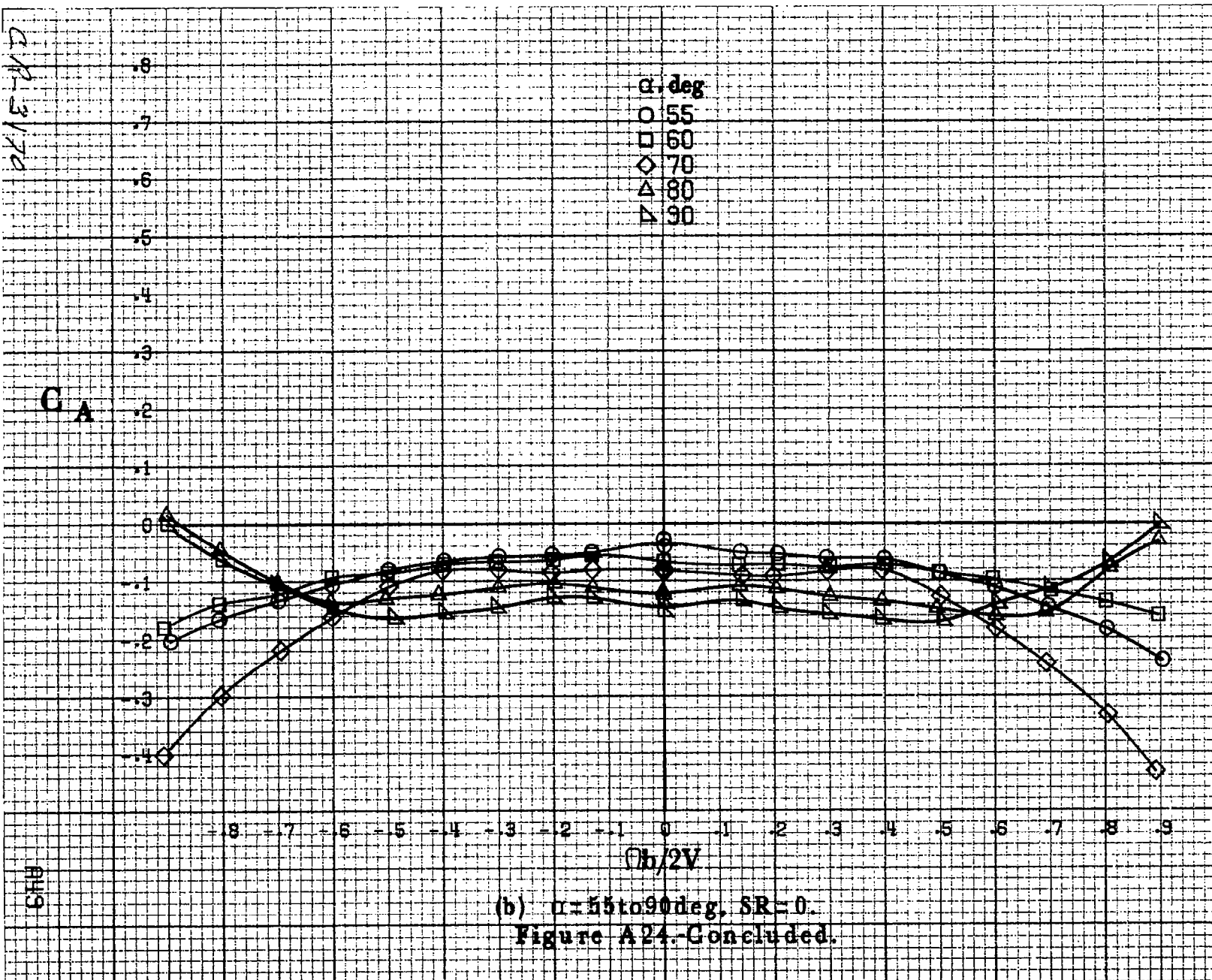


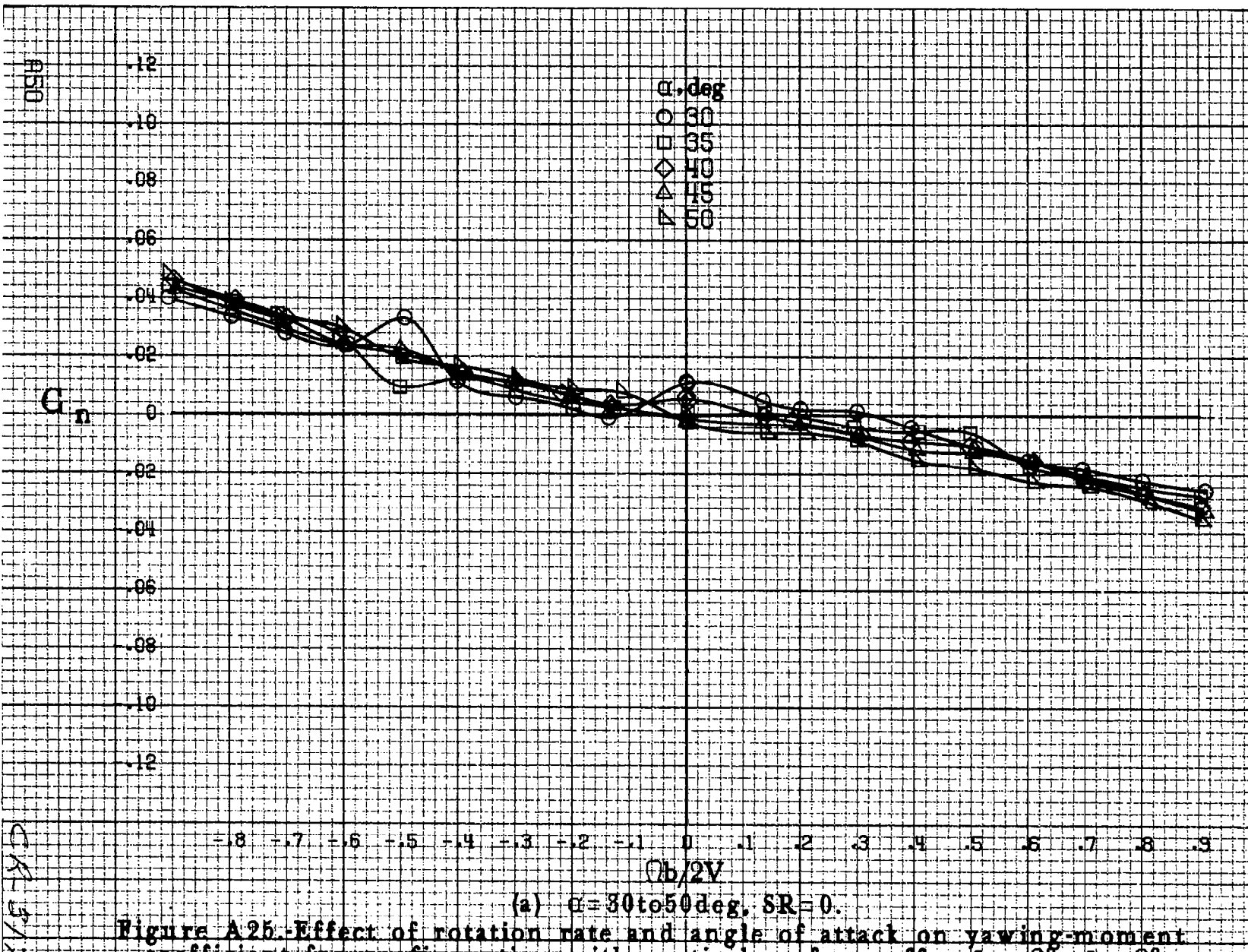
(a) $\alpha = 30$ to 50 deg, SR = 0.

Figure A23. Effect of rotation rate and angle of attack on side-force coefficient for configuration with wing LE cuff having increased nose radius. $\delta_{e_1} = 0^\circ$, $\delta_e = 0^\circ$, $\delta_r = 0^\circ$, $\beta = 0^\circ$.



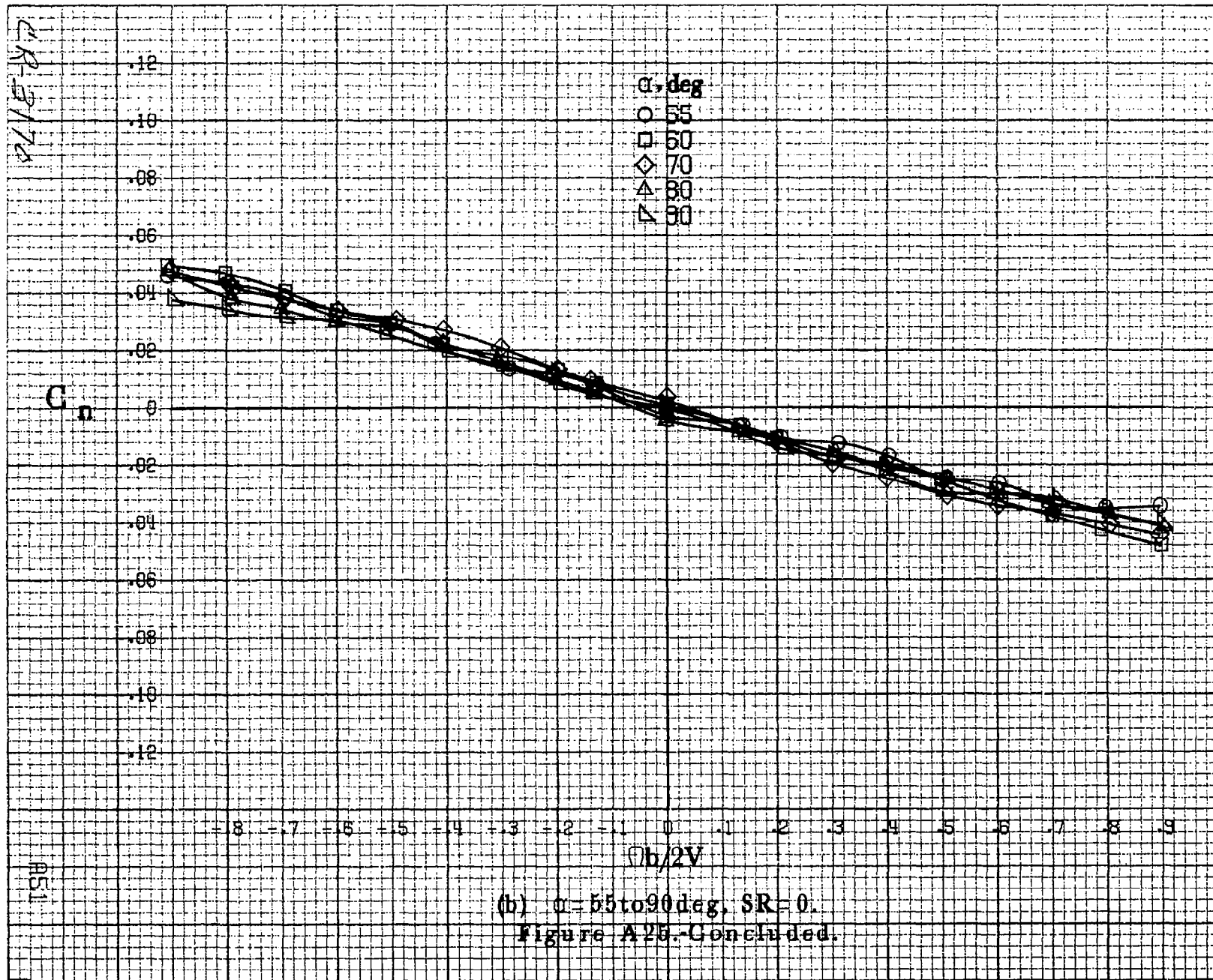


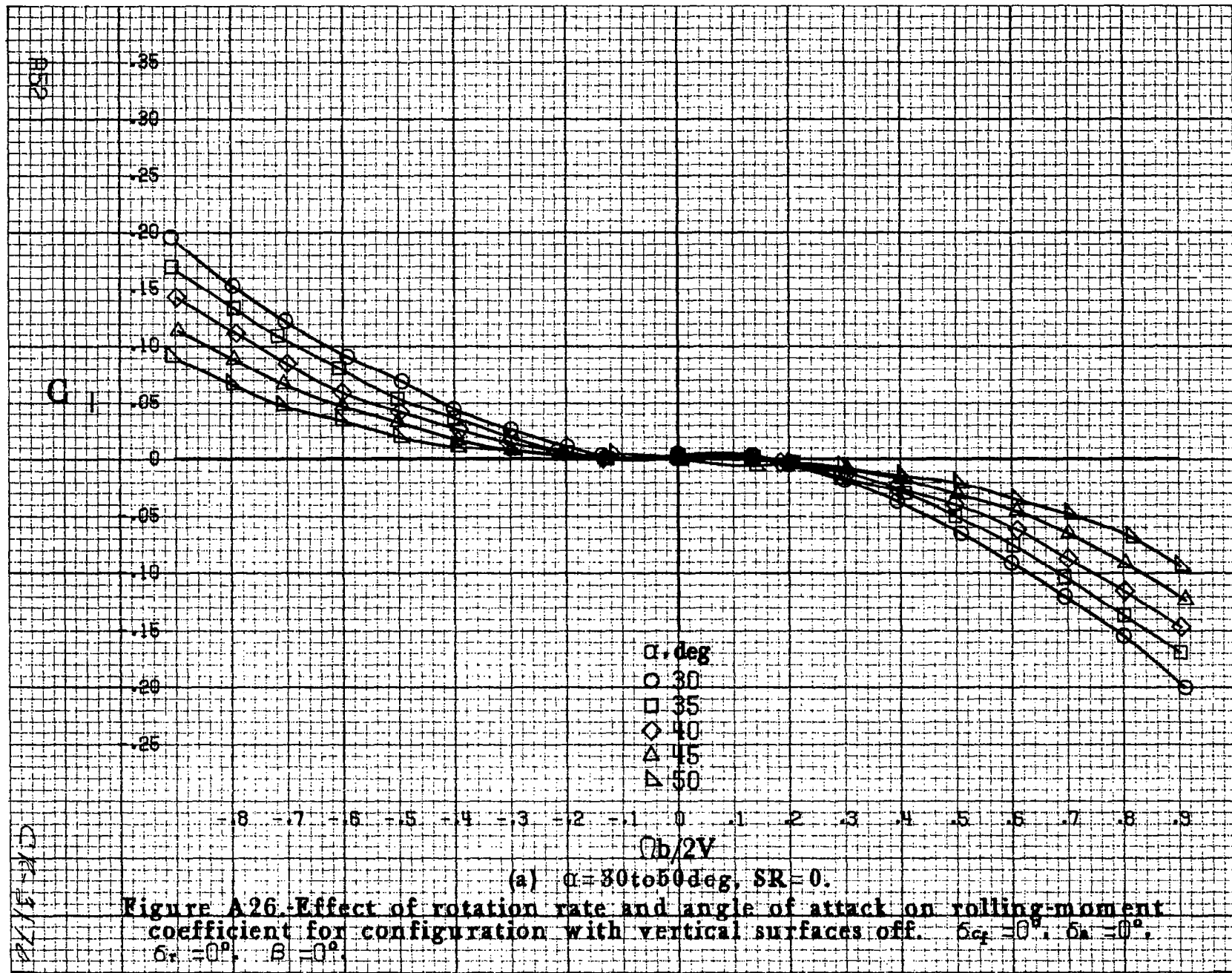




(a) $\alpha = 30$ to 50 deg, SR = 0.

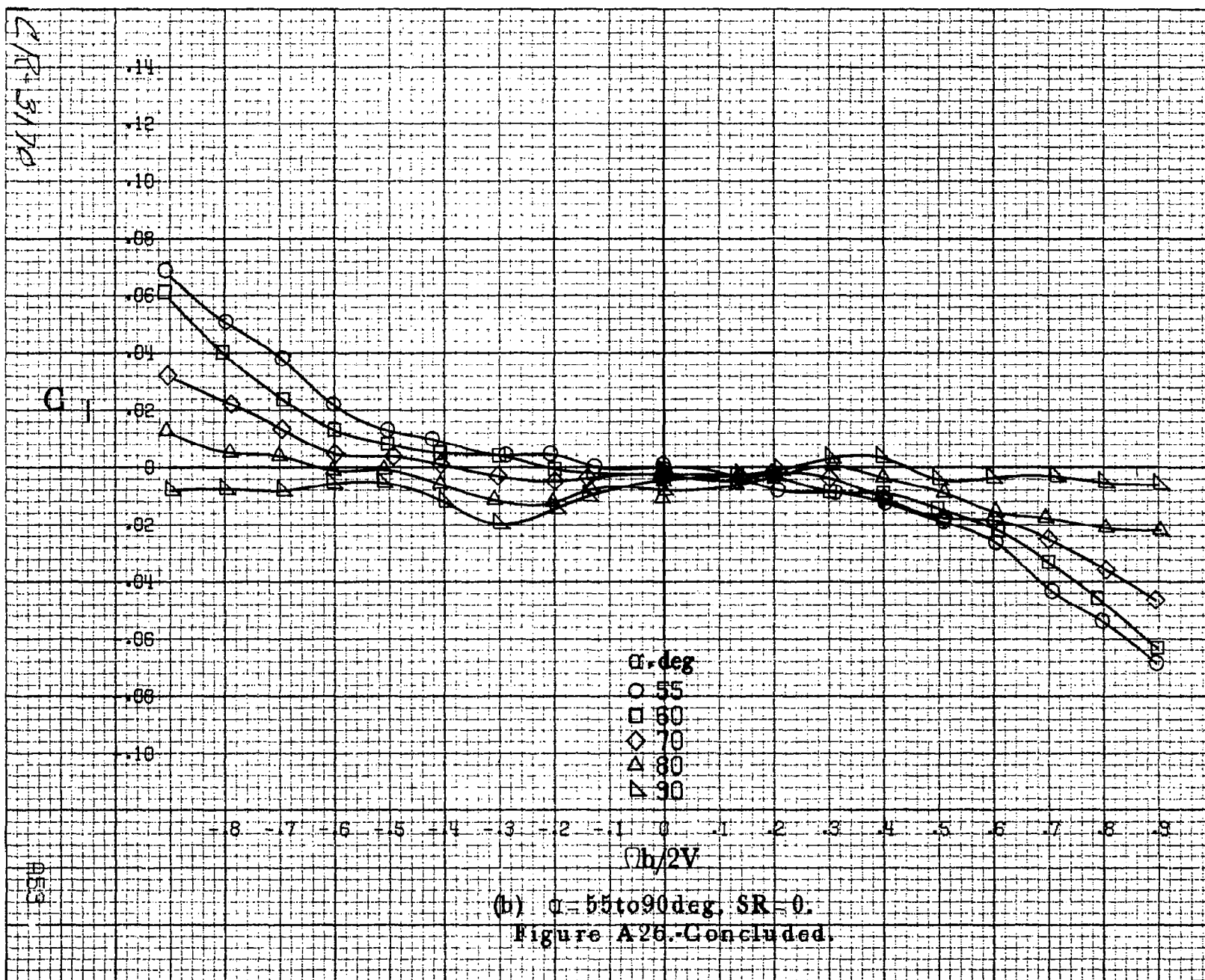
Figure A26. Effect of rotation rate and angle of attack on yawing-moment coefficient for configuration with vertical surfaces off. $\delta_{rf} = 0^\circ$, $\delta_a = 0^\circ$, $\delta_r = 0^\circ$, $\beta = 0^\circ$.





(a) $\alpha = 30$ to 50 deg, SR = 0

Figure A26. Effect of rotation rate and angle of attack on rolling-moment coefficient for configuration with vertical surfaces off. $\delta_{rf} = 0^\circ$; $\delta_a = 0^\circ$; $\delta_r = 0^\circ$.



(b) $\alpha = 55$ to 90° , SR = 0.

Figure A26.-Concluded.

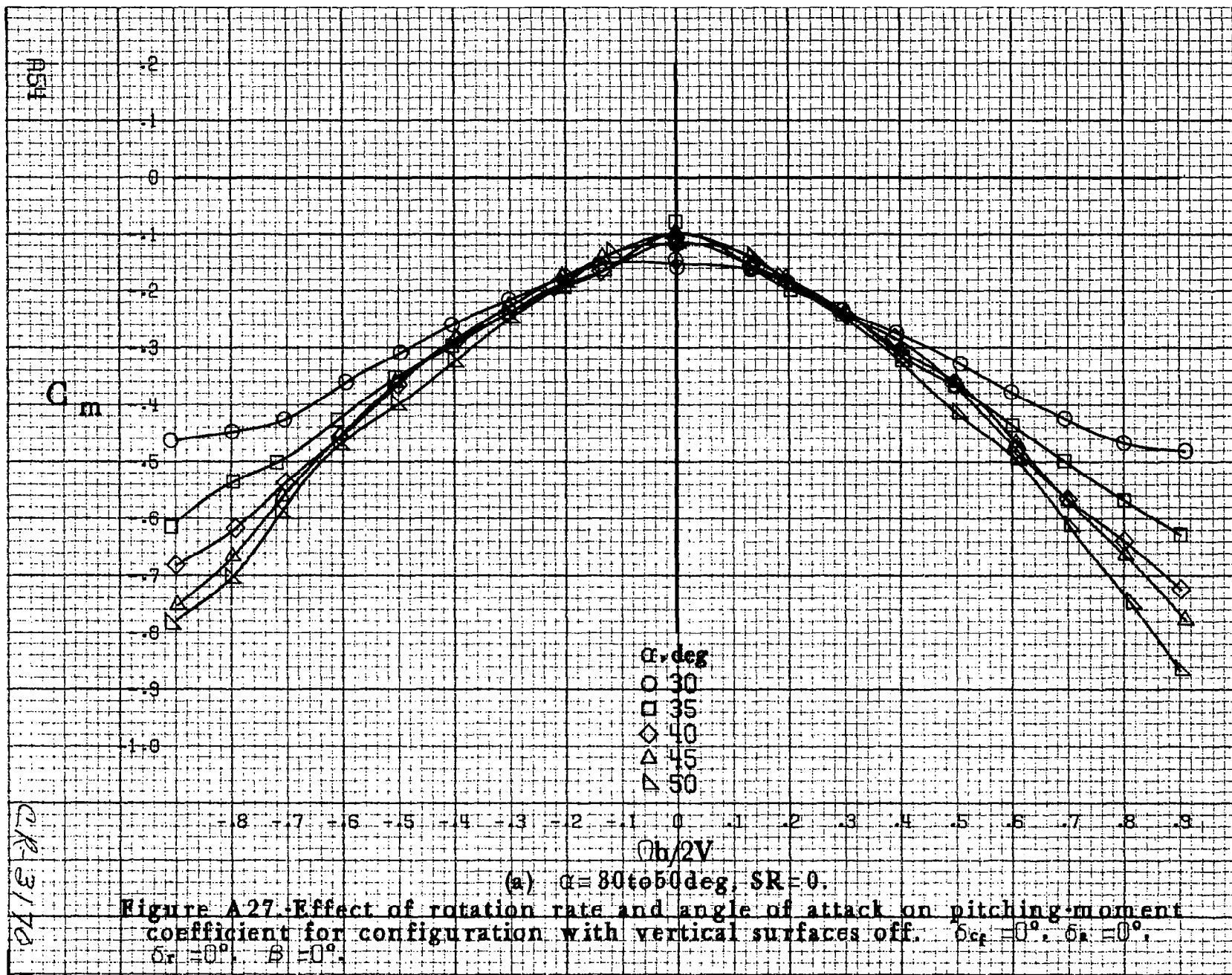
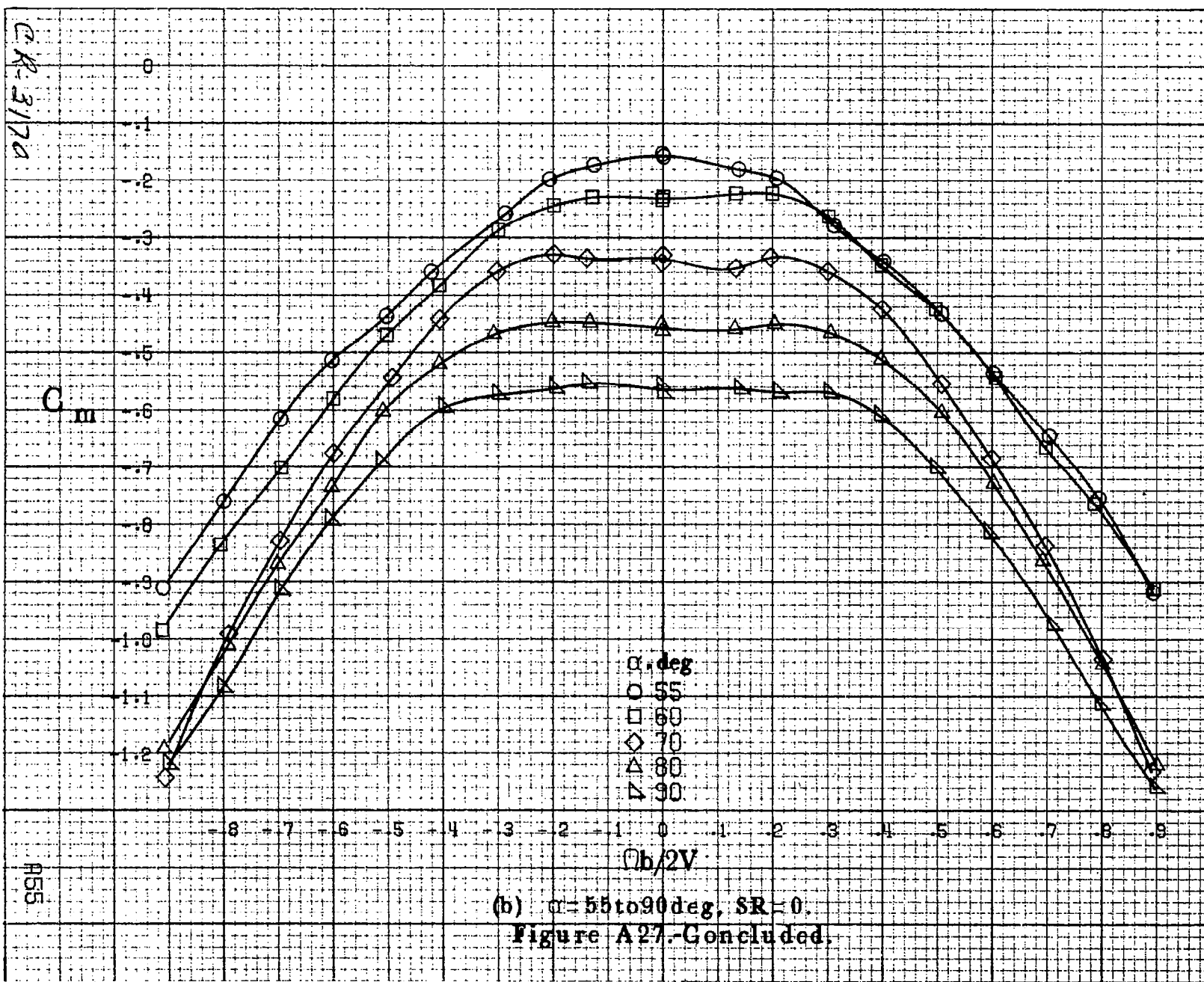
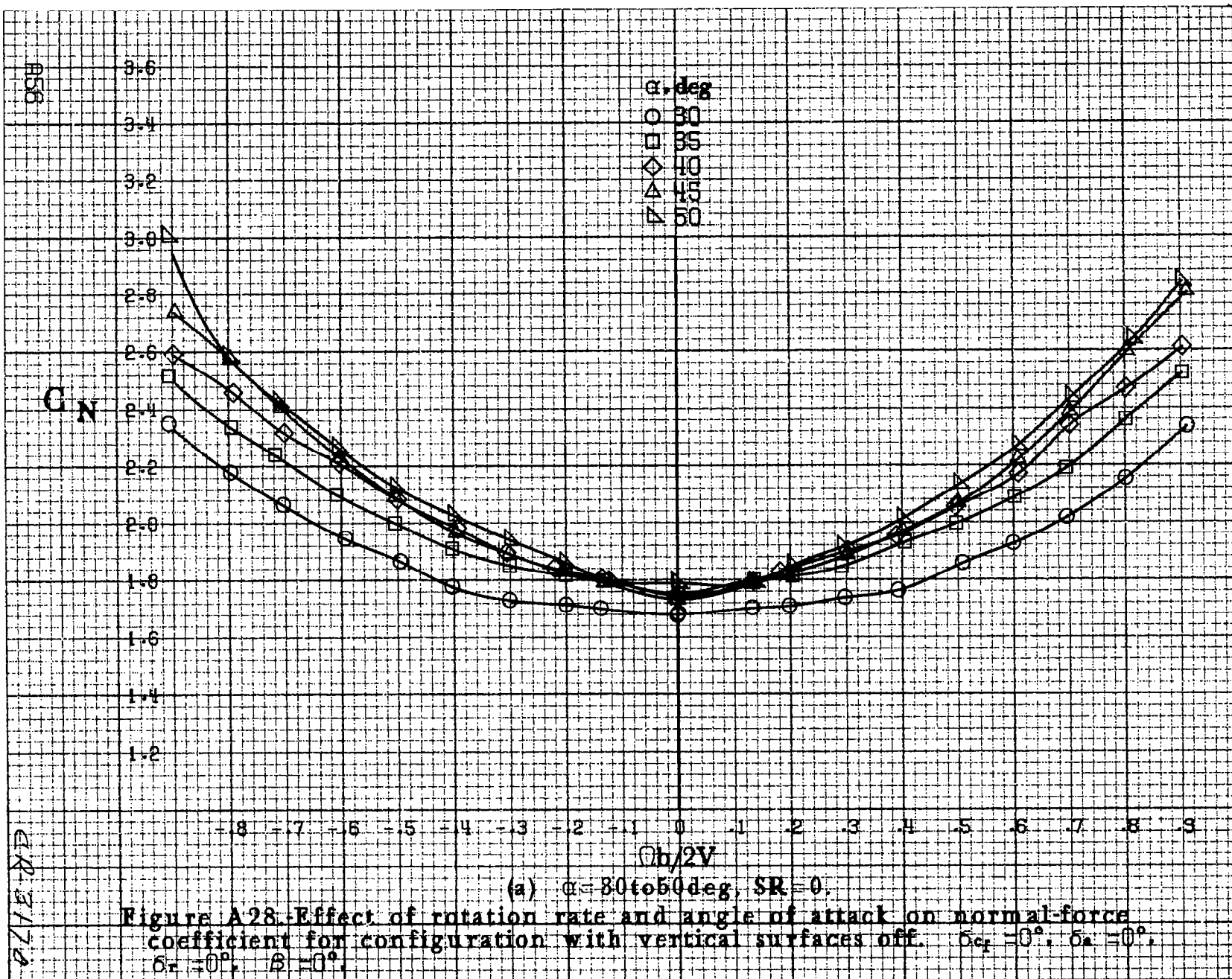


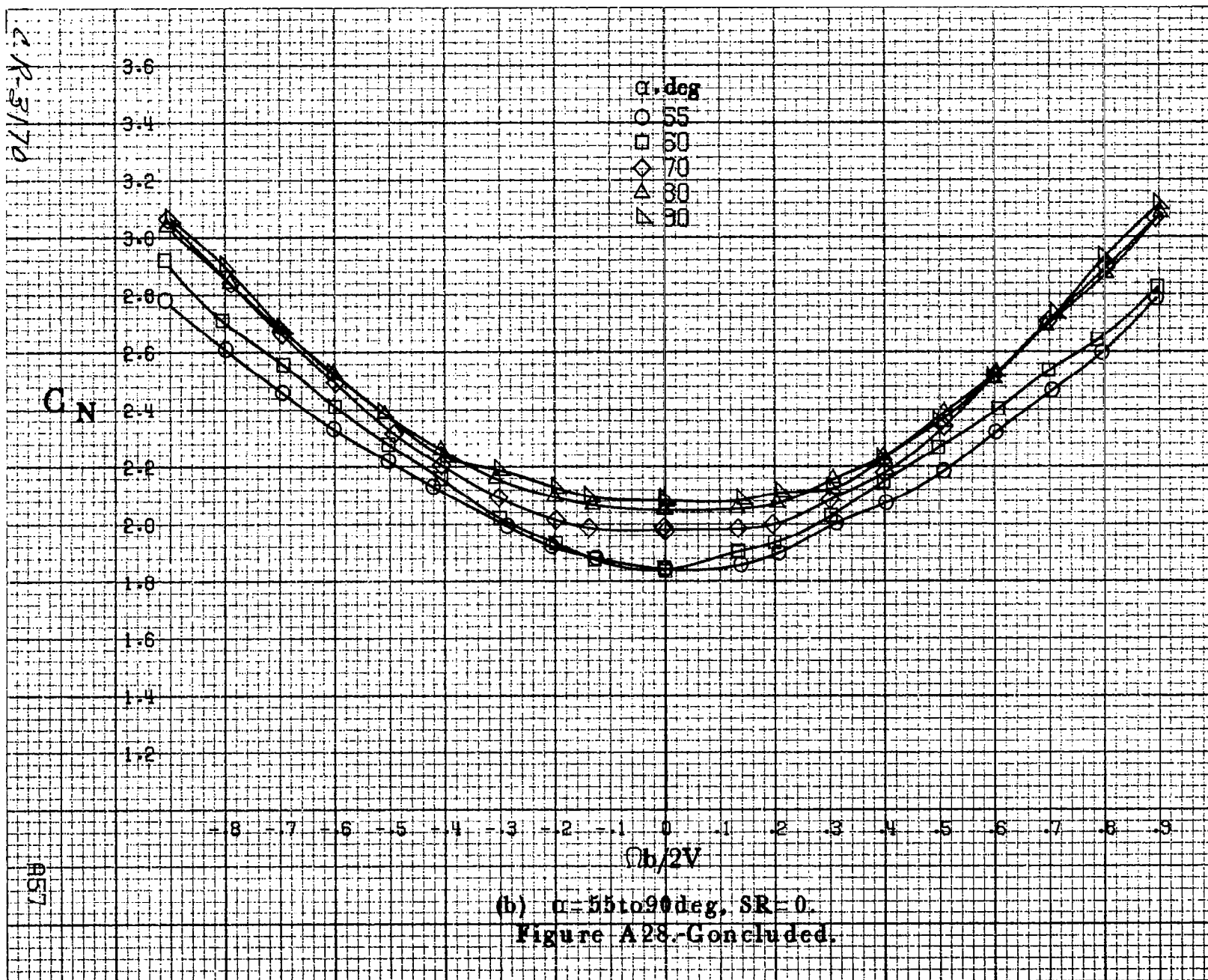
Figure A27. Effect of rotation rate and angle of attack on pitching moment coefficient for configuration with vertical surfaces off. $\delta_{rf} = 0^\circ$, $\delta_s = 0^\circ$, $\delta_r = 0^\circ$, $\beta = 0^\circ$.

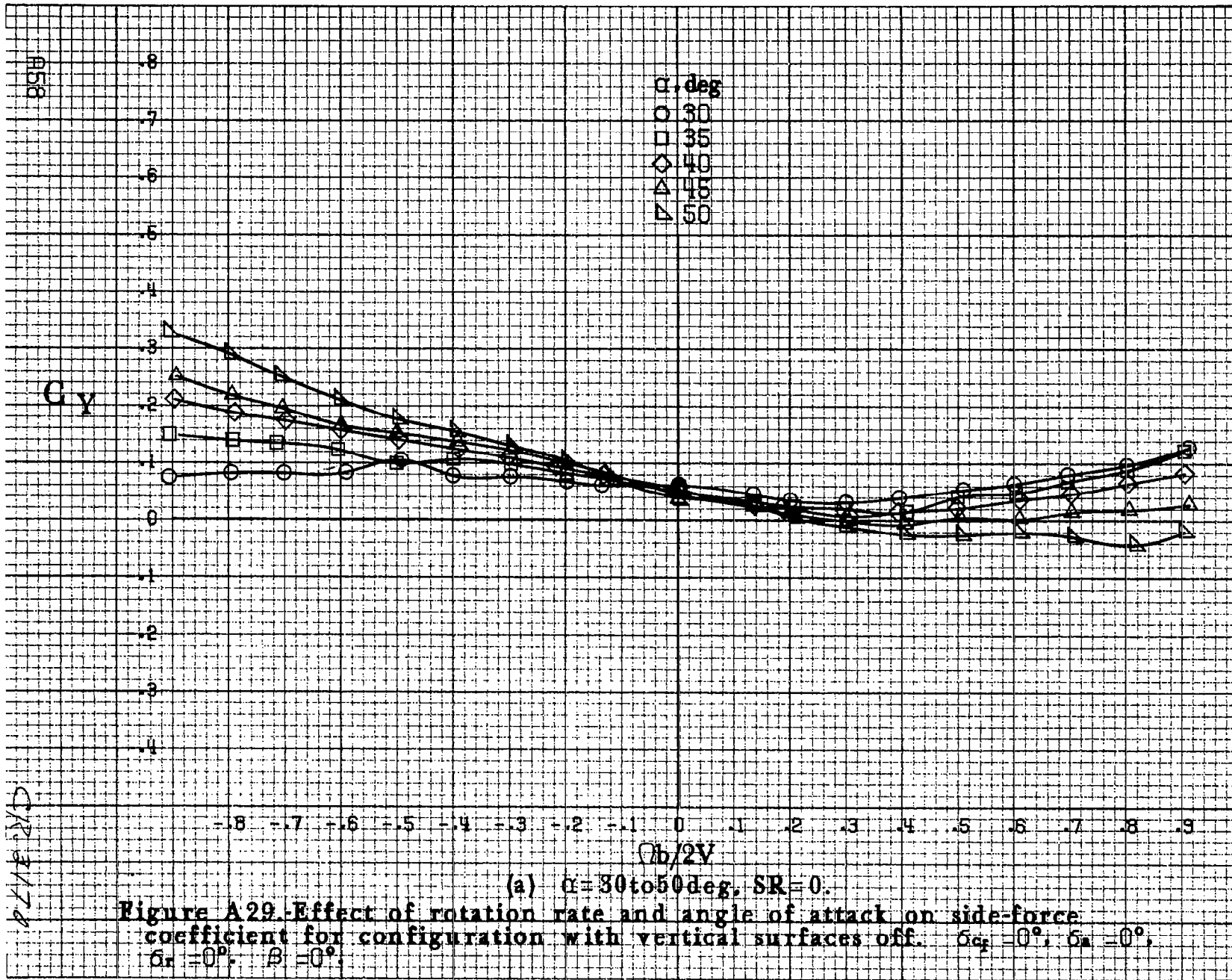
CR-3170

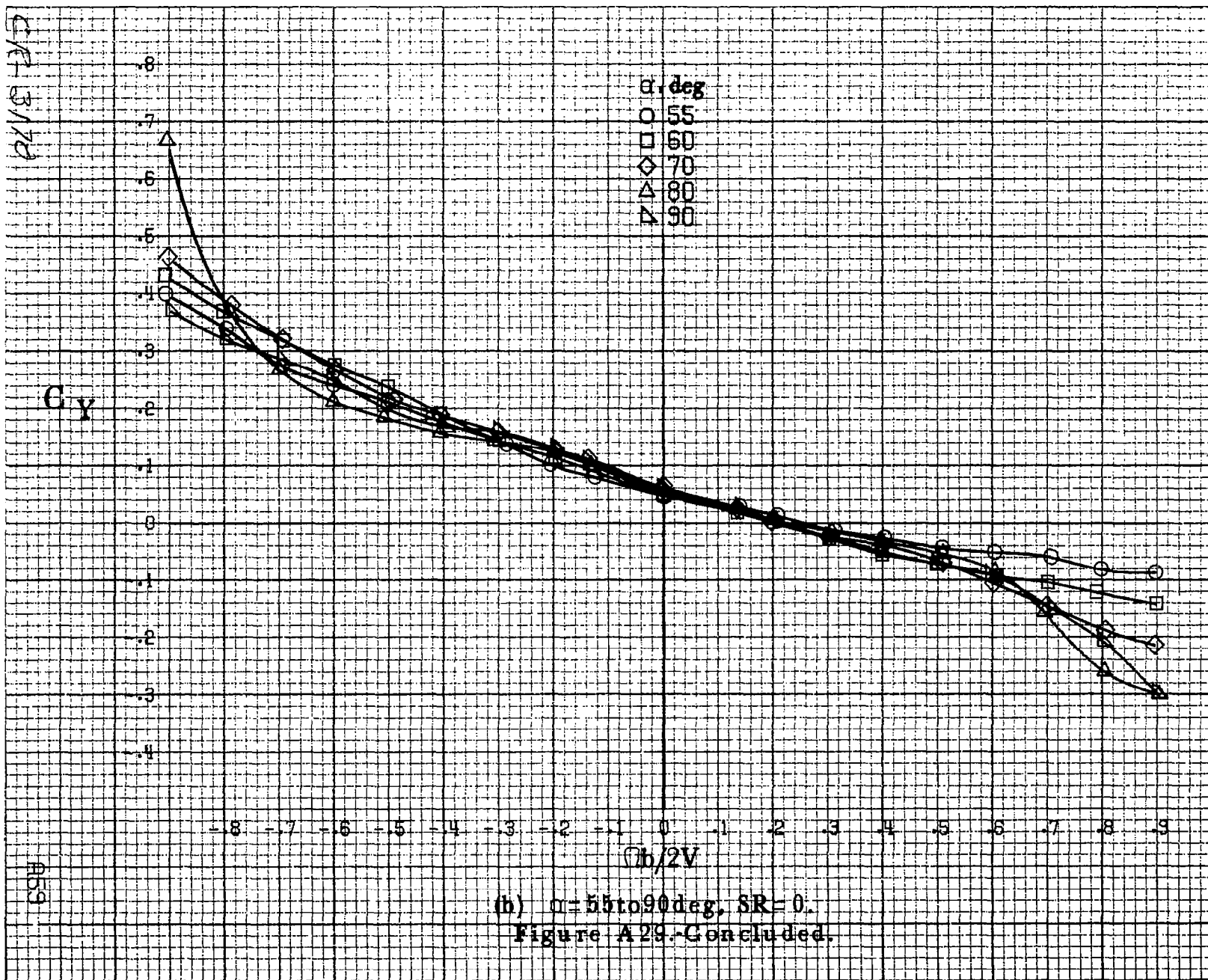


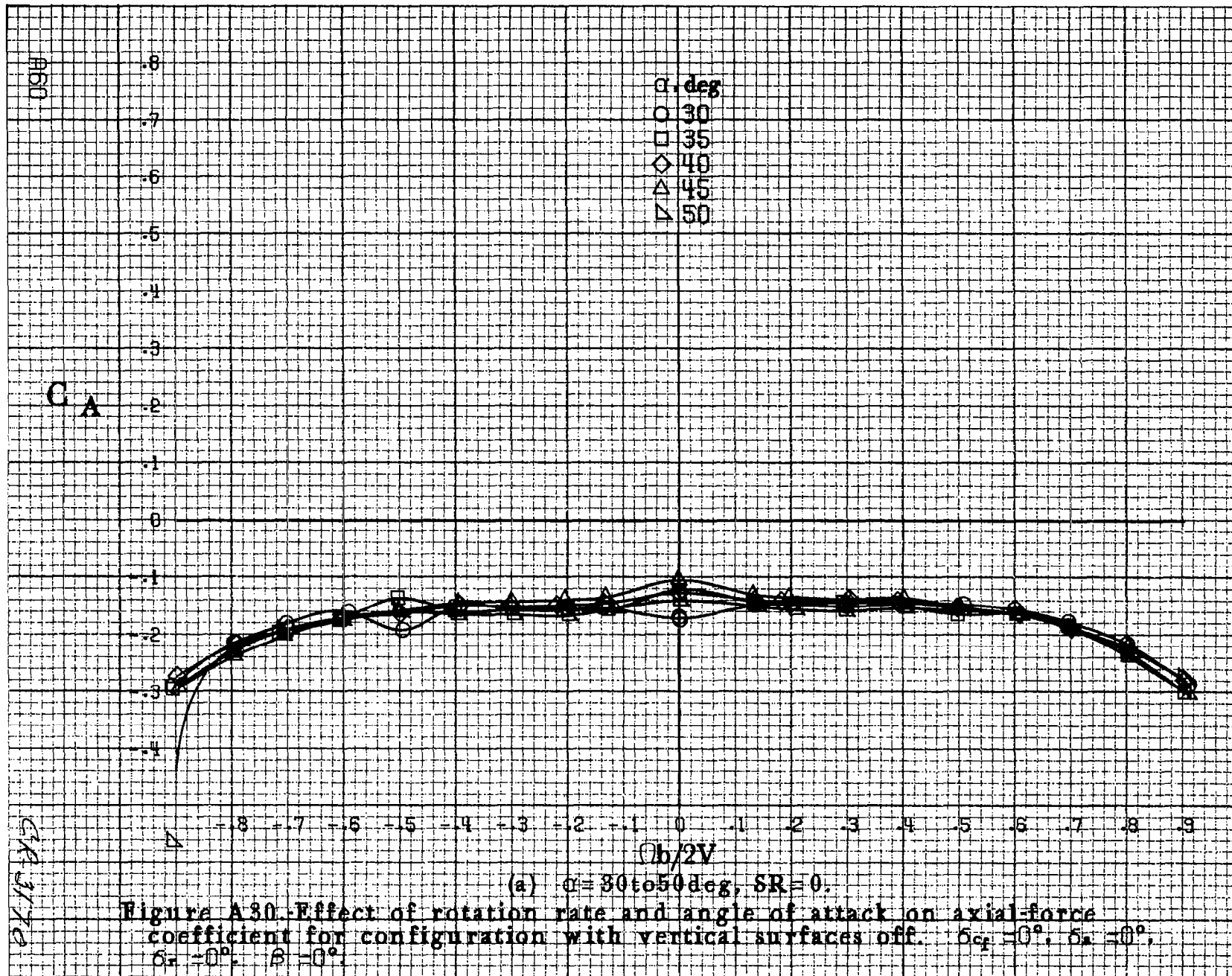
R55

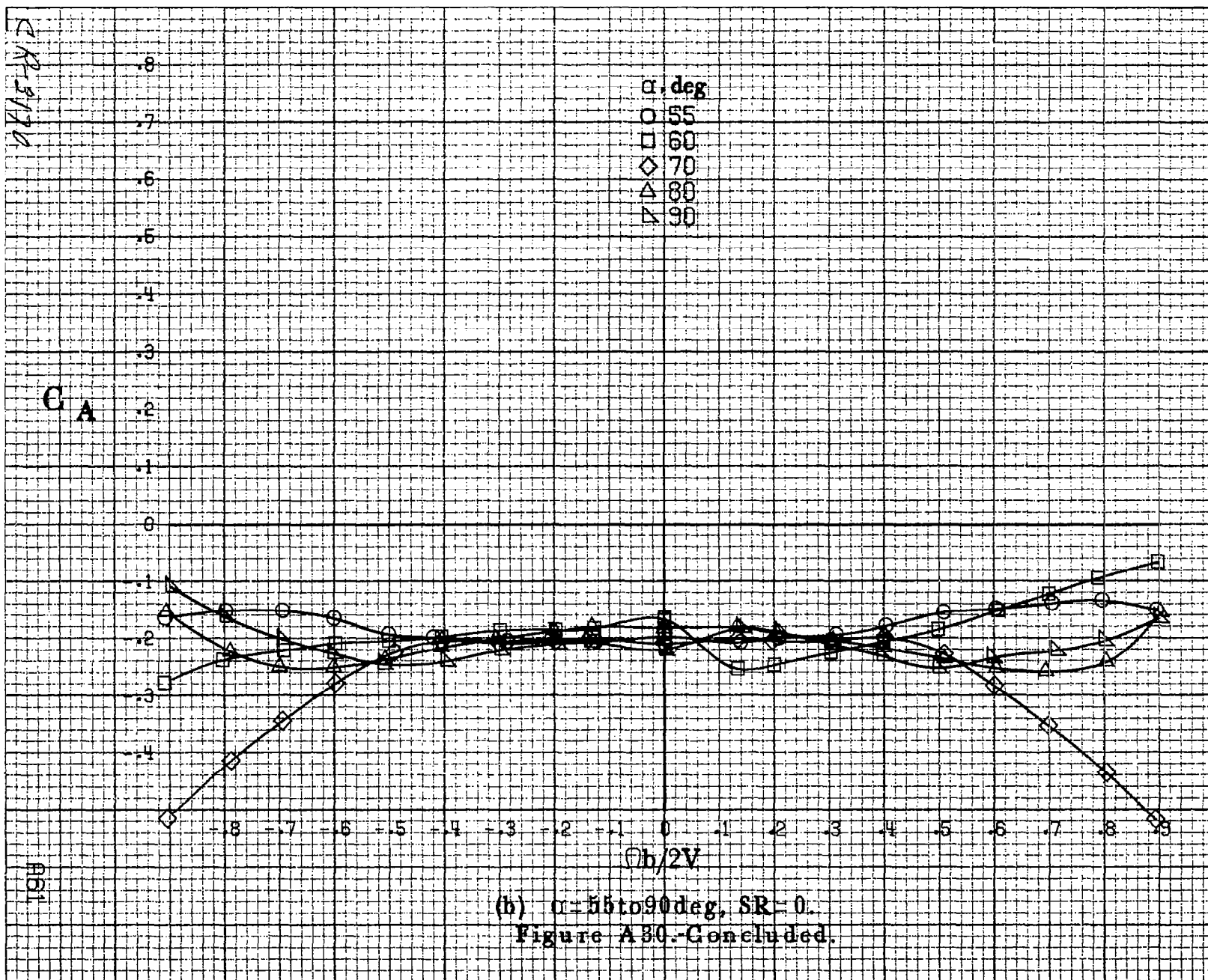


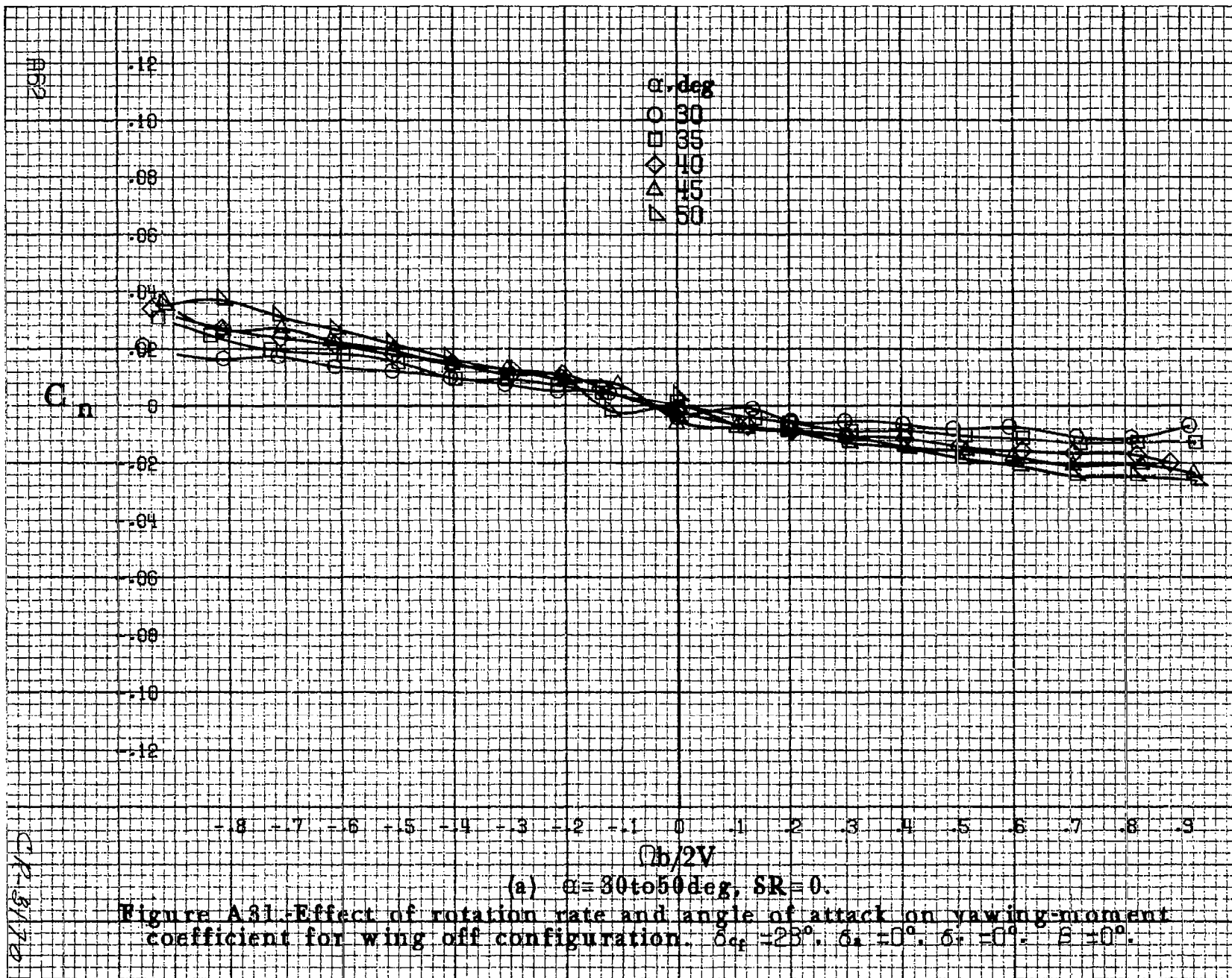






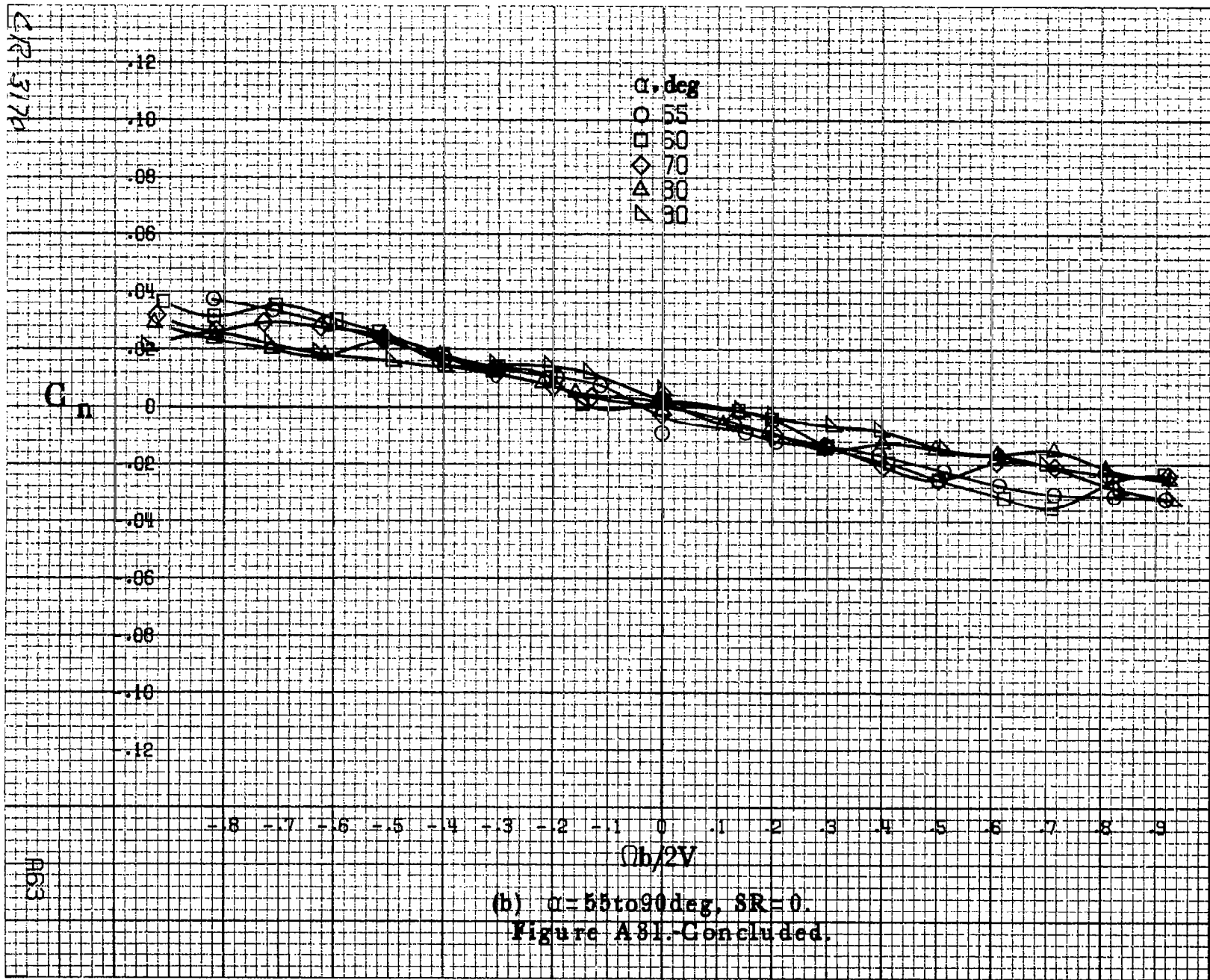


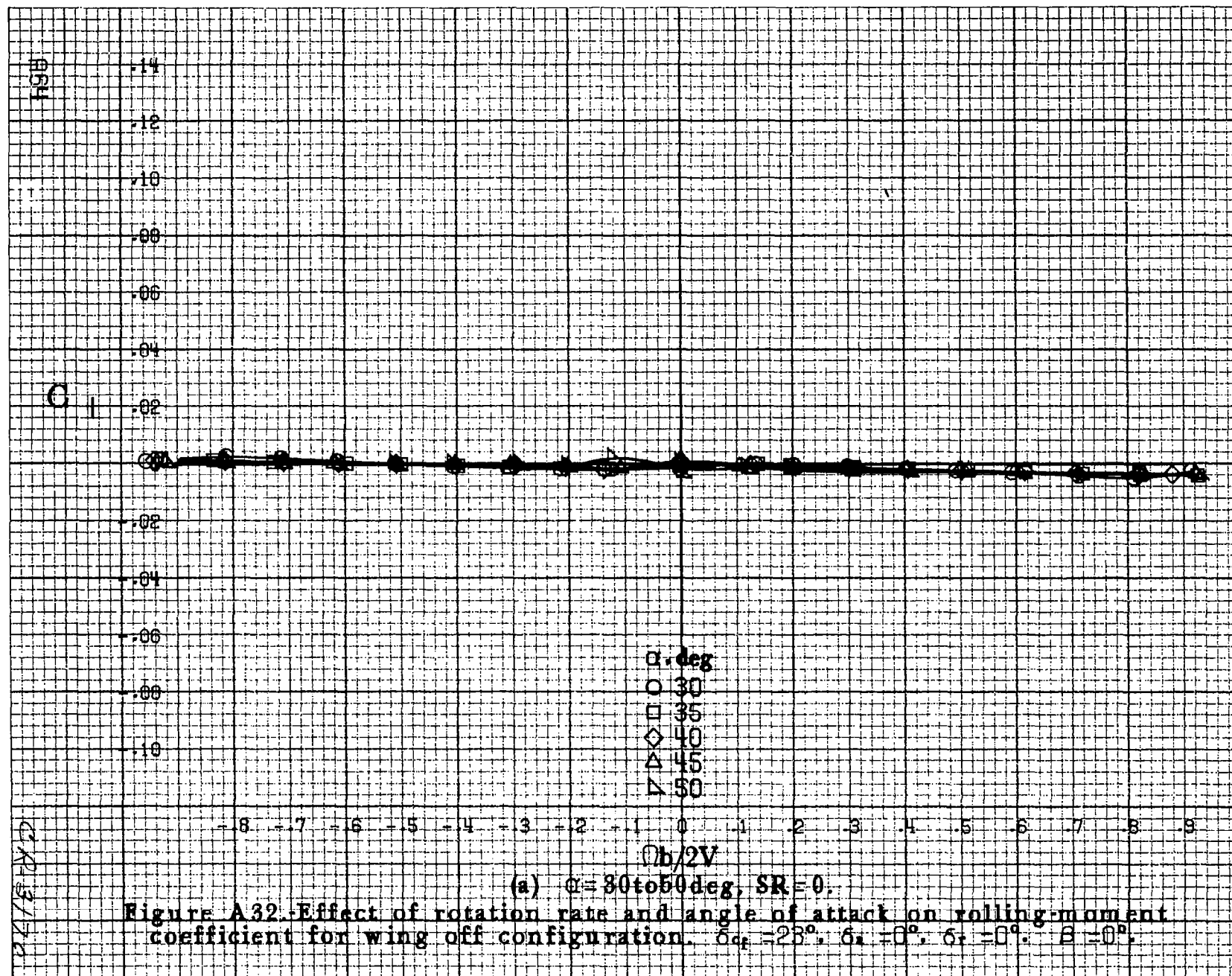




(a) $\alpha = 30$ to 50 deg, SR = 0.

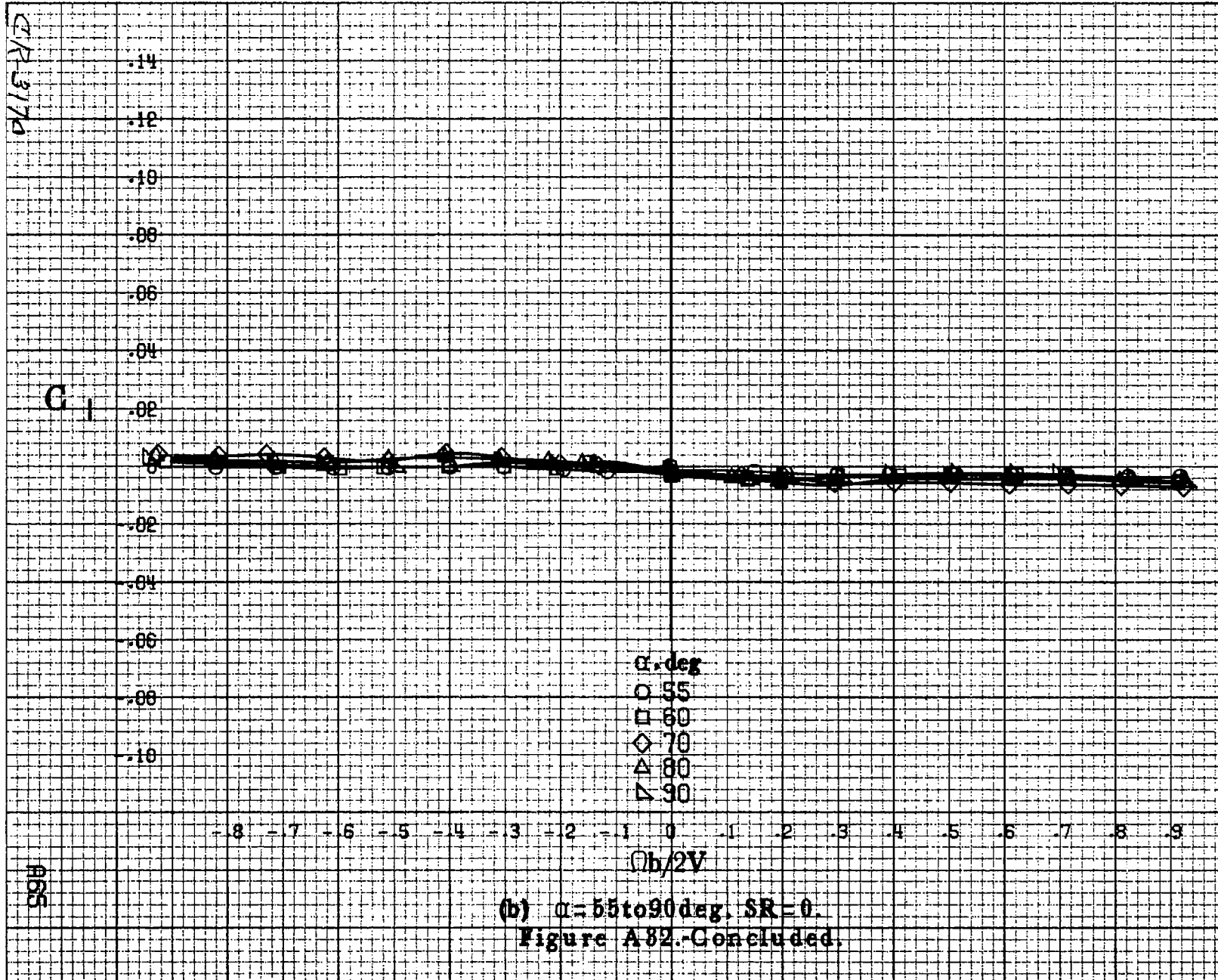
Figure A.31. Effect of rotation rate and angle of attack on yawing moment coefficient for wing off configuration. $\delta_{rf} = 20^\circ$, $\delta_s = 0^\circ$, $\delta_t = 0^\circ$, $\beta = 0^\circ$.

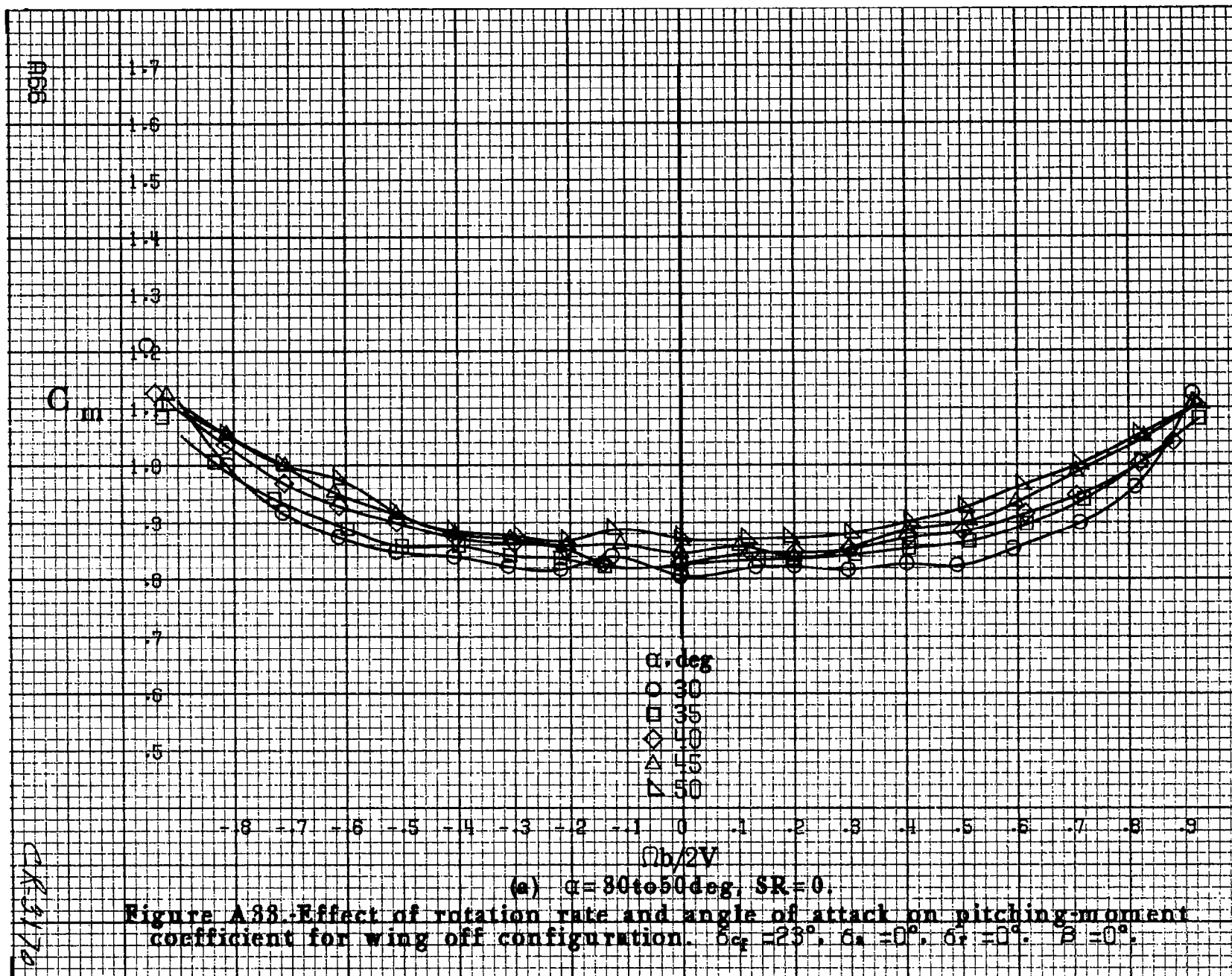


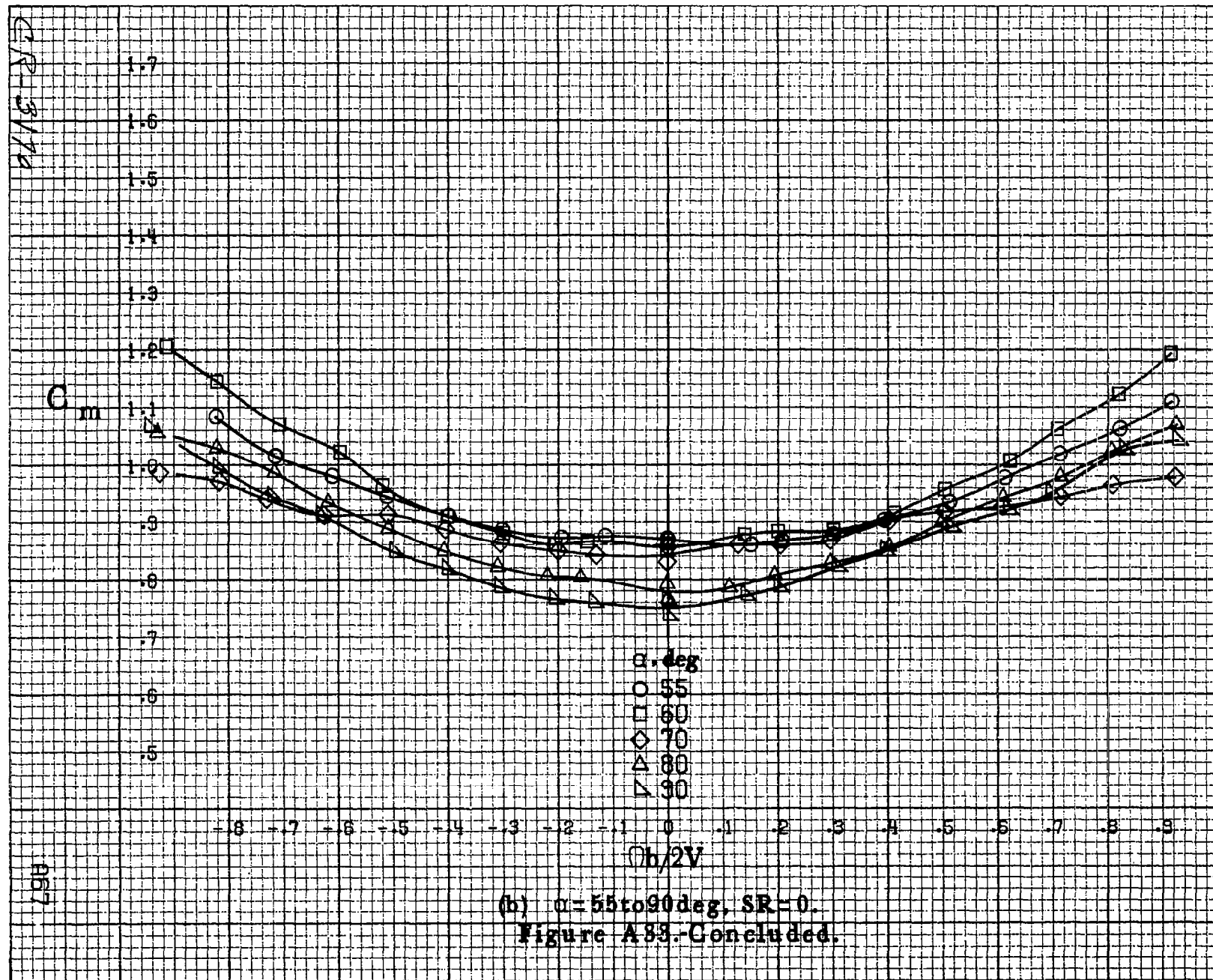


(a) $\alpha = 30$ to 50 deg, SR = 0.

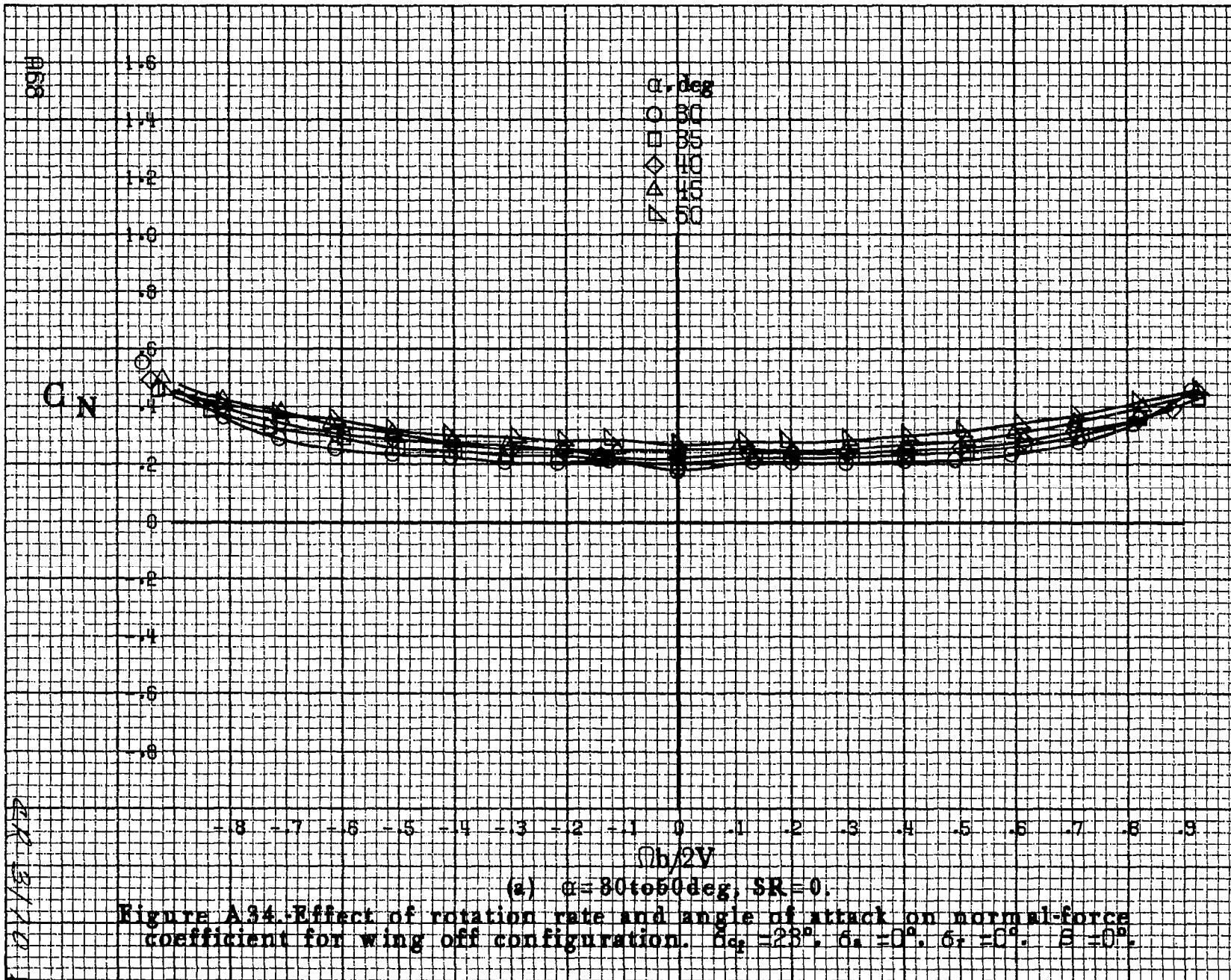
Figure A32. Effect of rotation rate and angle of attack on rolling-moment coefficient for wing off configuration. $\delta_{rf} = 25^\circ$, $\delta_s = 0^\circ$, $\delta_t = 0^\circ$, $B = 0^\circ$.

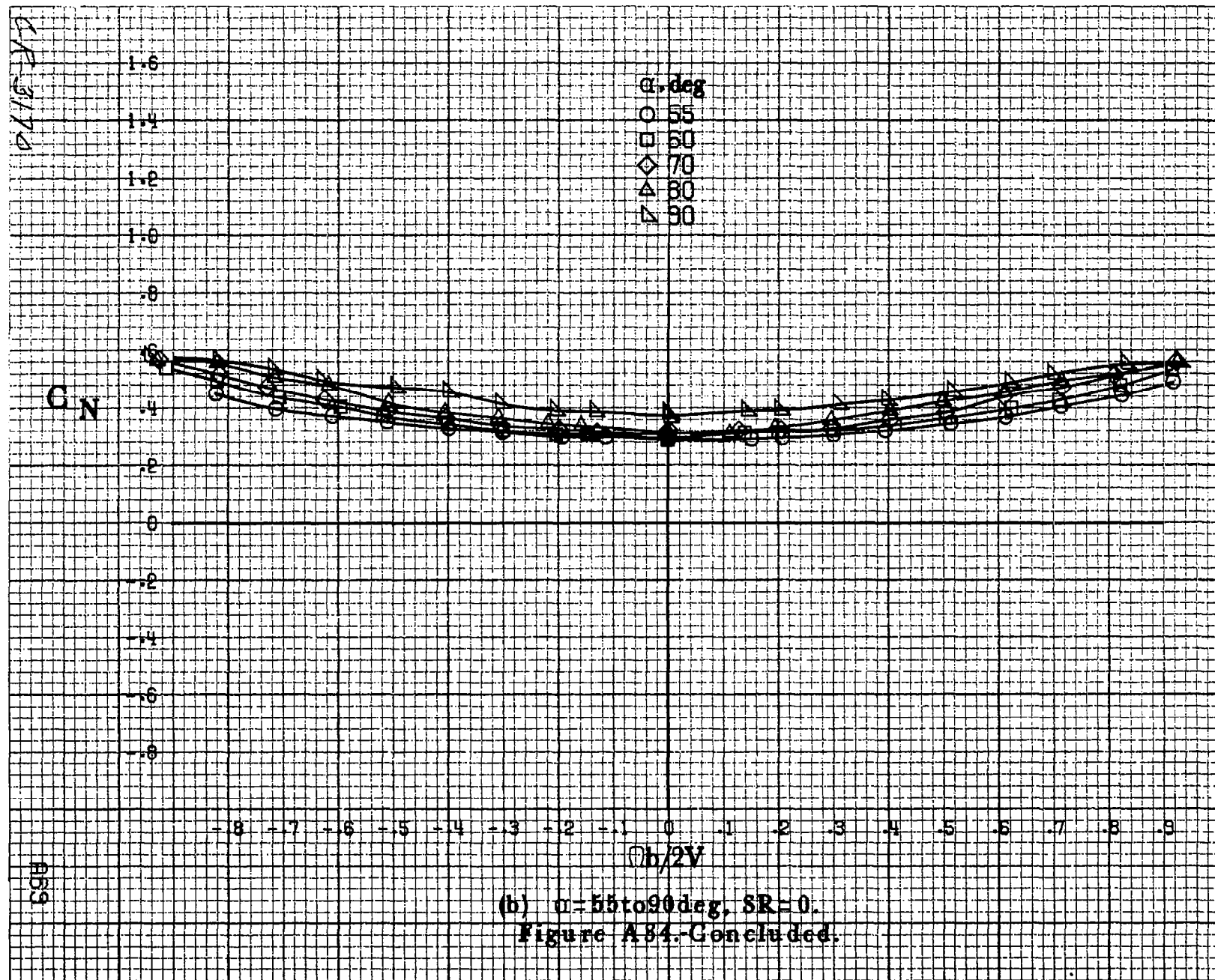


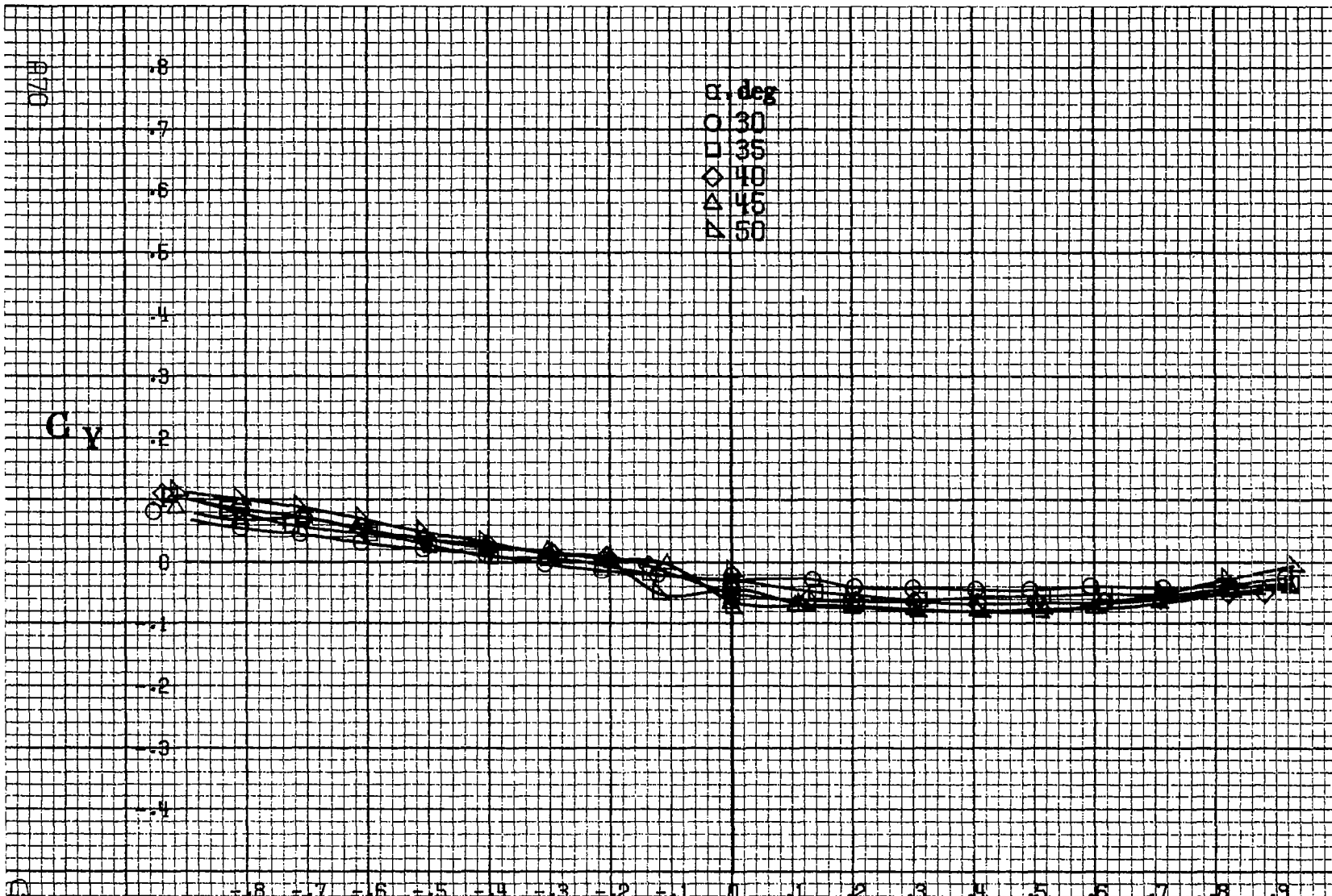




(b) $\alpha = 55$ to 90 deg, SR = 0.
Figure A 83.-Concluded.

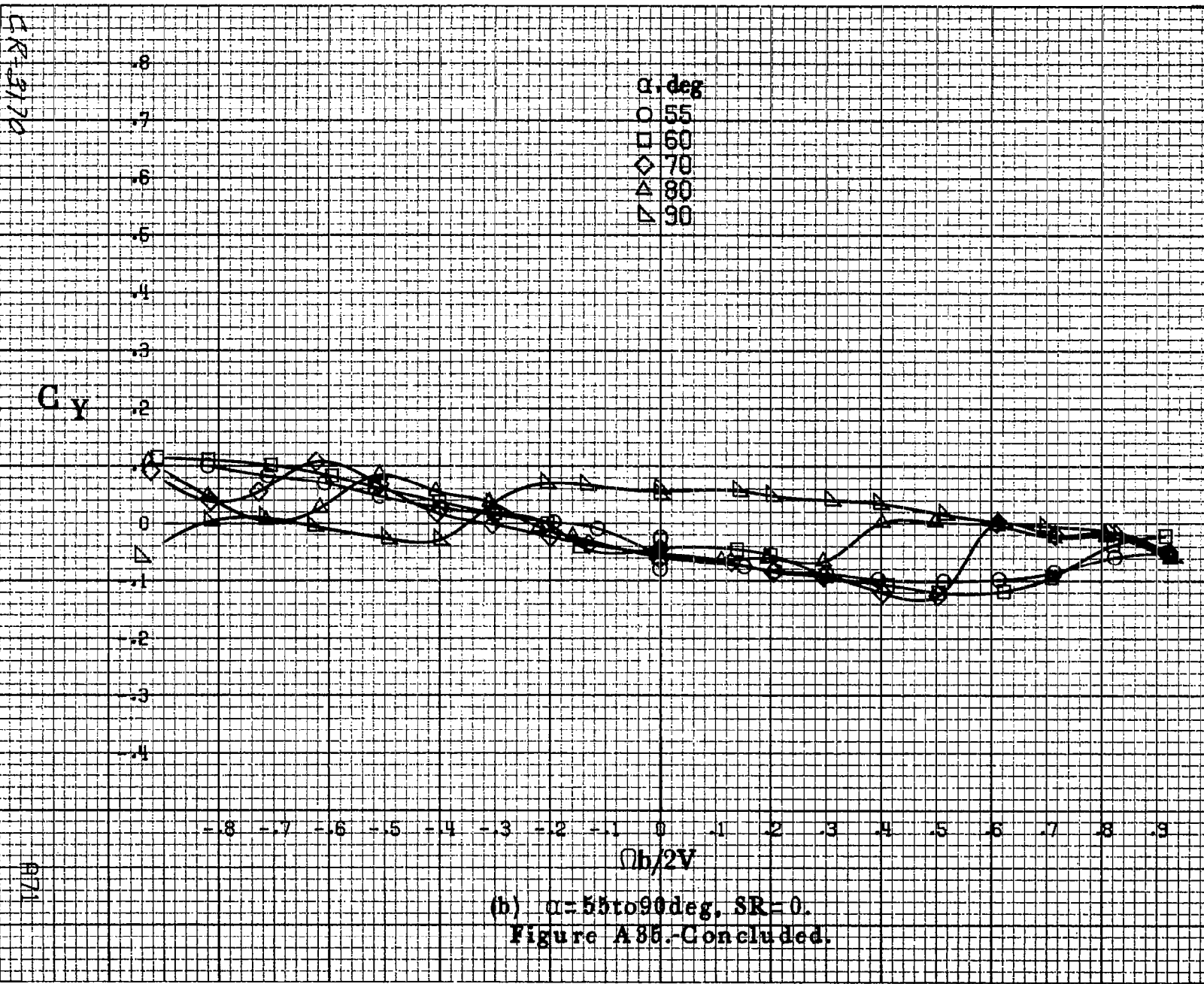


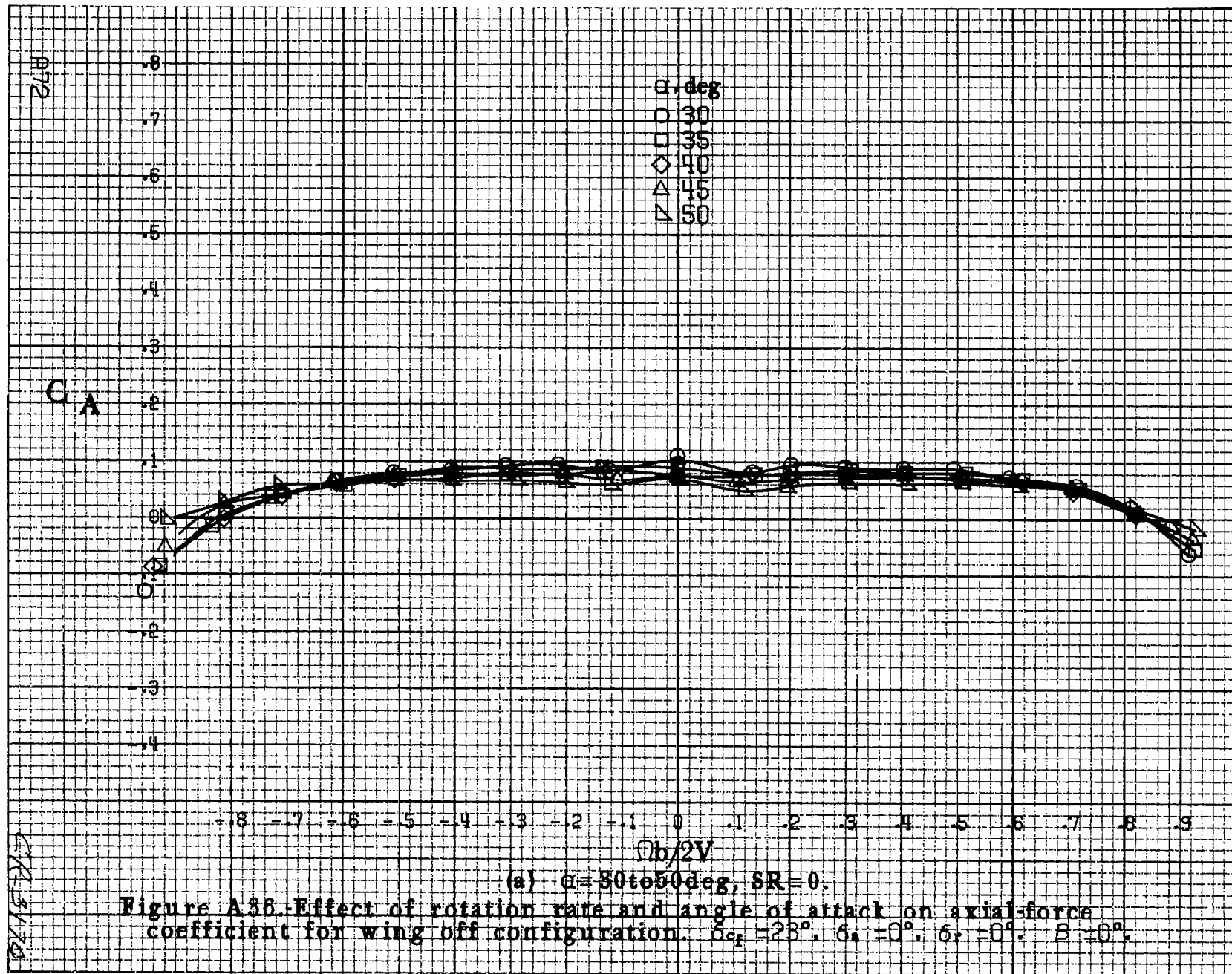


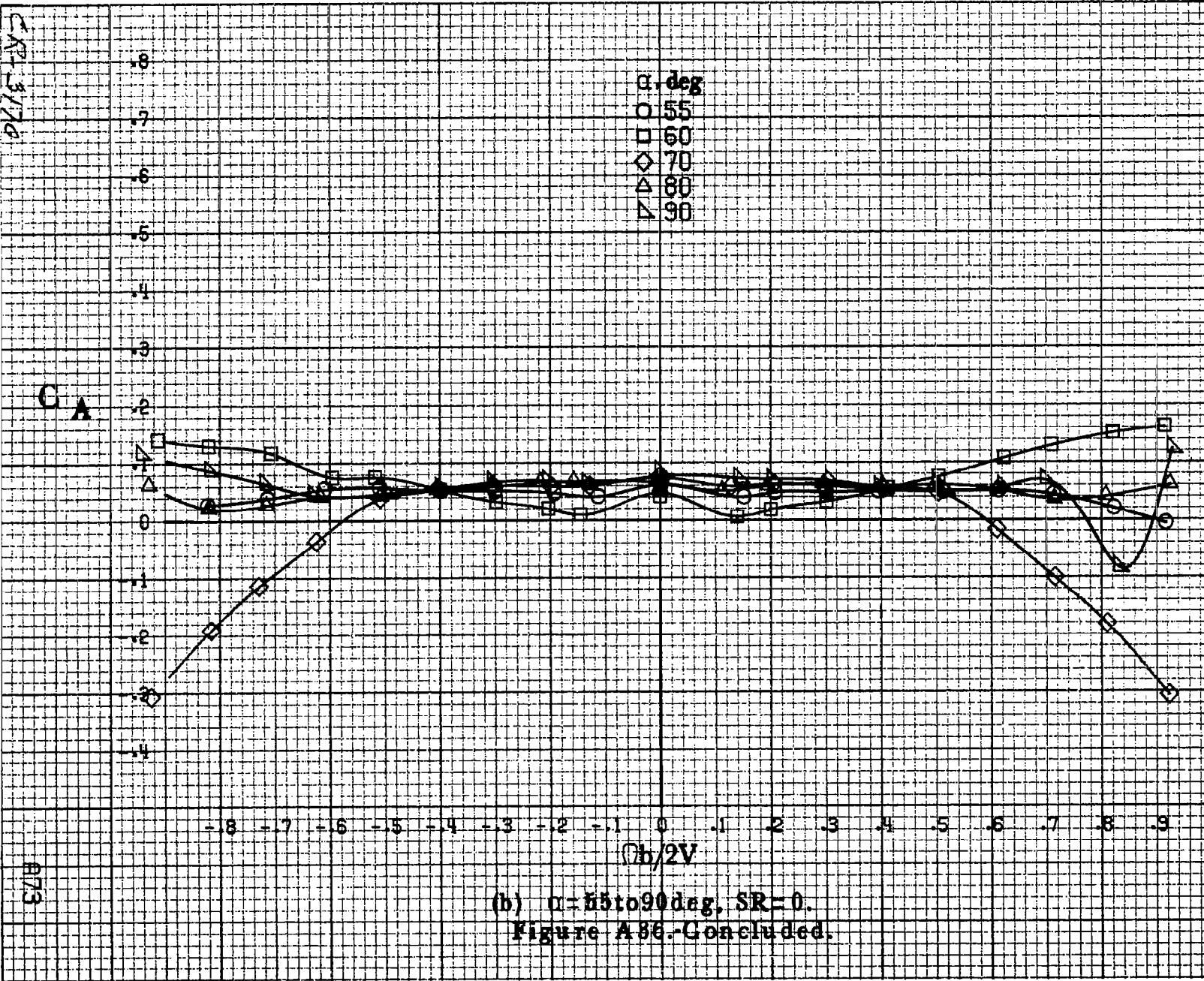


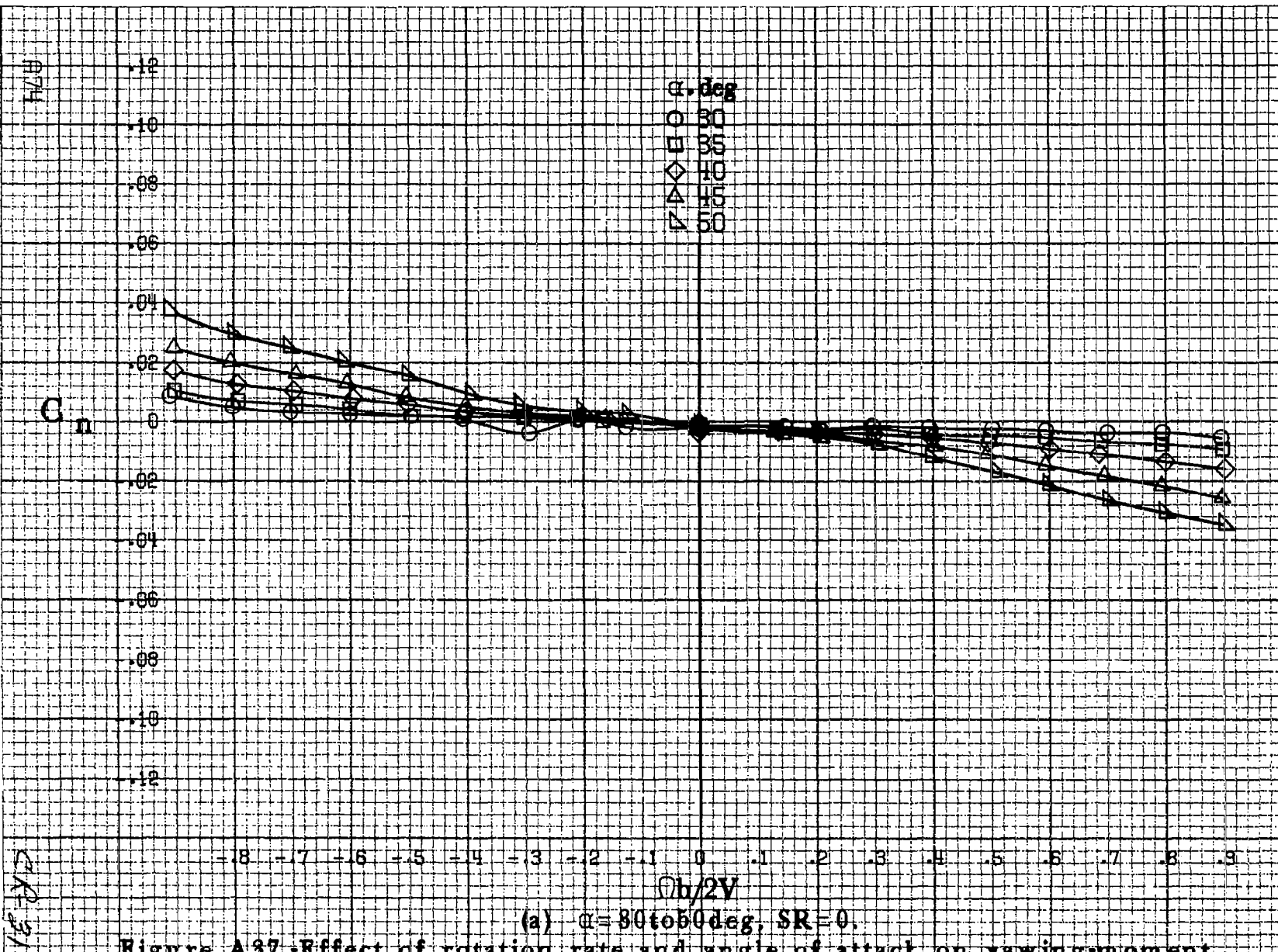
(a) $\alpha = 30$ to 50 deg, $SR = 0$.

Figure A.35 -Effect of rotation rate and angle of attack on side-force coefficient for wing off configuration. $\delta_{rf} = 25^\circ$, $\delta_s = 0^\circ$, $\delta_t = 0^\circ$, $\beta = 0^\circ$.



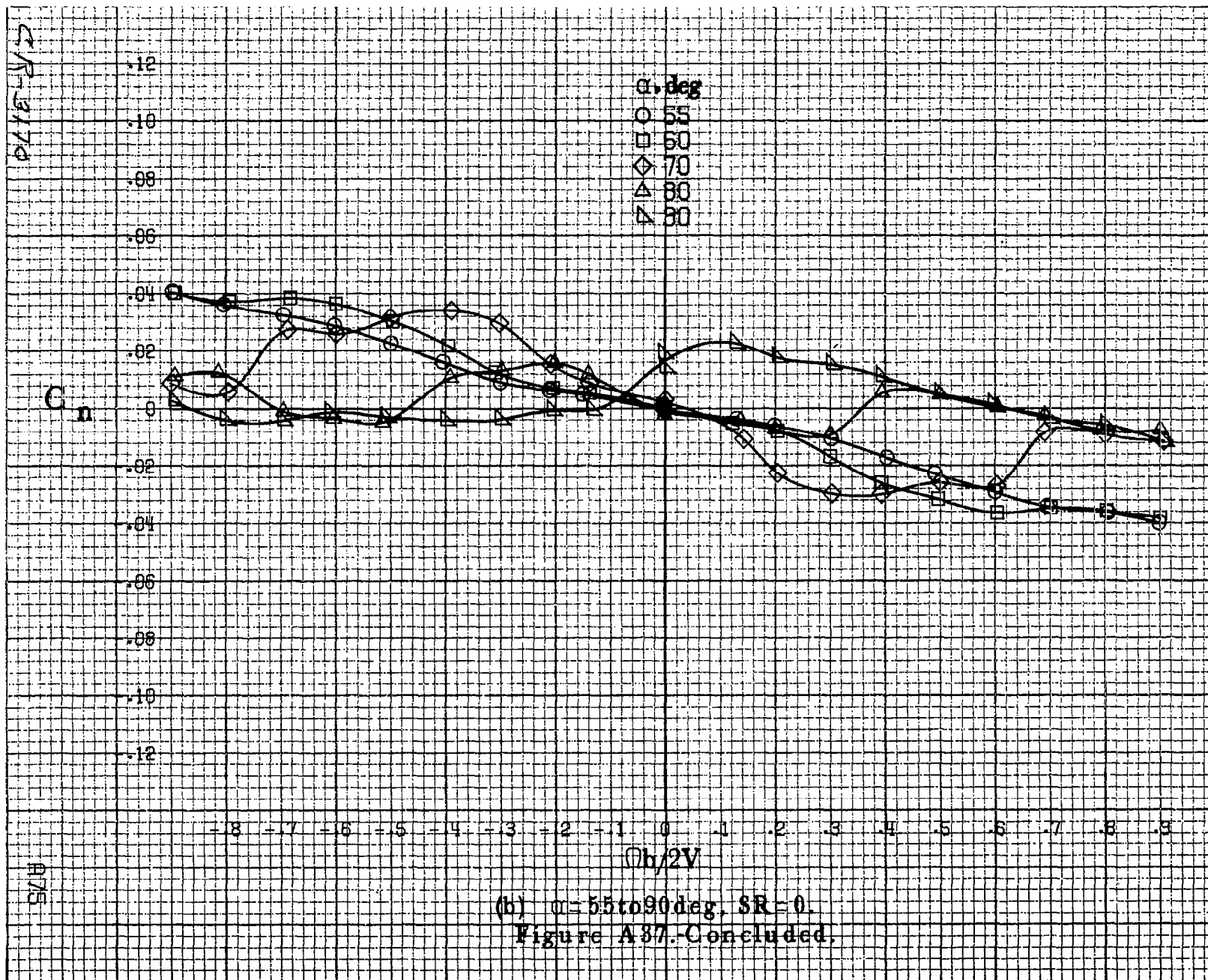


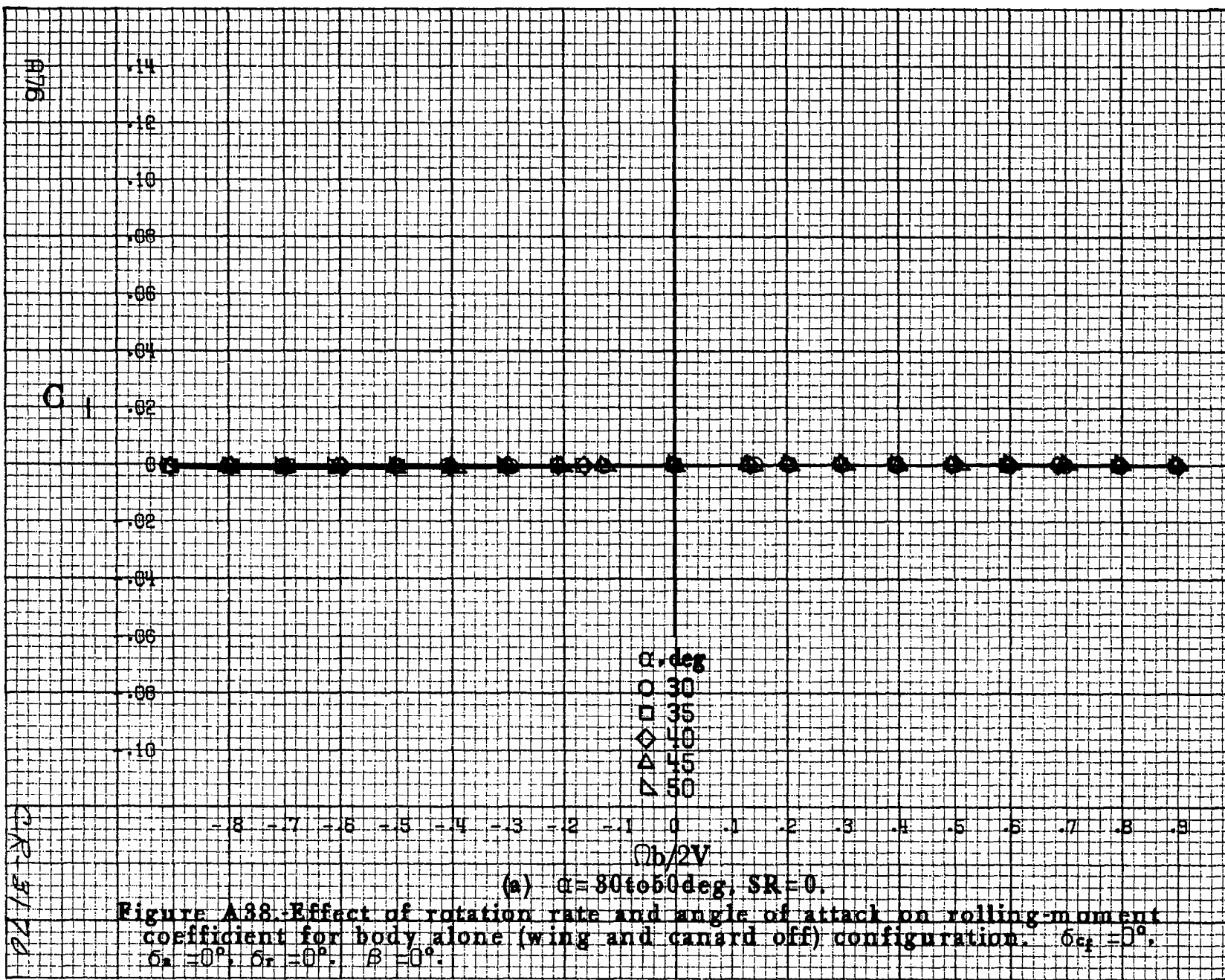




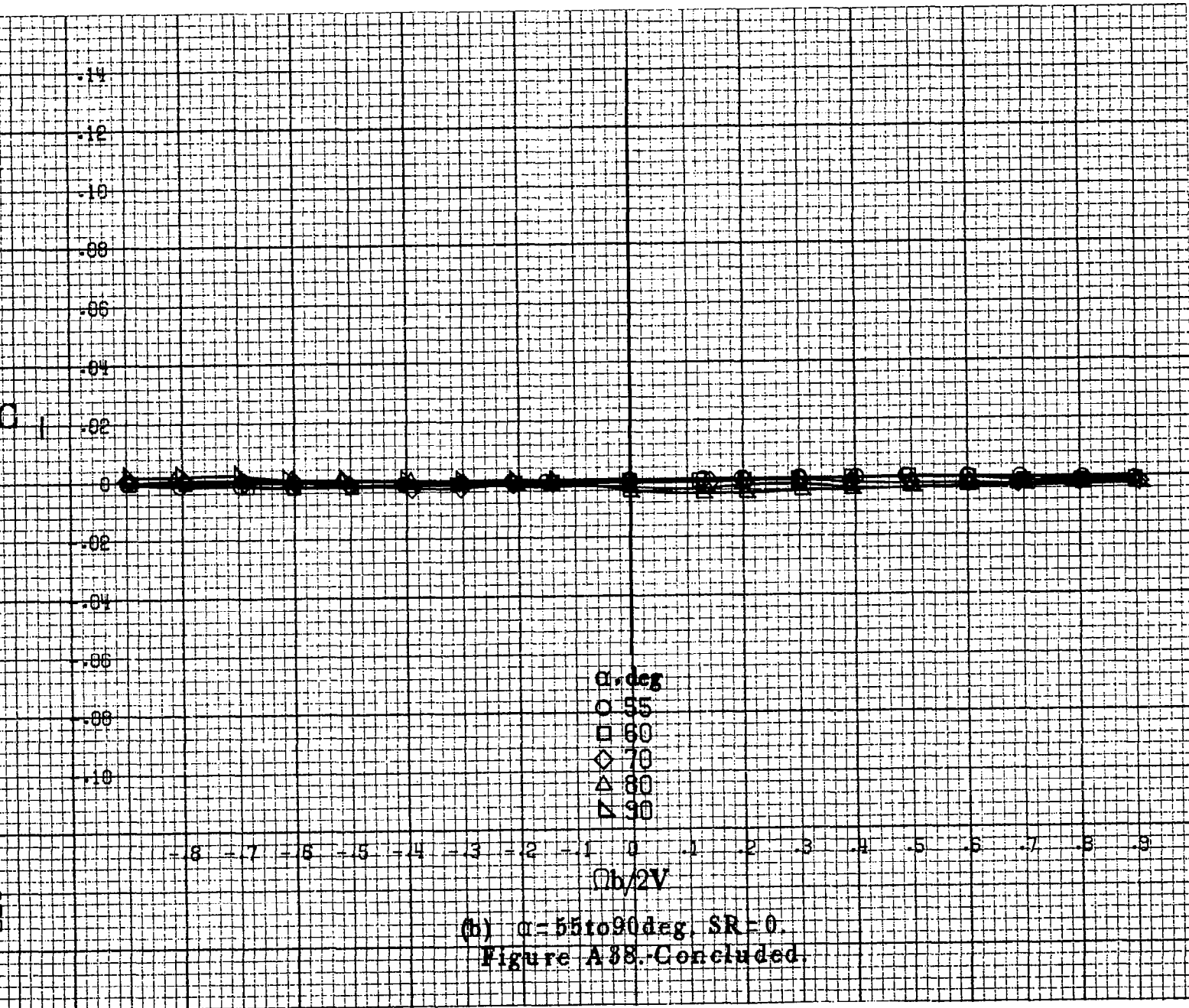
(a) $\alpha = 80$ to 50 deg, SR = 0.

Figure A.37. Effect of rotation rate and angle of attack on yawing-moment coefficient for body alone (wing and canard off) configuration. $\delta_{cf} = 0^\circ$, $\delta_a = 0^\circ$, $\delta_r = 0^\circ$, $\beta = 0^\circ$.





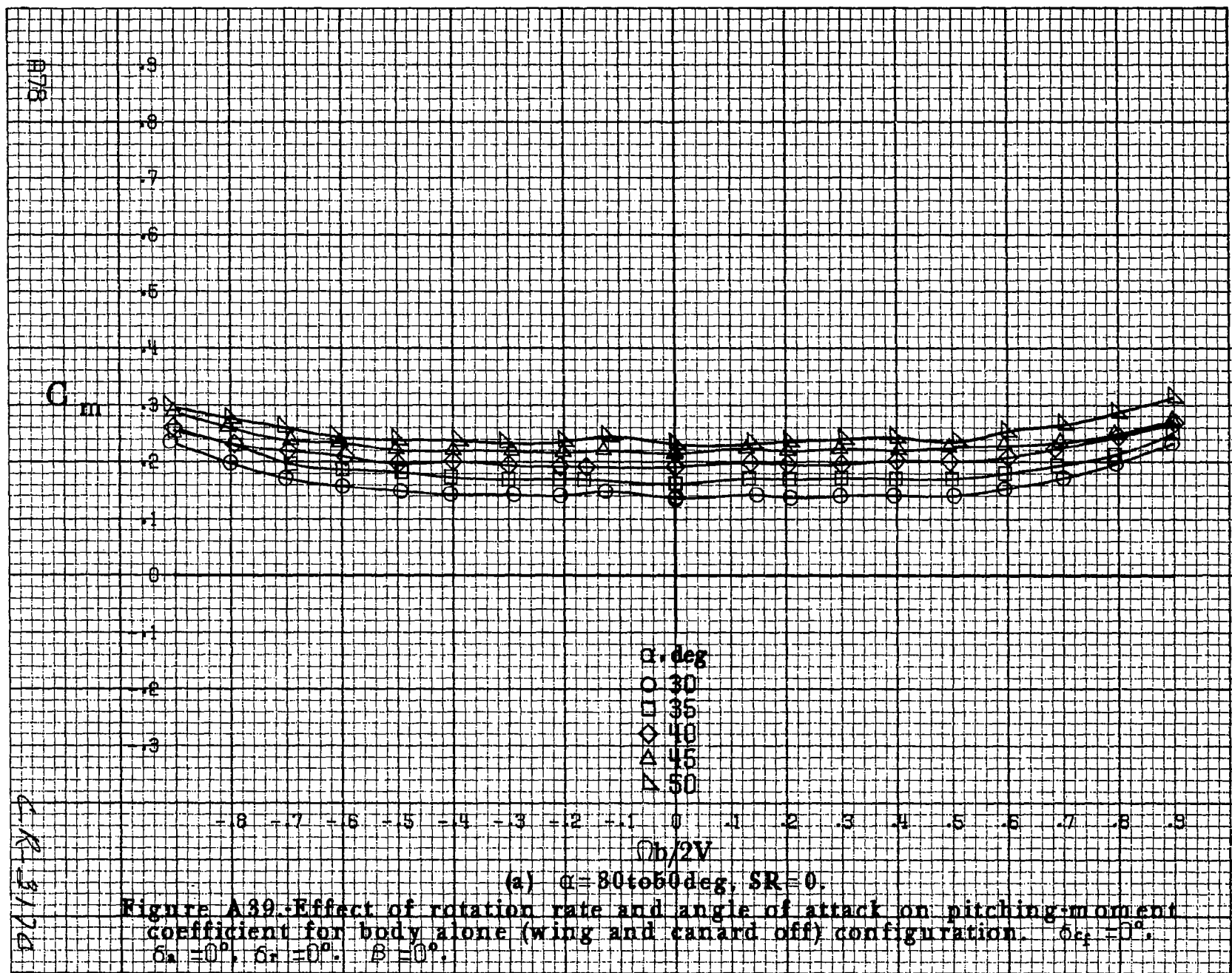
CR-3/1

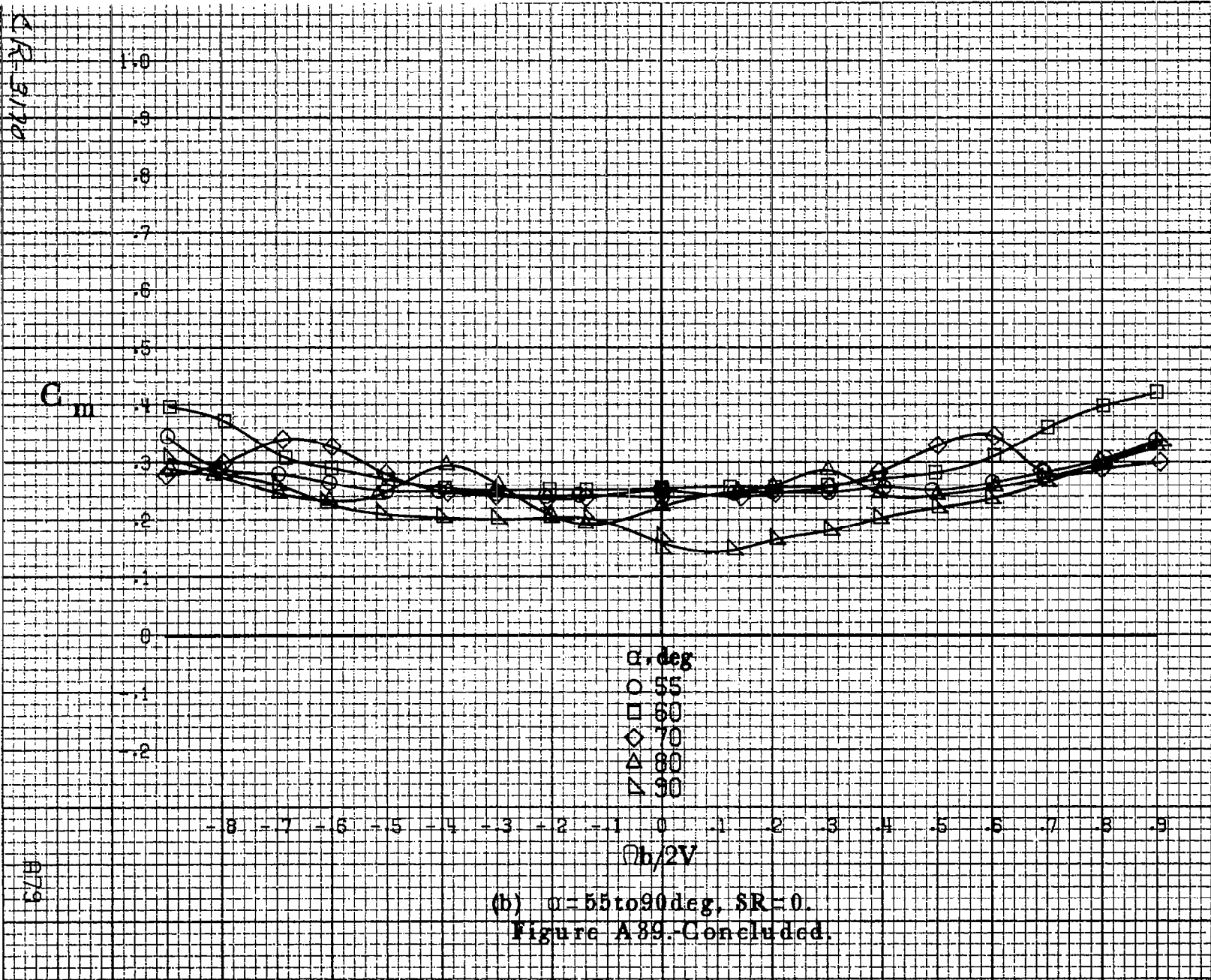


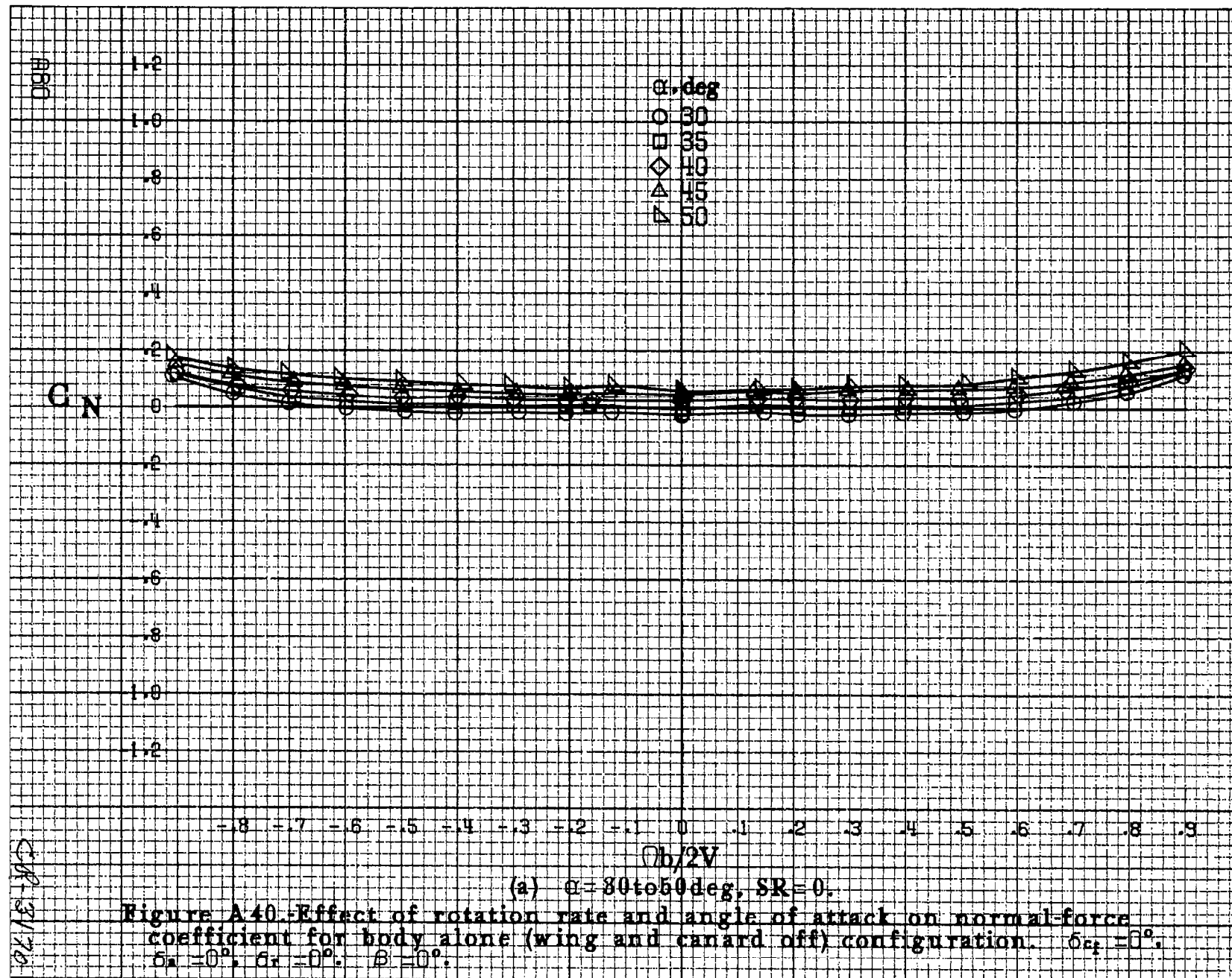
(b) $\alpha = 55 \text{ to } 90 \text{ deg. SR} = 0$.

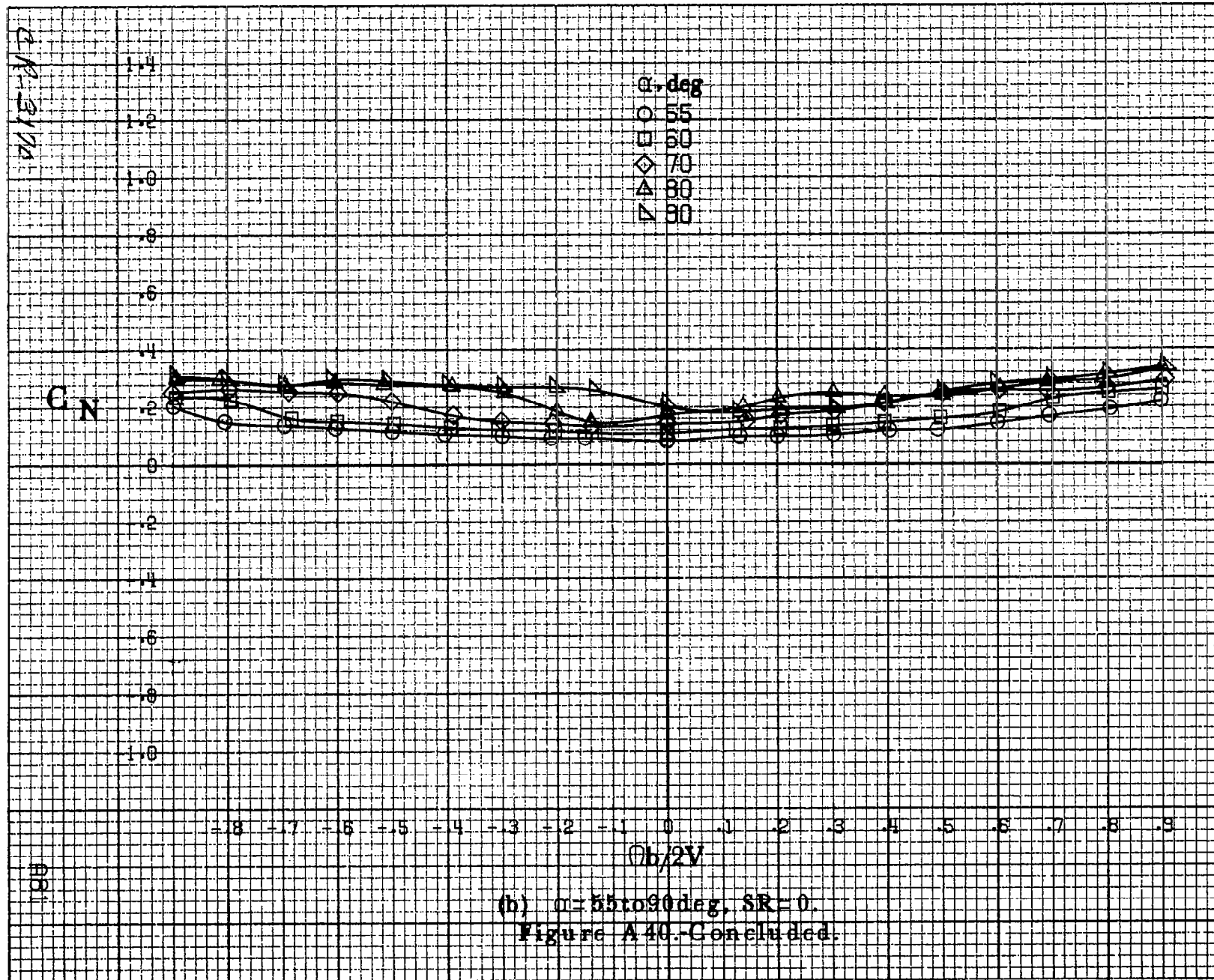
Figure A38.-Concluded.

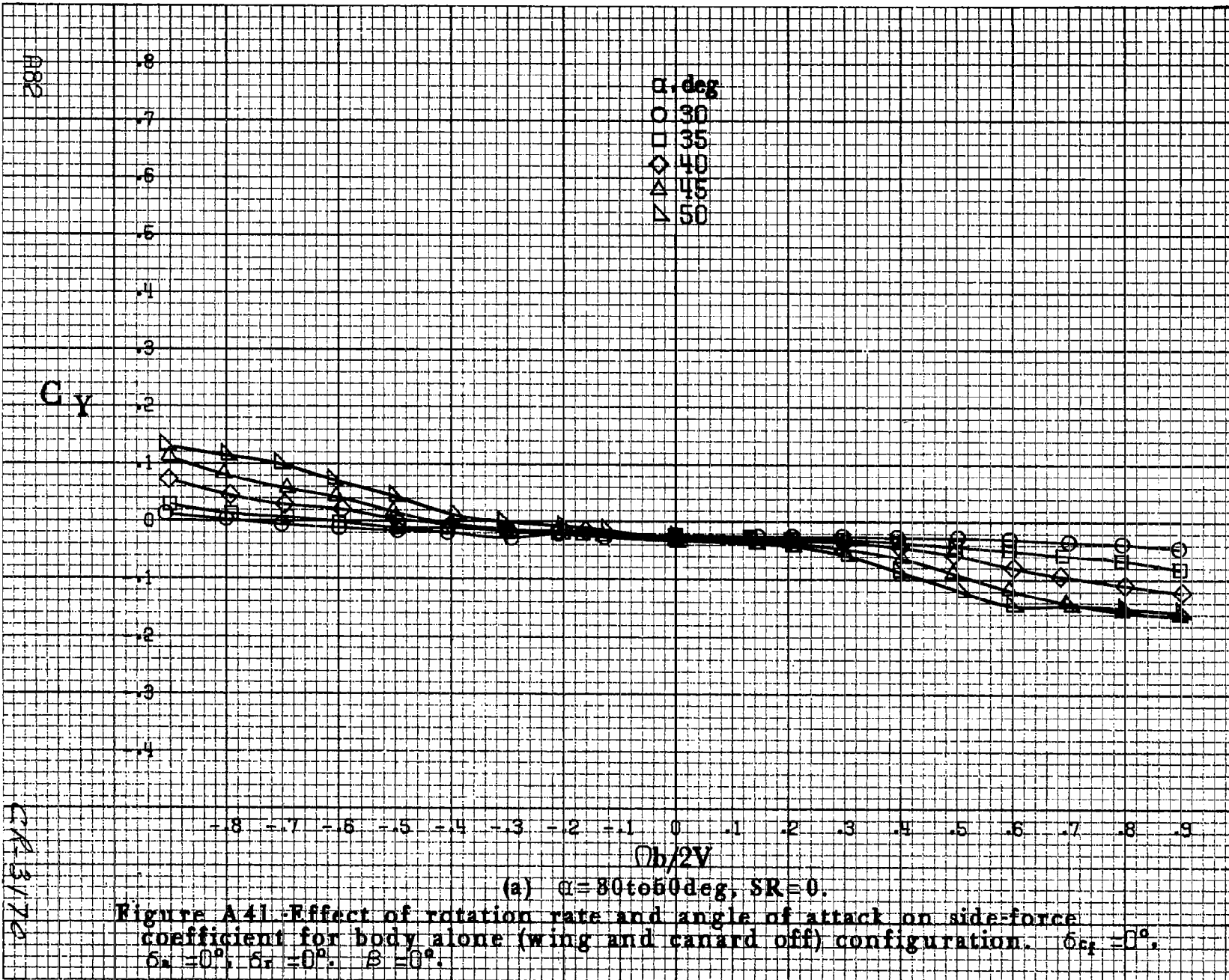
B77

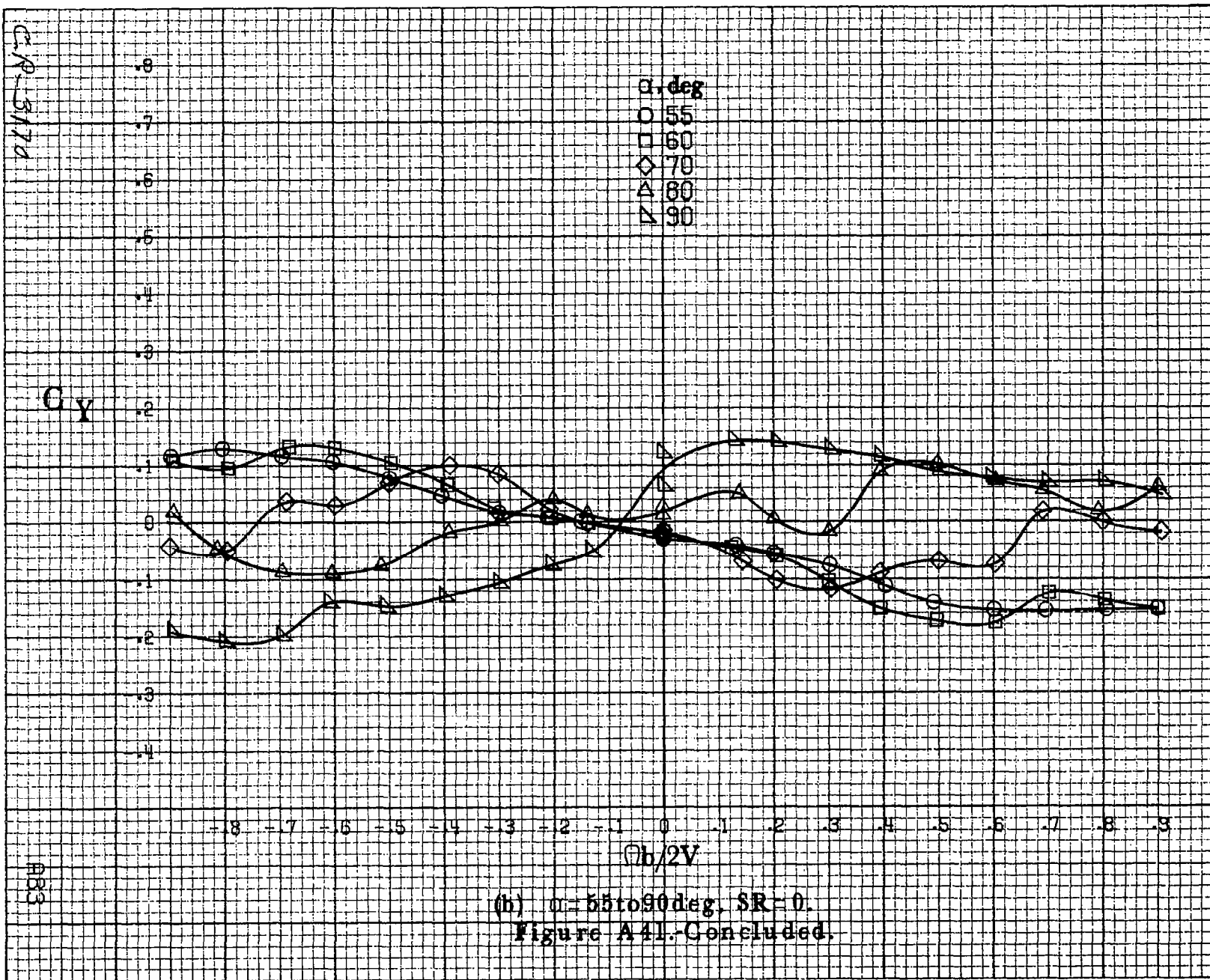


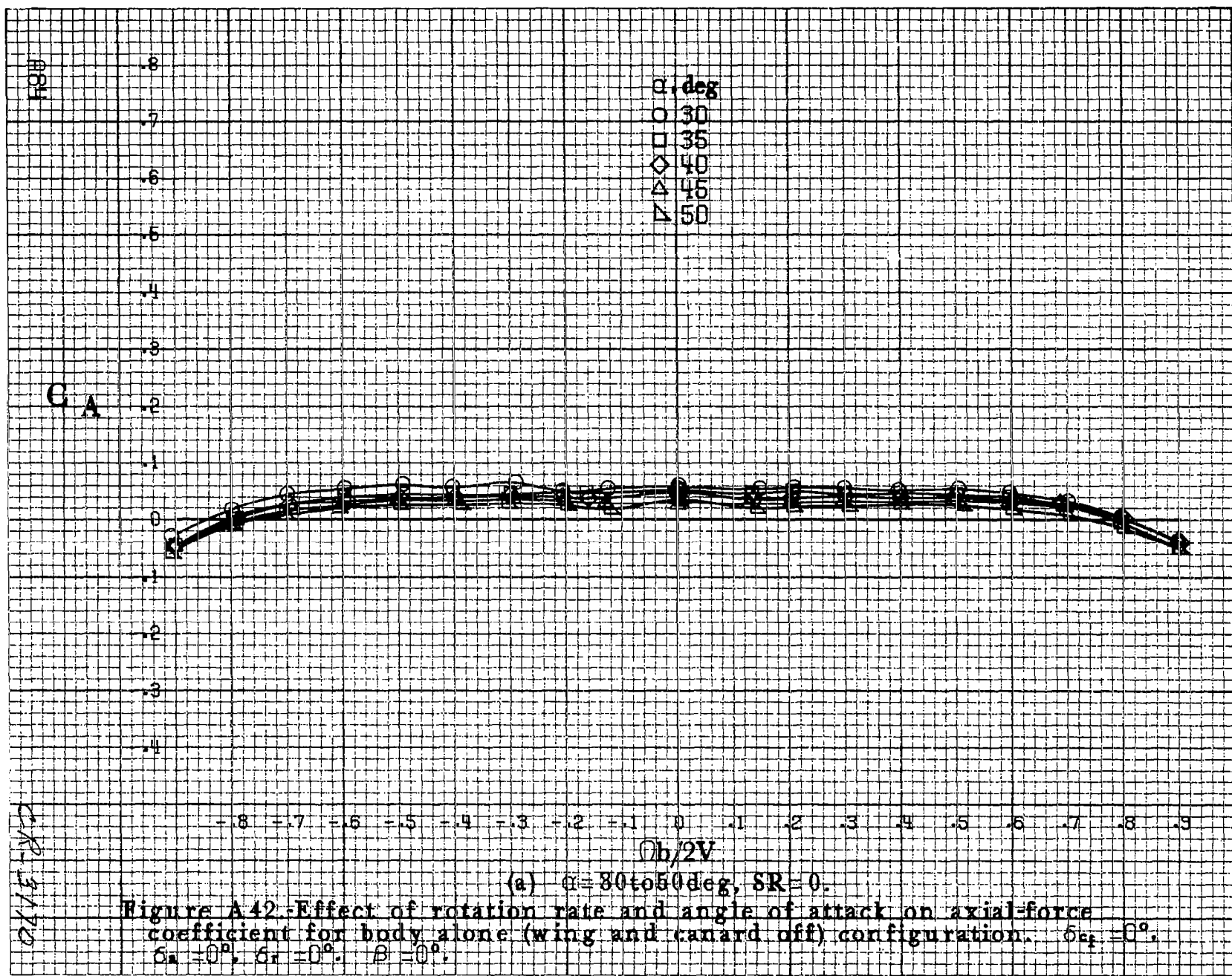


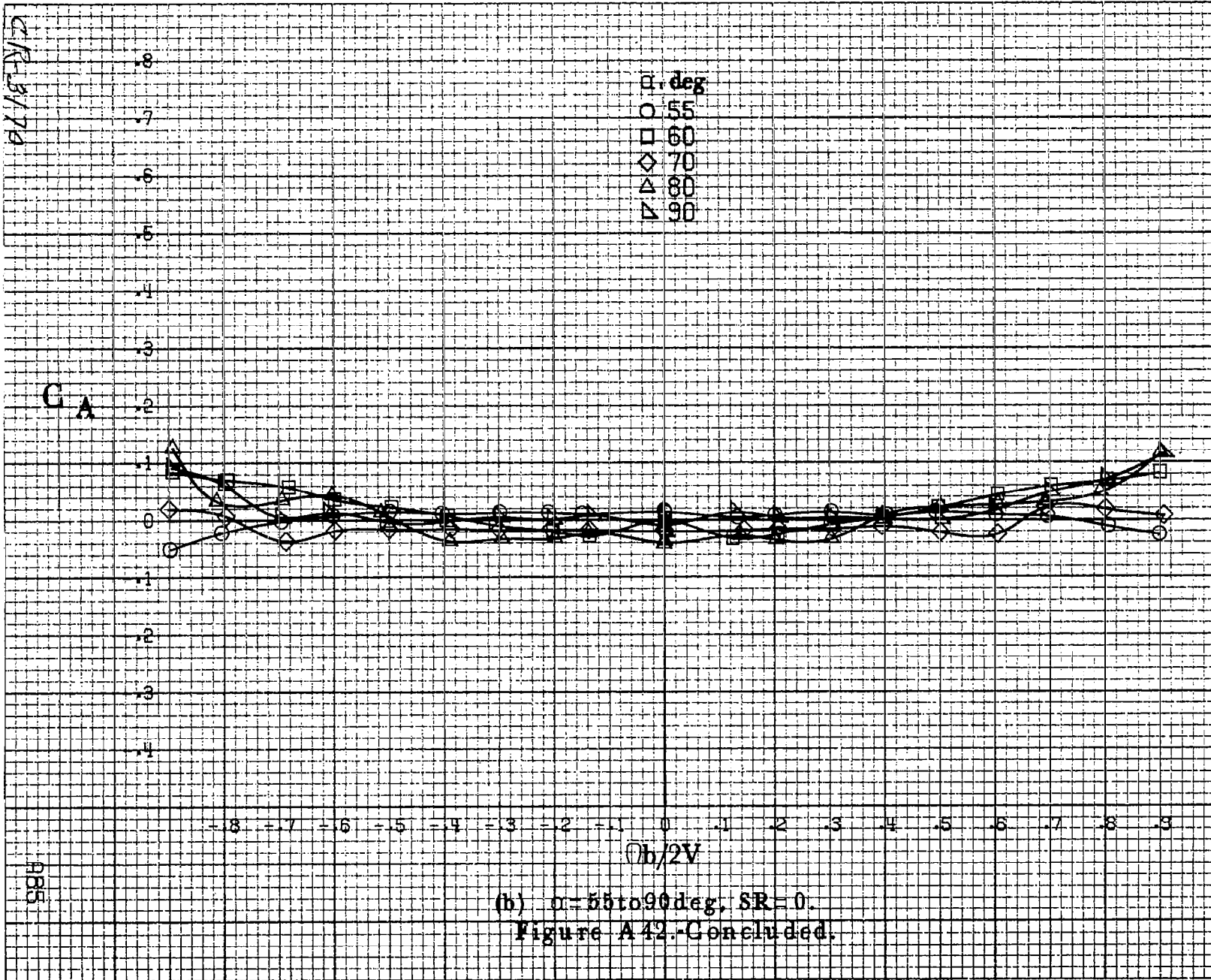












1. Report No. NASA CR-3170	2. Government Accession No.	3. Recipient's Catalog No.	
4. Title and Subtitle Rotary Balance Data for a Single-Engine General Aviation Design Having a High Aspect-Ratio Canard for an Angle-of-Attack Range of 30° to 90°		5. Report Date December 1980	
7. Author(s) William J. Mulcaj Robert Rose		6. Performing Organization Code	
9. Performing Organization Name and Address Bihrlle Applied Research, Inc. 400 Jericho Turnpike Jericho, New York 11753		8. Performing Organization Report No.	
12. Sponsoring Agency Name and Address National Aeronautics and Space Administration Washington, DC 20546		10. Work Unit No.	
15. Supplementary Notes Langley Technical Monitor: James S. Bowman, Jr. Topical report		11. Contract or Grant No. NAS1-14849, Task 34	
16. Abstract Aerodynamic characteristics obtained in a helical flow environment utilizing a rotary balance located in the Langley spin tunnel are presented in plotted form for a 1/4.5-scale single-engine general aviation model having a high aspect-ratio canard. The configurations tested included the basic airplane, various control deflections, two canard locations, and wing leading-edge modifications, as well as airplane components. Data are presented without analysis for an angle-of-attack range of 30° to 90° and clockwise and counter-clockwise rotations covering an $\frac{\Omega_b}{2V}$ range between 0 and 0.90.		13. Type of Report and Period Covered Contractor Report	
17. Key Words (Suggested by Author(s)) General Aviation Spinning Rotary Balance High angle of attack wind tunnel data Canard		18. Distribution Statement Unclassified - Unlimited Subject Category 02	
19. Security Classif. (of this report) Unclassified	20. Security Classif. (of this page) Unclassified	21. No. of Pages 103	22. Price A06

For sale by the National Technical Information Service, Springfield, Virginia 22161

NASA-Langley, 1980